

MASTER

Modelling dynamic behaviour of a yeast cell : simulation model of the TCA cycle and glyoxylate bypass

van Santen, M.A.E.

Award date:
1996

[Link to publication](#)

Disclaimer

This document contains a student thesis (bachelor's or master's), as authored by a student at Eindhoven University of Technology. Student theses are made available in the TU/e repository upon obtaining the required degree. The grade received is not published on the document as presented in the repository. The required complexity or quality of research of student theses may vary by program, and the required minimum study period may vary in duration.

General rights

Copyright and moral rights for the publications made accessible in the public portal are retained by the authors and/or other copyright owners and it is a condition of accessing publications that users recognise and abide by the legal requirements associated with these rights.

- Users may download and print one copy of any publication from the public portal for the purpose of private study or research.
- You may not further distribute the material or use it for any profit-making activity or commercial gain

EINDHOVEN UNIVERSITY OF TECHNOLOGY
DEPARTMENT OF ELECTRICAL ENGINEERING
Measurement and Control Group

MODELLING DYNAMIC BEHAVIOUR OF A YEAST CELL

Simulation model of the TCA cycle and glyoxylate bypass

by Miriam van Santen

M.Sc. Thesis

carried out from June 1995 to April 1996

commissioned by Prof.dr.ir. P.P.J. van den Bosch

under supervision of dr. H. Kuriyama, dr.ir. M. Keulers and dr.ir. A. van den Boom

The department of Electrical Engineering of the Eindhoven University of Technology accepts no responsibility for the contents of M.Sc. Theses.

SUMMARY

A simulation model of the Tricarboxylic acid (TCA) cycle and glyoxylate bypass has been developed. The simulation model is capable of calculating the amount of a metabolite that disappears each unit of time and the concentration of this metabolite. This simulation model could function as a tool in finding the cause of an autonomous, sustained, metabolic oscillation which is observed in a continuous culture of the yeast *Saccharomyces cerevisiae* grown on ethanol.

The simulation model consists of three different building blocks; a concentration block and a flux block for every metabolite and a reaction block for every reaction of the TCA cycle and glyoxylate bypass. In a concentration block the change in concentration of a metabolite is calculated from the amount of this metabolite made each unit of time (referred to as flux_{in}) and the amount that disappears each unit of time (referred to as flux_{out}). The flux block calculates the amount of flux_{out} as the rate constant of the metabolite times the concentration of the metabolite. A reaction block contains the stoichiometry of a reaction. The amount of flux which enters the glyoxylate bypass is determined through a so-called flux distribution function in the corresponding reaction block. This flux distribution function incorporates the negative feedback of two metabolites.

With the building blocks it is possible to construct a simulation model of a cyclic pathway with a bypass, which functions in a predictable way. It has been tested whether this simulation model can be fitted to experimental data. The experimental data which was available was an oscillating ethanol flux going into the cell, an oscillating acetate concentration and an oscillating CO_2 evolution rate. A number of simulations have been done to test whether the simulation model could reproduce the amplitude and the phase shift of the experimental data. The amplitude of the simulated acetate concentration could be tuned to the experimental acetate concentration through adjusting the rate constant. The phase shift between the experimental ethanol flux and the experimental acetate concentration could not be simulated. This could indicate that this phase shift is a result of the ethanol flux going into the cell. Adjusting the amplitude of the CO_2 evolution rate is more difficult, since it depends not only on several fluxes, but also on the flux distribution functions of the glyoxylate bypass and the ethanol input. To produce a correct simulation of the CO_2 evolution rate more experimental data is needed.

CONTENT

Glossary	i
1 Introduction	1
2 Literature review	7
2.1 Review of biochemical computer programs	7
2.1.1 Computer programs based on Metabolic Control Analysis	8
2.1.2 Computer programs based on Biochemical Systems Theory	9
2.1.3 Other computer programs	9
2.2 Discussion and conclusions	9
3 Principal aspects of the simulation model	11
3.1 Introduction	11
3.2 A chemical or a physical approach?	11
3.3 Hypotheses	13
3.4 TCA cycle and glyoxylate bypass	14
3.5 Building blocks of the simulation model	14
3.5.1 Concentration block	15
3.5.2 Flux block	15
3.5.3 Reaction block	16
3.6 Simulation model of a simplified version of the TCA cycle	18
3.7 Conclusions	21
4 Simulation model of the TCA cycle and glyoxylate bypass	23
4.1 Introduction	23
4.2 Extension of the simulation model	23
4.2.1 Glyoxylate bypass	25
4.2.2 Drains	27
4.3 Simulations	28
4.4 Deficiencies of the simulation model	31
4.4.1 If-then statement	31
4.4.2 Flux distribution	33
4.5 Conclusions	36
5 Fitting the simulation model with experimental data	39
5.1 Introduction	39
5.2 Denormalising the simulation model	39
5.3 Preparing the data	41
5.4 Simulations	43
5.5 Conclusions	48
6 Conclusions and future work	49
References	51
Nomenclatura	53

Appendix A	Chemical reactions	55
Appendix B	Listing of concentration block, flux block and reaction block	57
Appendix C	Listing of a reaction block and Simulink diagram of the normalised simulation model	61
Appendix D	Simulation results	65
Appendix E	If-then statement	73
Appendix F	Listing of MINXY, TCAMIN and WINDOW	85
Appendix G	Listing of altered concentration block, flux block and reaction block and Simulink diagram of denormalised simulation model	88
Japanese summary		91
Samenvatting		92
Acknowledgements		93

GLOSSARY

Abbreviations

ADP	Adenosine diphosphate
ATP	Adenosine triphosphate
DCW	dry cell weight
FADH ₂	Flavin adenine dinucleotide
NADH	Nicotinamide adenine dinucleotide
TCA	Tricarboxylic acid cycle

Metabolites of the Tricarboxylic acid cycle

ACE	Acetate
ACO	Acetyl-CoA
ADH	Acetaldehyde
CIT	Citrate
ETH	Ethanol
GLU	Glutamate
GLY	Glyoxylate
ISO	Isocitrate
KET	α -Ketoglutarate
MAL	Malate
OXA	Oxaloacetate
PEP	p-Enol-pyruvate
PYR	Pyruvate
SUC	Succinate

Constants

$r_{w/D}$	wet cell weight divided by dry cell weight ($g_{wet\ cell} \cdot g_{cell}^{-1}$)
V	volume (dm ³)
f	flux ($mmol \cdot s^{-1} \cdot dm_{cell}^{-3}$)

Subscripts

cell	cell
ex	extracellular
ferm	fermenter
i	in
in	intracellular
o	out
raw	unprepared data
tot	total

1

INTRODUCTION

The term yeast is a common name for a group of micro organisms which belong to the kingdom of Fungi. Yeasts are used, for example, for baking and alcoholic fermentation and approximately 600 different species are known and classified to date [Barnett *et al.* 1990]. The name *Saccharomyces cerevisiae* first appeared in 1838 when Meyen gave this name to a beer yeast. A more accurate description including physiological characteristics of *Saccharomyces cerevisiae* was given by Hansen in 1883 [Lodder *et al.* 1967]. Nowadays it is known as baker's yeast and it can be found in e.g., wines, beers, fruits, cheese, soft drinks, sugar cane, soil and also in human beings and other mammals [Barnet *et al.* 1990]. *Saccharomyces cerevisiae* forms white or cream colonies, is round to oval and measures 5-10 μm .

The yeast cell contains various elements like a nucleus, mitochondria and vacuoles. In the mitochondria the generation of energy takes place in the form of phosphorylation of ADP into ATP. This is referred to as the respiratory chain. To convert ADP into ATP, O_2 and NADH are necessary. The production of this NADH is one of the major functions of the Tricarboxylic acid (TCA) cycle. The TCA cycle, discovered in 1937 by Krebs [Krebs 1940], together with the glyoxylate bypass is shown in figure 1.1.¹

¹ A description of biochemical terms used in this thesis is given in 'Nomenclatura'.

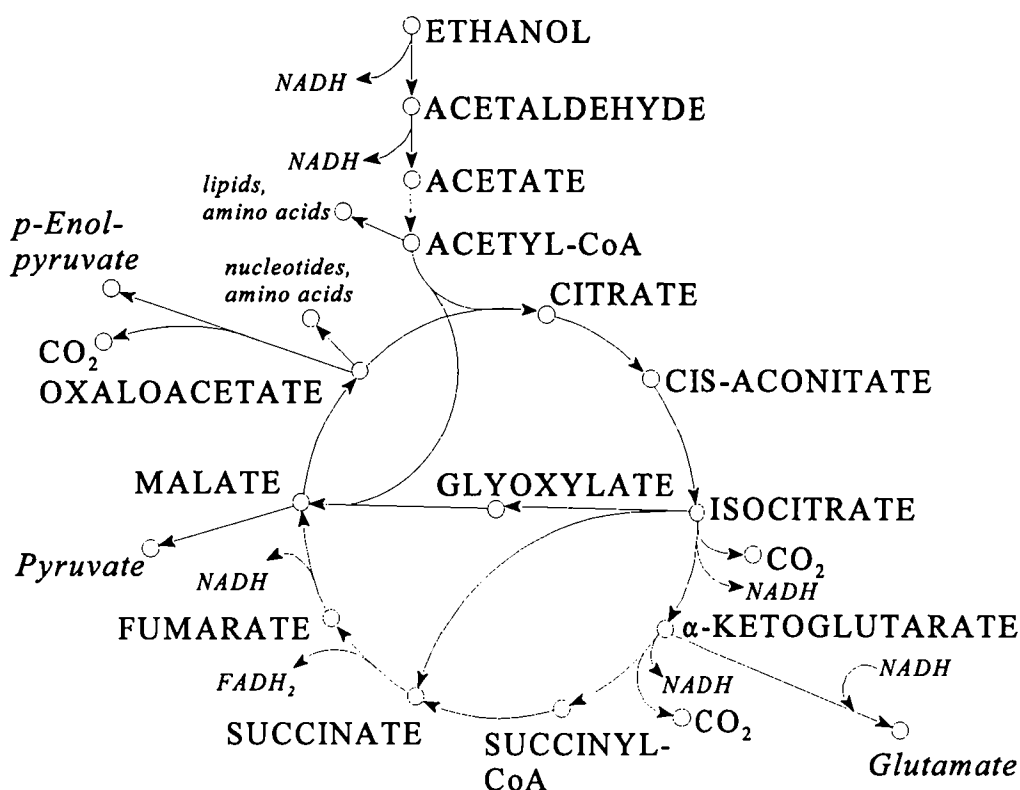


Figure 1.1. *TCA cycle and glyoxylate bypass. Metabolites of the TCA cycle and glyoxylate bypass are shown in capitals and the metabolites of the drains in small letters.*

The glyoxylate bypass, discovered in 1957 by Kornberg and Madsen [Kornberg *et al.* 1957], is a shortcut in the TCA cycle and consists of the conversion of isocitrate into glyoxylate and succinate and of the conversion of glyoxylate and acetyl-CoA into malate (for chemical reactions see Appendix A).

The TCA cycle not only generates energy, but also provides intermediates which are used in biomass formation. The drains which are used for this biosynthesis are the glutamate drain, the nucleotides and amino acids drain from oxaloacetate and the lipids and amino acids drain from acetyl-CoA. The pyruvate drain from malate and the p-enol-pyruvate drain from oxaloacetate enter the gluconeogenesis, which also produces intermediates for biosynthesis. In order to understand the functioning of the TCA cycle one has to look at the number of C-atoms of each metabolite involved, which is shown in figure 1.2. For the sake of clearness the metabolites cis-aconitate, succinyl-CoA and fumarate are left out. First the TCA cycle is regarded without the glyoxylate bypass and drains.

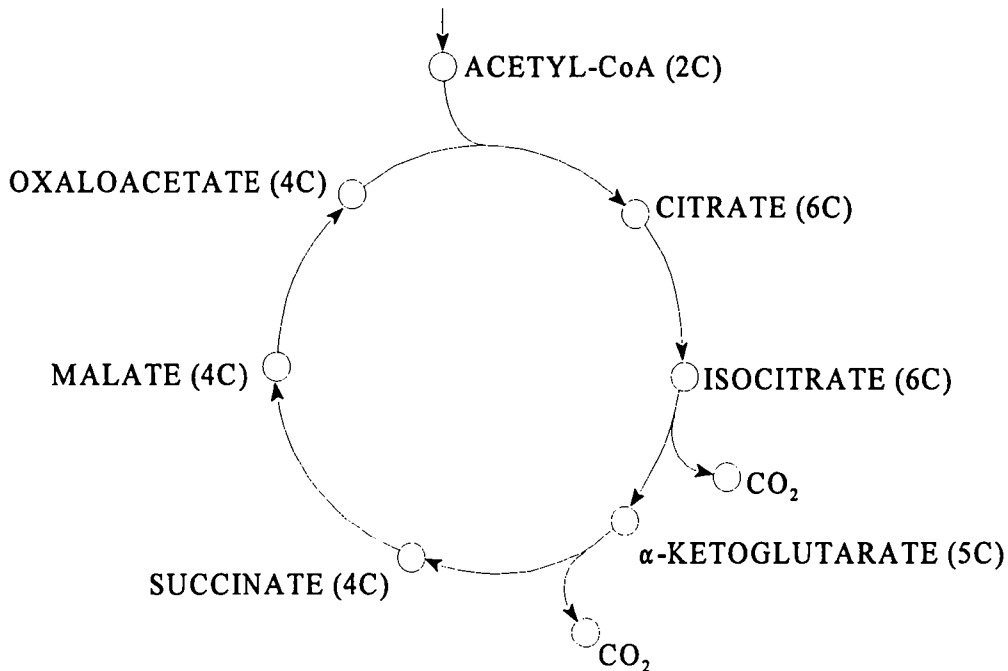


Figure 1.2. *TCA cycle without the glyoxylate bypass and drains. Between brackets the number of C-atoms of each metabolite is given.*

Acetyl-CoA (2 C-atoms) enters the TCA cycle and reacts with oxaloacetate (4 C-atoms) into citrate (6 C-atoms). Citrate is converted into isocitrate (6 C-atoms) without a change in the number of C-atoms. Next, isocitrate is converted into α -ketoglutarate (5 C-atoms) and 1 CO_2 is produced. α -Ketoglutarate reacts to succinate (4 C-atoms) and again 1 CO_2 molecule is produced. Succinate is transformed into oxaloacetate (4 C-atoms) without a loss of C-atoms. Oxaloacetate can react again with acetyl-CoA into citrate and in this way 1 mol of acetyl-CoA results in 1 mol of oxaloacetate. The number of C-atoms of each metabolite in the TCA cycle indicates that the two C-atoms from acetyl-CoA which enter the TCA cycle, compensate the two CO_2 molecules that are produced. As long as acetyl-CoA is available, the TCA cycle is able to keep on turning.

A problem arises for the TCA cycle when drains are attached to some metabolites. For example, the glutamate drain from α -ketoglutarate, the pyruvate drain from malate and the p-enol-pyruvate drain from oxaloacetate. Every C-atoms that leaves the TCA cycle through one of these drains is not compensated. In this way 1 mol acetyl-CoA results no longer in 1 mol of oxaloacetate and as a result the TCA cycle runs down and stops. To compensate for these losses in the TCA cycle, a shortcut known as the glyoxylate bypass is present. Figure 1.3 shows the number of C-atoms of the metabolites of the TCA cycle, of the metabolites of the glyoxylate bypass and of the drains.

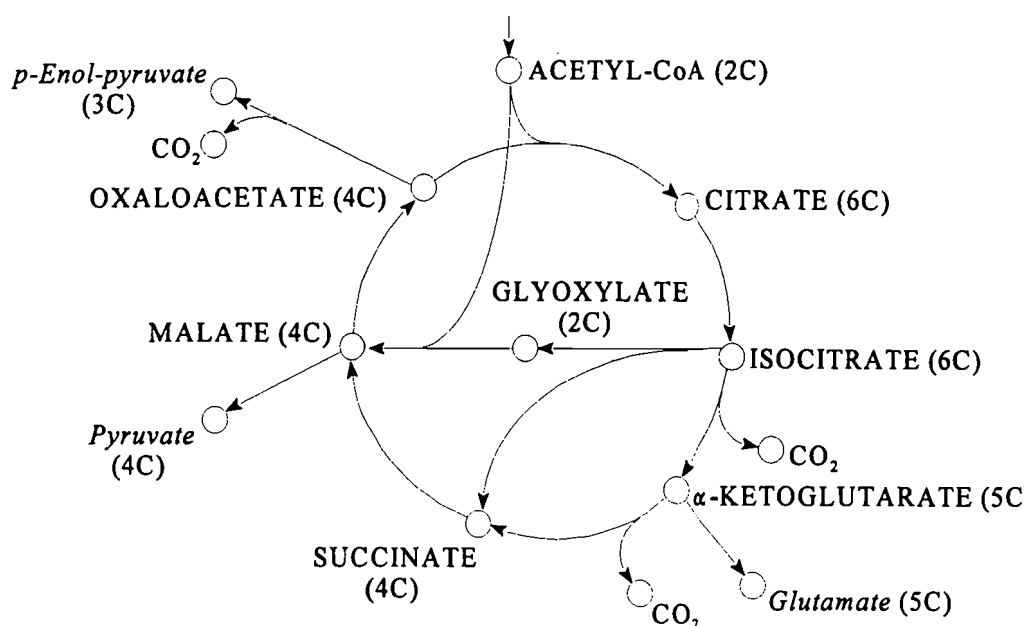


Figure 1.3. *TCA cycle, glyoxylate bypass and three drains. Metabolites of the TCA cycle and glyoxylate bypass are given in capitals and metabolites of the drains in small letters. For every metabolite the number of C-atoms is given.*

The functioning of the glyoxylate bypass can be clarified as follows. Suppose 1 mol isocitrate is converted into 0.5 mol glyoxylate (2 C-atoms), 0.5 mol succinate (4 C-atoms), 0.5 mol α -ketoglutarate (5 C-atoms) and 0.5 mol of CO_2 . Assume 10% of α -ketoglutarate is converted into glutamate. The remaining part of α -ketoglutarate forms 0.45 mol succinate. Assume that 0.5 mol acetyl-CoA (2 C-atoms) is available to react with 0.5 mol glyoxylate (2 C-atoms) into 0.5 mol malate (4 C-atoms). The total amount of malate being made is 1.45 mol. If the pyruvate drain and the p-enol-pyruvate drain together use no more than 0.45 mol, then 1 mol oxaloacetate remains to react with 1 mol acetyl-CoA into 1 mol citrate. Through controlling the amount of isocitrate that converts into either glyoxylate and succinate or into α -ketoglutarate, the TCA cycle is able to compensate for the losses of the drains.

SCOPE OF THIS THESIS

Under certain circumstances an autonomous, sustained, metabolic oscillation is observed in a continuous culture of *Saccharomyces cerevisiae* when it is grown on glucose or ethanol medium. This oscillation appears in a number of parameters e.g., the oxygen uptake rate, the ethanol uptake rate (when grown on ethanol), the CO_2 evolution rate, the dissolved oxygen tension and the concentration of acetate. Until now little is known about such oscillations. A better understanding of it could result in control of dynamic yeast processes. Nowadays yeast processes are maintained in a steady state and they are already optimised to a high degree. Being able to control dynamic yeast processes could enhance production and could form a new way to produce special product, for example fine chemicals and drugs.

So far the cause of the oscillation is unknown. A hypothesis is that this oscillation is caused by a negative feedback mechanism. Such negative feedback mechanisms are abundant in the metabolic pathways. For example, in the TCA cycle the concentration of malate and succinate have a negative feedback on the conversion of isocitrate into glyoxylate and succinate. However, this is not the only known feedback mechanism in the TCA cycle and glyoxylate bypass and there are also negative feedbacks involved in the pathways leading towards and from the TCA cycle. A simulation model of the TCA cycle and glyoxylate bypass could facilitate goal-directed experiments to find the cause of the oscillation. The object of this thesis can therefore be described as follows:

Develop a simulation model of the TCA cycle and glyoxylate bypass that simulates concentrations and fluxes of the autonomous, sustained, metabolic oscillation observed in a continuous culture of *Saccharomyces cerevisiae* grown on ethanol.

OUTLINE OF THIS THESIS

First a literature review is given on the available biochemical computer programs in chapter 2. To date several biochemical programs exist and it is checked whether they could form as a basis for the simulation model described in this thesis. Since neither of the programs is able to handle steady states and dynamic behaviour as well as calculate concentrations and fluxes at the same time, none could serve as a basis. In chapter 3 the hypotheses on which the simulation model is based are stated. Also a distinction is made between a chemical and a physical approach of the simulation model. Furthermore, the three building blocks of the simulation model are described. With these building blocks a simulation model of a simplified version of the TCA cycle is made and the results of two simulations are discussed. In chapter 4 the simulation model of the previous chapter is extended with several metabolites, with the glyoxylate bypass and with several drains. Simulation results showed some deficiencies of the simulation model and possible solutions for these deficiencies are investigated. In chapter 5 the simulation model is adjusted in a way that it can handle experimental data and the experimental data is prepared. With the simulation model and the experimental data several simulations have been done and the results are discussed. In the last chapter conclusions and suggestions for future work are given.

2

LITERATURE REVIEW

A literature research has been done to find out whether there are computer programs available which could serve as the basis for a simulation model. When a paper of a computer program was found, it was checked whether the program could handle steady states as well as dynamic behaviour of the system and whether it was able to calculate fluxes and concentrations of the metabolites involved. First a short review of the field of biochemical computer programs will be given after which several computer programs will be discussed.

2.1 REVIEW OF BIOCHEMICAL COMPUTER PROGRAMS

One of the pioneers on biochemical system simulation was Chance. In the 1940's he simulated the behaviour of a simple enzyme system [Garfinkel *et al.* 1970]. By the end of the 1960's the use of more powerful computers resulted in a machine-independent and biochemist-oriented language, called BIOSSIM [Garfinkel *et al.* 1970, Mendes 1993]. At the same time a first step towards a biochemical control theory was made by Higgins [Higgins 1965]. He presented a theoretical method for determining the 'rate-limiting' reaction of a metabolic pathway. In the following years several biochemical control theories were developed of which the most important ones are 'Metabolic Control Analysis' [Kascser *et al.* 1973, Heinrich *et al.* 1974, Westerhoff *et al.* 1984, Burns *et al.* 1985, Fell *et al.* 1985, Sauro *et al.* 1987, Reder 1988, Brown *et al.* 1990, Westerhoff *et al.* 1991, review articles: Kell *et al.* 1986, Fell 1992, Cornish-Bowden 1995] and 'Biochemical System Theory' [Savageau 1969, 1976, 1990]. A number of simulation programs are written of which several are based on one of these theories.

2.1.1 COMPUTER PROGRAMS BASED ON METABOLIC CONTROL ANALYSIS

Metabolic Control Analysis (MCA) is a small signal analysis method to determine the rate-limiting reaction or control site of a metabolic pathway. The most important features in MCA are the control coefficients. They describe how a variable, such as a metabolic flux or the concentration of a metabolite, responds to a small variation of a parameter, usually an enzyme concentration. Another important feature is called the elasticity coefficient. An elasticity coefficient represents the kinetics of an individual enzyme. A number of simulation programs are made based on MCA e.g., MetaCon [Thomas *et al.* 1993], MetaModel [Cornish-Bowden *et al.* 1991], SCAMP [Sauro *et al.* 1991], CONTROL [Letellier 1991], a program developed by Schulz [Schulz 1991] and GEPASI [Mendes 1993].

With MetaCon, the control coefficients of a pathway can be evaluated. The reaction scheme is the only required input. In this program the combination of alfa-numerical and numerical information can be incorporated into a model. Depending on the particular system being investigated, and the amount of data available, the control coefficients may evaluate to a number, or may be expressed as polynomials containing enzyme kinetic constants, equilibrium constants, reaction fluxes etc .

With MetaModel steady state fluxes and concentrations can be calculated if all rate equations, initial concentrations, K_m and v_{max} values are known. With this calculated steady state an elasticity and control coefficients matrix is obtained to analyse the control structure of the metabolic pathway in question.

SCAMP can handle reaction schemes of any complexity, including conserved cycles. It is capable of steady state analysis and time-dependent analysis (time-dependent movement between states). The required inputs are rate equations, K_m and v_{max} values and initial concentrations.

CONTROL is able to calculate control coefficients from elasticity coefficients of any metabolic pathway. However, it does not calculate steady states. The program is based on a method developed by Reder [Reder 1988].

The computer program made by Schulz derives control coefficients for linear and branched metabolic pathways. The skeleton of the pathway, the number of metabolites involved and the effect of each metabolite on each enzyme of the system (the elasticity coefficient) form the inputs of the program. The appropriate equations are expressed in matrix form. The program accommodates unlimited feedforward and feedback loops and a maximum of two branches from each metabolite on the main pathway.

GEPASI calculates steady states and trajectories of metabolite concentrations for any system consisting of maximal 45 metabolite and 45 reactions. With a steady state, elasticity and control coefficients can be calculated. Inputs are the reaction scheme and type of enzyme kinetics with rate constants.

2.1.2 COMPUTER PROGRAMS BASED ON BIOCHEMICAL SYSTEMS THEORY

Biochemical Systems Theory (BST) is based on the fact that biochemical systems are highly non-linear. The starting point of BST is the rate law, from which the following expression is derived:

$$\dot{[X_i]} = \alpha_i \prod_{j=1}^n [X_j]^{g_{ij}} - \beta_i \prod_{j=1}^n [X_j]^{h_{ij}} \quad (2-1)$$

with $[X_i]$ = concentration of metabolite X_i ;
 α_i, β_i = rate constants;
 g_{ij}, h_{ij} = kinetic order of the reaction.

The first term of equation (2-1) represents the net synthesis of X_i and the second term takes the degradation of X_i into account.

There is one computer program available for BST, named ESSYNS (Evaluation and Simulation of SYnergistic Systems). It calculates dynamic solutions for complex systems containing up to 25 simultaneous non-linear ordinary differential equations. No further information was available on this program.

2.1.3 OTHER COMPUTER PROGRAMS

So far, one simulation program has been found which is not directly related to either MCA or BST. This simulation program [Regan *et al.* 1993] offers a visual programming environment for the flux analysis of metabolic pathways.

The simulation program contains several icons representing different kind of chemical reactions. To form a pathway the necessary icons, with stoichiometries, need to be connected with each other. To be able to calculate the pathway fluxes, comprehensive measurements of substrates, biomass and of individual excreted metabolites have to be made as they serve as inputs to the program as well.

2.2 DISCUSSION AND CONCLUSIONS

The computer programs based on MCA and BST almost all require as inputs at least rate constants, often completed with enzyme kinetics such as K_m and v_{max} values. Exceptions are CONTROL and the program made by Schulz, because they use elasticity coefficients of MCA as inputs. The program made by Regan *et al.* is the only one for which no measurements of rate constants, K_m or v_{max} are needed. This program, however, needs measurements of substrates, biomass and of individual excreted metabolites. It's main goal is to calculate pathway fluxes whereas the main purpose of the other programs is to reveal the control sites of a pathway through calculation of specific MCA features.

All programs, except the one of Regan *et al.*, are based on a chemical approach of the biochemical system, for which enzyme kinetics and rate constants need to be known. Neither of the programs described above is able to handle steady states and dynamic behaviour and at the same time calculate fluxes and concentrations. For these reasons, none of the above mentioned programs will be used.

3

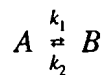
PRINCIPAL ASPECTS OF THE SIMULATION MODEL

3.1 INTRODUCTION

A simulation model of the TCA cycle and glyoxylate bypass can be based on either a chemical or a physical description of the processes involved. Whether the physical description is valid depends on the time constant of the chemical reactions with respect to the time constant of the real process. In the first paragraph the chemical and physical description will be discussed and one of them is taken as a basis for the simulation model. In the following sections the hypotheses are stated and a description of the building blocks of the simulation model are given. Finally a simulation model of a simplified version of the TCA cycle is made to test the building blocks and to investigate whether the simulation model satisfies the hypotheses.

3.2 A CHEMICAL OR A PHYSICAL APPROACH ?

The concentrations of the metabolites in the reactions of the TCA cycle and the rate constants can be written as a set of coupled differential equations. For example, assume the reversible reaction of metabolite A and B:



with k_1 = rate constant of the conversion of A into B;
 k_2 = rate constant of the conversion of B into A.

This reaction scheme can be written as two differential equations in the following way:

$$\frac{d[A]}{dt} = -k_1[A] + k_2[B] \quad (3-1A)$$

$$\frac{d[B]}{dt} = k_1[A] - k_2[B] \quad (3-1B)$$

with $[A]$ = concentration of metabolite A ($\text{mol}\cdot\text{dm}^{-3}$);
 $[B]$ = concentration of metabolite B ($\text{mol}\cdot\text{dm}^{-3}$);
 k_1, k_2 in s^{-1} .

In the chemical description it is assumed that equations (3-1A) and (3-1B) determine the kinetics of the system, and therefore the rate constants k_1 and k_2 must be known. When this chemical description is used to make a simulation model of the TCA cycle and glyoxylate bypass a practical problem arises: not all rate constants of the TCA cycle and glyoxylate bypass of *Saccharomyces cerevisiae* are known to date.

The TCA cycle and glyoxylate bypass can also be seen from a physical point of view. In this case it is assumed that all chemical reactions occur instantaneously. The dynamics of the system are determined by processes such as inhibitions, the supply or removal of products, or the diffusion of metabolites between the different organelles of the cell or between the cell and the environment.

The amount of a metabolite A that is present in a cell, Q (unit mol), is defined as follows:

$$Q(t) = [A(t)] \cdot V(t) \quad (3-2)$$

with $[A]$ = concentration of metabolite A ($\text{mol}\cdot\text{dm}^{-3}$);
 V = volume (dm^3).

The volume in this equation is the volume of one yeast cell. The change in the amount Q of metabolite A depends on how much of A is made per unit time (referred to as flux in (f_i , unit $\text{mol}\cdot\text{s}^{-1}$)) and how much disappears per unit time (referred to as flux out (f_o , unit $\text{mol}\cdot\text{s}^{-1}$)):

$$\frac{dQ(t)}{dt} = f_i(t) - f_o(t) \quad (3-3)$$

When equations (3-2) and (3-3) are combined, the following expression results:

$$\frac{d[A(t)]}{dt} = \frac{f_i(t) - f_o(t)}{V(t)} \quad (3-4)$$

For the solution of equation (3-4) the cell volume, $f_i(t)$ and $f_o(t)$ need to be known.

As stated before, whether the physical description can be used instead of the chemical description depends on the time constant of the chemical reactions involved with respect to the time constant of the real process. Only when the chemical time constant is smaller than the time

constant of the experiments, it is valid to use the physical description instead of the chemical description. The time constant of the chemical processes is determined by the smallest rate constant of the TCA cycle and glyoxylate bypass. It is difficult to determine this value since not all rate constants are known. The time constant of the real process is of the order of magnitude of 40 minutes, the period of oscillation. The fact that not all rate constants are known and it would take a lot of time to determine them is the main reason to choose for the physical approach at this moment. Note that the chemical description approaches the physical description for high values of the rate constants k_i .

3.3 HYPOTHESES

The simulation model of the TCA cycle and glyoxylate bypass is based on several hypotheses. The first six hypotheses are related to biochemistry, whereas hypotheses 7, 8 and 9 are made to facilitate the simulation model.

- H1. The yeast cell is assumed to have a constant volume, containing a constant amount of liquid.
- H2. The concentrations of all metabolites are homogeneously distributed over the cell volume.
- H3. The bioreactor, containing the continuous culture of yeast cells, is a continuous stirred bioreactor. This means that chemical substances which are in the reactor or added to the bioreactor, as well as the yeast cells, are homogeneously distributed over the bioreactor.
- H4. All cells are assumed to be synchronised. This means they all respond at the same time with the same reaction towards a disturbance of any kind¹.
- H5. There is no other carbon source available for the TCA cycle than ethanol.
- H6. Only the carbon balance is taken into account.
- H7. The concentration of a metabolite has a maximum value. This maximum value, however, has no physiological meaning.
- H8. The flux from one metabolite to the next depends on the concentration of the first metabolite².
- H9. When all concentrations are at the maximum level, the amount of metabolite made per unit of time should be the same as the amount that disappears per unit of time. In this case a change in the ethanol flux causes all fluxes to change accordingly. In other words, the speed or conversion rate at which the TCA cycle turns can be changed.

Furthermore the following should be considered.

1. In the reaction 'A + B → C' as much of metabolite C is made as the minimum available amount of metabolite A and metabolite B. When the concentrations of either metabolite A or B reach zero no metabolite C is made.
2. To avoid estimating the maximum concentration of each metabolite, these variables are normalised. The maximum value is chosen one.

¹ Not the life cycle of the yeast cells is synchronised but the metabolic breakdown of ethanol is synchronised.

² In §3.5.3 this hypotheses will be rewritten as: "The *maximum possible* flux from one metabolite to the next depends on the concentration of the first metabolite".

3.4 TCA CYCLE AND GLYOXYLATE BYPASS

A closer look at the TCA cycle and glyoxylate bypass in figure 1.1 in chapter 1 shows that there are certain metabolites which have a biological meaning but can be omitted from a simulation model. These metabolites, cis-aconitate, succinyl-CoA and fumarate, form intermediate steps in which the number of carbon atoms is constant. Furthermore, they are assumed to have no feedforward or feedback on any of the reactions occurring in the TCA cycle. They would only cause a delay in the chemical approach, but this is not relevant in the physical approach this simulation model is based on. Therefore they can easily be excluded from the simulation model. Since only carbon fluxes are taken into account, NADH and FADH₂ are omitted too. Figure 3.1 shows the TCA cycle, glyoxylate bypass and drains on which the simulation model is based.

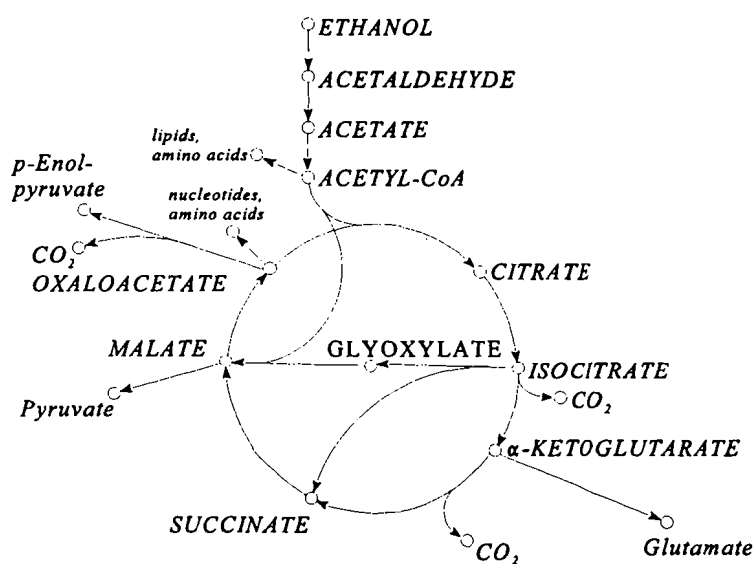


Figure 3.1. *The metabolites of the TCA cycle, glyoxylate bypass and drains which are incorporated in the simulation model. The metabolites of the TCA cycle and glyoxylate bypass are shown in capitals and the metabolites of the drains in small letters.*

3.5 BUILDING BLOCKS OF THE SIMULATION MODEL

The simulation model is composed of three different building blocks. These three blocks are a concentration block, a flux block and a reaction block. The blocks will be discussed in detail in the following three sections. The inputs and outputs of each block can be divided into two groups. The first group consists of flux signals, represented as flux lines. Over these lines an amount of molecules is transported each unit of time. The second group exists of information signals, referred to as information lines. As the name reveals, they transport information about the status of the parameter.

3.5.1 CONCENTRATION BLOCK

In the simulation model the concentration of each metabolite can be seen as the content of a vessel of volume V with a minimum and a maximum level. This content (unit $\text{mol}\cdot\text{dm}^{-3}$) exists of molecules of the metabolite in question. The concentration of a metabolite depends on the amount of flux (unit $\text{mol}\cdot\text{s}^{-1}$) flowing into the vessel, f_i , and the amount of flux flowing out of the vessel, f_o ¹. The vessel is mathematically represented as a limited integrator with an upper and a lower bound, with the upper bound equal to the maximum concentration level and the lower bound equal to zero.

The concentration block of metabolite A, like all metabolites, is implemented in Simulink as a S-function. It contains the following expressions:

```

if { [A(t)] ≤ 0 and (fi(t) - fo(t)) < 0 } or { [A(t)] ≥ [A]max and (fi(t) - fo(t)) > 0 }
  d[A(t)]/dt = 0
else d[A(t)]/dt = fi(t) - fo(t)
end

```

with $[A]_{\text{max}}$ = maximum concentration of metabolite A.

A figure together with a complete listing of the concentration block is given in appendix B.

3.5.2 FLUX BLOCK

As stated before in hypothesis H8, the flux from one metabolite to the next depends on the concentration of the first. The flux f_o of metabolite A is linked to f_i and the concentration of A in the following way. If f_i is zero and the concentration of metabolite A is zero, f_o should be zero. When the concentration of A is between zero and maximum level, f_o should also be between zero and the maximum level. If f_i is greater than zero and the concentration of metabolite A is at the maximum level, f_o should be equal to f_i . These situations are summarized in the following expressions:

$$\left. \begin{array}{l} f_i = 0 \\ [A] = 0 \end{array} \right\} f_o = 0 \quad (3-5A)$$

$$0 < [A] < [A]_{\text{max}} \rightarrow 0 < f_o < \max f_o \quad (3-5B)$$

$$\left. \begin{array}{l} f_i > 0 \\ [A] = [A]_{\text{max}} \end{array} \right\} f_o = f_i \quad (3-5C)$$

¹All fluxes in the simulation model have the unit of $\text{mol}\cdot\text{s}^{-1}$ instead of $\text{C}\cdot\text{mol}\cdot\text{s}^{-1}$ (if metabolite A has 5 C-atoms then 1 mol of A is equal to 5 C-mol of A). Although the option to write fluxes in $\text{C}\cdot\text{mol}\cdot\text{s}^{-1}$ is often used in biochemistry, it is not chosen for this simulation model. Writing fluxes in units of $\text{C}\cdot\text{mol}\cdot\text{s}^{-1}$ makes it more difficult to compare the fluxes; one has to know the number of C-atoms of every metabolite to be able to compare the fluxes quantitatively.

The first two expressions and the facts that f_o depends on the concentration and that all concentrations have a maximum level of one, lead to the following equation for f_o :

$$f_{o,\max}^A(t) = \frac{[A](t)}{[A]_{\max}} \quad (3-6)$$

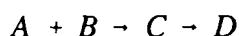
In equation (3-6) f_o is replaced by $f_{o,\max}^1$, because equation (3-6) determines the maximum amount of metabolite A that can take part in a reaction. That is, $f_{o,\max}$ depends on the fact whether another metabolite takes part in the reaction and how much of this metabolite is available, how much is used of metabolite A. Therefore, equation (3-6) sets the upper limit for the amount of metabolite A that can be used in a reaction. Because of equation (3-6) hypothesis H8 has to be rewritten as: "The maximum possible flux from one metabolite to the next depends on the concentration of the first metabolite".

With equation (3-6) $f_{o,\max}$ is normalised between zero and one. The flux block is also implemented in Simulink as a S-function and a figure together with the listing is given in appendix B.

3.5.3 REACTION BLOCK

The stoichiometry of every reaction occurring in the TCA cycle and glyoxylate bypass is embedded in a so-called reaction block. First, the principals of the reaction block will be explained. Next, judging from these principals, the inputs and outputs of the block will be determined.

The reaction block 'A + B → C' determines how many molecules of metabolite A and metabolite B have to be put together to make metabolite C. Assume the following pathway in which metabolite A and B react into metabolite C and C is subsequently converted into metabolite D.



As much C is made as the minimum available amount of A and B. When there is enough A and B available to make C, it has to be checked whether the concentration of C is at the maximum level. If the concentration of C is not at the maximum level, A and B can be converted into C. If the concentration of C is at the maximum level, the amount of C being made depends on the amount of C being converted into D, because in this case f_i^C has to be less or equal to f_o^C . It may occur that enough A and B is available to make C, but C is not converted into D and therefore no C is made from A and B. Table 3.1 gives a summary of these situations.

¹ 'Max f_o ' used in expression (3-5B) and ' $f_{o,\max}$ ' used in equation (3-6) are not synonymous. The term 'max f_o ' refers to the maximum level f_o can reach. This maximum level of f_o depends on $[A]_{\max}$ in this case. On the other hand, ' $f_{o,\max}$ ' is the maximum possible f_o of a metabolite vessel and depends on the concentration of this metabolite instead of on the maximum concentration.

Table 3.1. *The working of reaction block 'A + B → C' as a part of the pathway 'A + B → C → D'.*

available amount of A (mol·s ⁻¹)	available amount of B (mol·s ⁻¹)	[C] (mol·dm ⁻³)	amount of C converted into D (mol·s ⁻¹)	amount of C made from A and B (mol·s ⁻¹)
0.1	0.3	<[C] _{max}	don't care	0.1
0.2	0.1	<[C] _{max}	don't care	0.1
0.75	0.75	= [C] _{max}	0.5	0.5

The first four columns of table 3.1 are inputs of the reaction block. The last column is an output. The remaining inputs and outputs of the reaction block are defined next.

Metabolite A and B first offer their maximum available amount of f_o , referred to as $f_{o,max}^A$ and $f_{o,max}^B$, to the reaction block. The reaction block determines how much of A and B is actually needed and a signal with this information, referred to as f_o^A and f_o^B , is returned to metabolite A and B. Then the exact amount of A and B that will convert into C is send to the reaction block. As a result f_o^A and f_o^B are added to the reaction block, both as input and output.

Table 3.2 contains the inputs and outputs of reaction block 'A + B → C' and displays whether it is an information or a flux line.

Table 3.2. *Inputs and outputs of reaction block 'A + B → C'.*

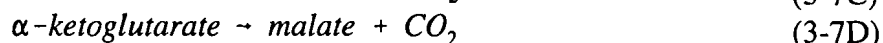
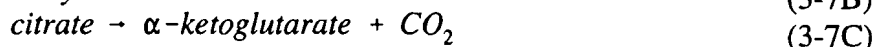
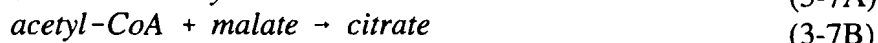
$f_{o,max}^A$	input	information line
$f_{o,max}^B$	input	information line
[C]	input	information line
f_o^C	input	information line
f_o^A	input	flux line
	output	information line
f_o^B	input	flux line
	output	information line
f_i^C	output	flux line

In general, each metabolite taking part in the reaction has two inputs and one output within the reaction block. A figure of the reaction block together with the listing is given in appendix B.

The flux block and concentration block together have to provide the inputs for the reaction block, whereas the reaction block has to provide the inputs for the concentration block and flux block.

3.6 SIMULATION MODEL OF A SIMPLIFIED VERSION OF THE TCA CYCLE

In order to study the behaviour of the building blocks described in §3.5, first a simplified version of the TCA cycle is considered. In this simplified version, shown in figure 3.2, the following reactions are taken into account:



This model contains no drains and the glyoxylate bypass is omitted.

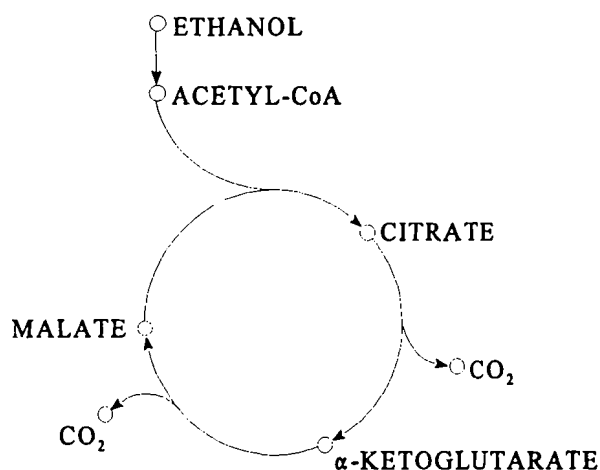


Figure 3.2. *Simplified version of the TCA cycle.*

For every metabolite of the simplified TCA cycle a concentration block and a flux block are made and put together in a metabolite block. For example, the concentration and flux block of acetyl-CoA are embedded in the metabolite block named "ACO". Each reaction has its own reaction block. For example, the reaction block 'ACO+MAL-CIT' performs the reaction 'acetyl-CoA + malate → citrate' (equation (3-7B)). Figure 3.3 shows a block diagram of the simulation model of the simplified version of the TCA cycle. Note that the amount of CO₂ being made is equal to the amount of α-ketoglutarate respectively malate that is made, since the simulation model is on a mole base instead of on a C-mole base. With this simulation model a number of simulations have been done of which two will be discussed.

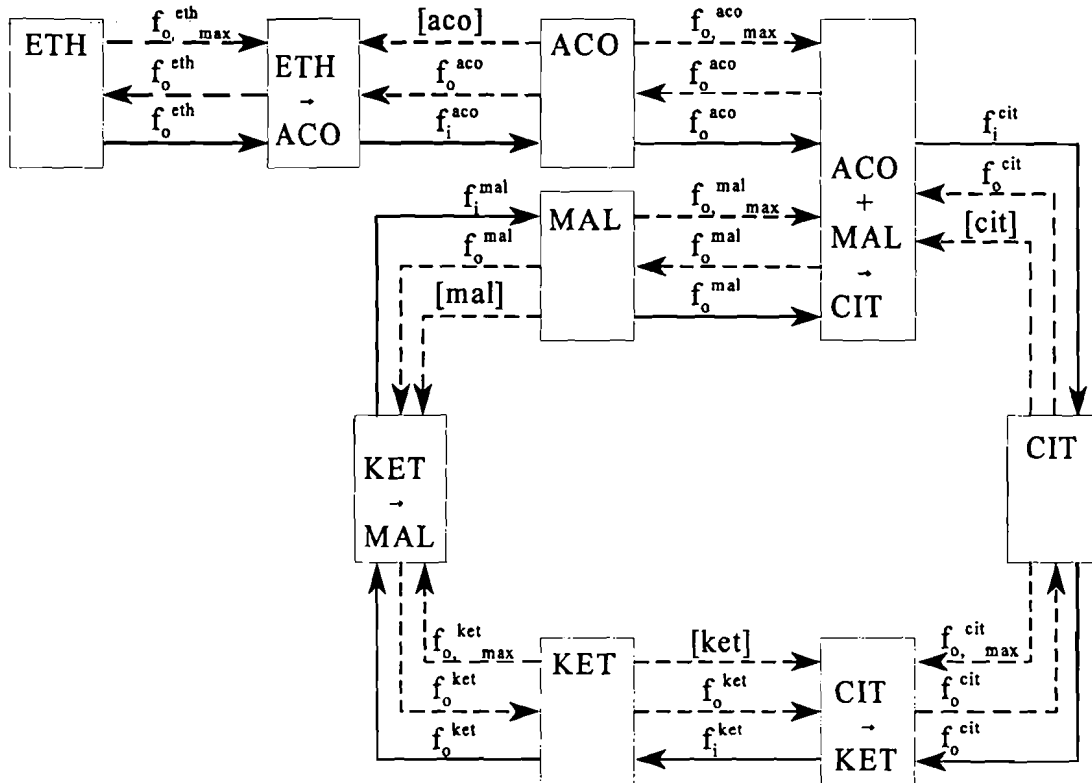


Figure 3.3. Block diagram of the simulation model of the simplified version of the TCA cycle.

$f_o^{X,max}$ = maximum possible f_o of metabolite X;

f_o^X = f_o of metabolite X;

f_i^X = f_i of metabolite X;

— = flux line;

--- = information line;

[X] = concentration of metabolite X.

The concentration block and the flux block of every metabolite are embedded in a metabolite block, indicated by 3 letters:

ETH = ethanol;

ACO = acetyl-CoA;

CIT = citrate;

KET = α -ketoglutarate;

MAL = malate.

Simulation 1 shows the correct working of the reaction block named “ACO + MAL → CIT”. The initial concentration of acetyl-CoA is chosen zero, while the other concentrations are chosen arbitrary. The ethanol input is zero for $0s < t < 7s$, from $t=7s$ until $t=17s$ it increases to one and at $t=17s$ it decreases again and reaches zero at $t=27s$. The total simulation time is 30s. What is to be expected is that at the moment the acetyl-CoA concentration reaches zero, no citrate is made regardless the concentration of malate. Also, when both acetyl-CoA and malate are available, as much citrate is made as the minimum available amount of acetyl-CoA and malate. The results are shown in figure 3.4. Both expectations are met in simulation 1. Between $t=4s$ and $t=7s$ there

is no acetyl-CoA available and therefore no citrate is made. From $t=13\text{s}$ until $t=22\text{s}$ enough acetyl-CoA is available but malate is the limiting factor. So in this case malate determines the amount of citrate being made.

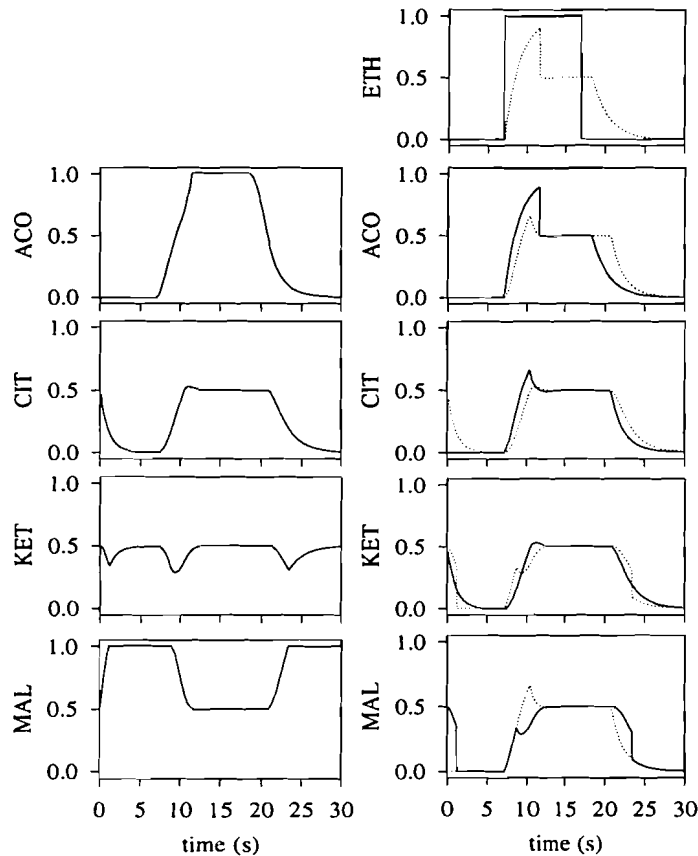


Figure 3.4. Results of simulation 1.

Graphs in left column, solid line: concentration of each metabolite ($\text{mol} \cdot \text{dm}_{\text{cell}}^{-3}$).
Graphs in right column, solid line: f_i of every metabolite; dotted line: f_o of every metabolite ($\text{mol} \cdot \text{s}^{-1} \cdot \text{dm}_{\text{cell}}^{-3}$).

Simulation 2 shows that when all concentrations have reached the maximum level and the ethanol input is changed, the conversion rate of the TCA cycle is changed. This means all fluxes change according to the changes of the ethanol flux. To make the concentrations increase to the maximum level an extra source of either citrate, α -ketoglutarate or malate should be available. This is a result of the fact that there are no drains and there is no other source available for the TCA cycle than ethanol, causing the summation of the concentrations of citrate, α -ketoglutarate and malate to be constant throughout a simulation¹. The ethanol input is 0.5 from $t=0\text{s}$ until $t=11\text{s}$. From $t=11\text{s}$ until $t=18\text{s}$ it increases to one and remains at this level until $t=24\text{s}$. From $t=24\text{s}$

¹ This can be explained as follows. Since there are no drains in this simplified version of the TCA cycle, ethanol ($\text{C}_2\text{H}_6\text{O}$) is used to cover the losses caused by 2CO_2 in the cycle (see figure 3.2). Since the TCA cycle is cyclical, preventing malate to accumulate, this leads to the summation of the concentrations of citrate, α -ketoglutarate and malate being constant throughout a simulation.

it decreases to 0.5. Between $t=16s$ and $t=23s$ an extra citrate source is available. The initial concentrations are the same as in simulation 1 and the total simulation time is 35s. The results are depicted in figure 3.5. The results show indeed that when all concentrations are at the maximum level a change of the ethanol output is followed by the same change in the other fluxes.

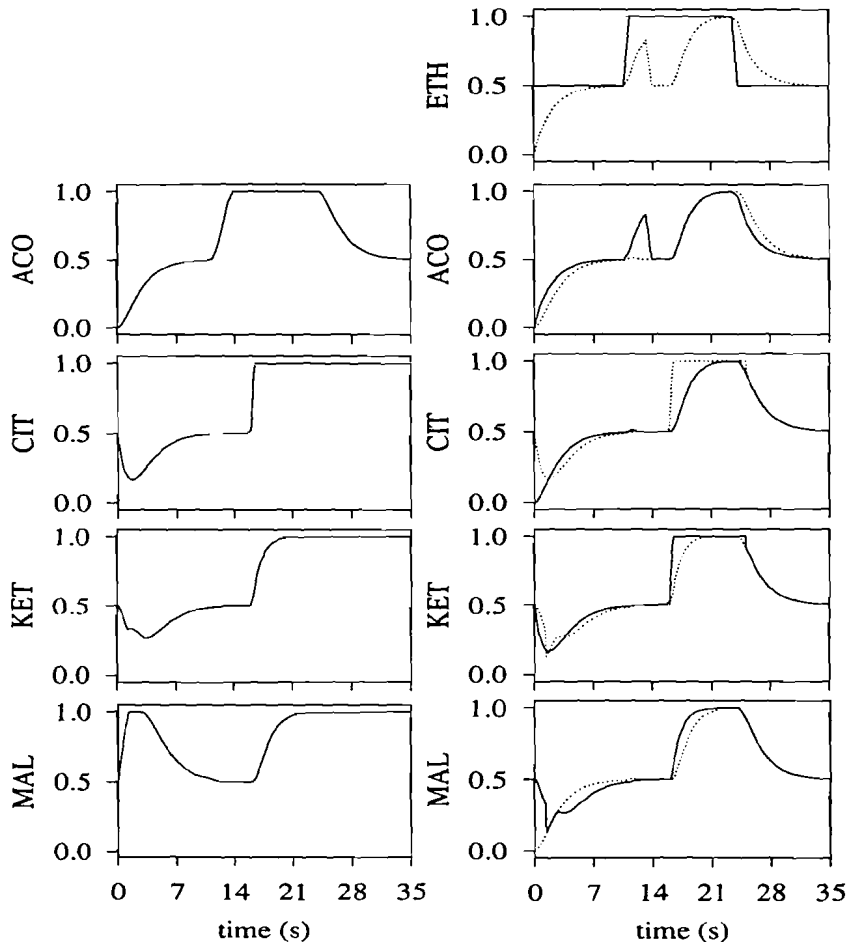


Figure 3.5. Results of simulation 2.

Graphs in left column, solid line: concentration of each metabolite ($\text{mol} \cdot \text{dm}_{\text{cell}}^{-3}$).
 Graphs in right column, solid line: f_i of every metabolite; dotted line: f_o of every metabolite ($\text{mol} \cdot \text{s}^{-1} \cdot \text{dm}_{\text{cell}}^{-3}$).

3.7 CONCLUSIONS

In this chapter the building blocks of the simulation model are described and tested. The most important requirements for the simulation model are that it can represent a cyclical pathway, that f_o is equal to f_i when all concentrations reach the maximum level and that it can represent chemical reactions like one mole of metabolite A and one mole of metabolite B convert into one mole of metabolite C. Simulations done with a simulation model of a simplified version of the TCA cycle show that it satisfies all the above mentioned requirements.

4

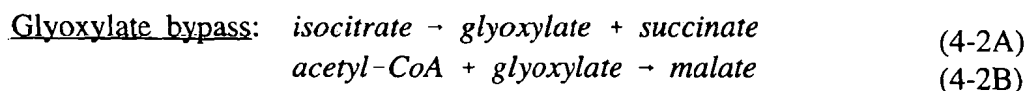
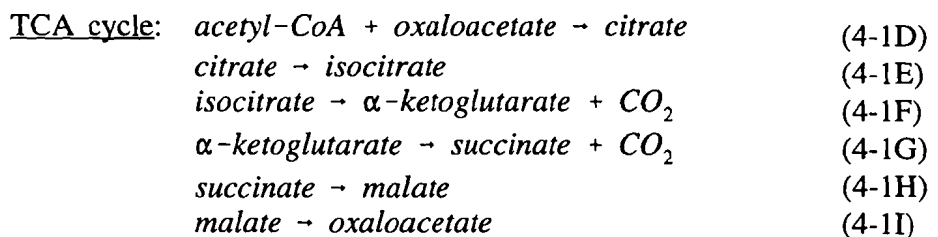
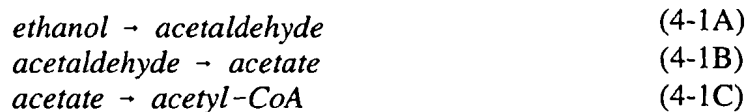
SIMULATION MODEL OF THE TCA CYCLE AND GLYOXYLATE BYPASS

4.1 INTRODUCTION

The simulation model which was described in chapter 3, will be extended with the glyoxylate bypass, drains and several metabolites and reactions. With this extended simulation model a number of simulations will be done. From these simulations several problems arise, which will be dealt with in this chapter.

4.2 EXTENSION OF THE SIMULATION MODEL

The metabolites of the TCA cycle and glyoxylate bypass which will be incorporated into the extended simulation model (from now on referred to as 'simulation model') are shown in figure 3.1 in §3.4. The following reactions take place in this simulation model.



<u>Drains:</u> acetyl-CoA → lipids + amino acids	(4-3A)
α-ketoglutarate → glutamate	(4-3B)
malate → pyruvate	(4-3C)
oxaloacetate → p-enol-pyruvate	(4-3D)
oxaloacetate → nucleotides + amino acids.	(4-3D)

The extension of the simulation model consists of three parts:

- Adding the metabolites isocitrate, succinate, oxaloacetate, acetaldehyde and acetate¹.
- Adding the glyoxylate bypass (4-2A and 4-2B). This means that isocitrate can be converted not only into α-ketoglutarate, as a part of the TCA cycle, but also into glyoxylate and succinate as a part of the glyoxylate bypass. Acetyl-CoA can react with glyoxylate to make malate as a part of the glyoxylate bypass, or react with oxaloacetate to form citrate in the TCA cycle.
- Adding drains; the glutamate drain from α-ketoglutarate (4-3B), the pyruvate drain from malate (4-3C), the p-enol-pyruvate and nucleotides and amino acids drains from oxaloacetate (4-3D and 4-3E) and the lipids and amino acids drain from acetyl-CoA (4-3A).

Although every reaction in the TCA cycle and glyoxylate bypass has its own enzyme to control the reaction, only seven of them are taken into account in this simulation model. Enzymes which are incorporated into the simulation model have a simple function; they are used as a switch to put the reaction they catalyse on or off. The enzymes of reaction (4-1A) until (4-1I) are omitted, because there is no need to switch these reactions on or off. The reactions of the glyoxylate bypass ((4-2A) and (4-2B)) and the reactions which form products of the TCA cycle ((4-3A) until (4-3E)) are assumed to be enzyme catalysed reactions, which can be turned on or off by their enzymes. These enzyme catalysed reactions together with the enzymes are listed in table 4.1.

Table 4.1. Enzyme catalysed reactions with the corresponding enzymes.

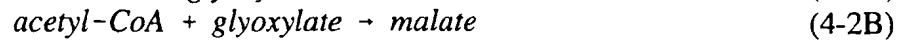
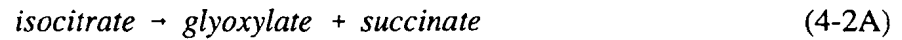
reaction	enzyme
isocitrate → glyoxylate + succinate	isocitrate lyase
acetyl-CoA + glyoxylate → malate	malate synthase
acetyl-CoA → lipids + amino acids	acetyl-CoA carboxylase
α-ketoglutarate → glutamate	glutamate dehydrogenase
malate → pyruvate	malate dehydrogenases
oxaloacetate → p-enol-pyruvate	phosphorpyruvate carboxylase
oxaloacetate → nucleotides + amino acids	aspartate transaminase

¹This is still not a complete model of the TCA cycle since not all metabolites of the TCA cycle are incorporated (see §3.4).

For the metabolites isocitrate, succinate, oxaloacetate, acetaldehyde and acetate a concentration and a flux block are made. These concentration and flux blocks are exactly the same as described in §3.5.1 and §3.5.2 respectively. For each metabolite the concentration block and flux block are put together in a metabolite block, named after the metabolite. The reaction blocks for the reactions (4-1A-I) and (4-2A,B) are also similar to the one described in §3.5.3.

4.2.1 GLYOXYLATE BYPASS

To implement the glyoxylate bypass in the TCA cycle one additional metabolite needs to be incorporated: glyoxylate. The concentration and flux block of glyoxylate are again exactly the same as the other concentration and flux blocks. To add the reactions of the glyoxylate bypass:



two reaction blocks need to be altered. The reaction block which represents the conversion of isocitrate into α -ketoglutarate is extended with reaction (4-2A). For this a so-called 'flux distribution' needs to be implemented. This flux distribution determines how much isocitrate is turned into α -ketoglutarate and how much isocitrate is used to form glyoxylate and succinate. First of all this flux distribution is influenced by the enzyme isocitrate lyase. In the simulation model described here, the effect of isocitrate lyase is kept simple; it is either abundant or not available at all. Only when this enzyme is present isocitrate can be converted into glyoxylate and succinate. Secondly, the concentration of both succinate and malate have a negative feedback on the conversion from isocitrate into glyoxylate and succinate. Up to now it is only known that these concentrations have a negative feedback, but it is not known how this feedback depends on the concentrations of both metabolites. Another condition for the flux distribution is that it has to be gradual.

From the functions which could serve as a flux distribution function, equation (4-4) is chosen. This function depends on two variables and shows a smooth change in the flux distribution when the concentration of malate and succinate change, as shown in figure 4.1.

$$a = \left(1 - \frac{[suc]}{[suc]_{\max}} \right) \cdot \left(1 - \frac{[mal]}{[mal]_{\max}} \right) \quad (4-4)$$

with $[suc]_{\max}$ = maximum concentration of succinate;

$[mal]_{\max}$ = maximum concentration of malate.

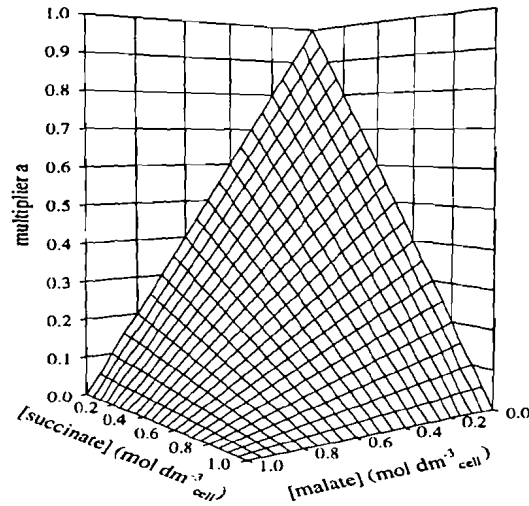


Figure 4.1. The flux distribution function; multiplier a as a function of the concentration of malate and succinate.

The factor 'a' in equation (4-4) is the fraction of $f_{o,\max}^{\text{iso}}$ which is available for the glyoxylate bypass. When both concentrations of malate and succinate are zero, isocitrate is converted completely into glyoxylate and succinate. When the concentrations of malate and succinate are at the maximum level, isocitrate is completely converted into α -ketoglutarate. Between these two bounds there is a gradual transition. The flux distribution from isocitrate is summarized in table 4.2. The last column indicates the state of the glyoxylate bypass.

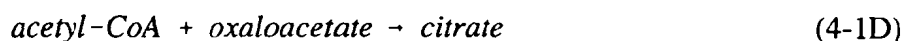
Table 4.2. Summary of the flux distribution from isocitrate.

$f_i^{\text{gly}} = f_i$ of glyoxylate; $f_o^{\text{gly}} = f_o$ of glyoxylate.

[gly]	[suc]	[mal]	[isocitrate lyase]	glyoxylate bypass
don't care	$=[\text{suc}]_{\max}$	don't care	don't care	off
don't care	don't care	$=[\text{mal}]_{\max}$	don't care	off
don't care	don't care	don't care	0	off
$<[\text{gly}]_{\max}$	$<[\text{suc}]_{\max}$	$<[\text{mal}]_{\max}$	1	on
$=[\text{gly}]_{\max}$	$<[\text{suc}]_{\max}$	$<[\text{mal}]_{\max}$	1	on and $f_i^{\text{gly}} \leq f_o^{\text{gly}}$

The last row of table 4.2 shows the situation in which the glyoxylate concentration is at the maximum level. In this case the amount of glyoxylate made per second (f_i^{gly}) has to be equal to or smaller than the amount of glyoxylate that disappears per second (f_o^{gly}).

The reaction block which contains the formation of citrate out of acetyl-CoA and oxaloacetate is extended with reaction (4-2B):



In this block there is a flux distribution from acetyl-CoA to either citrate or malate. The enzyme malate synthase which is necessary for the conversion of acetyl-CoA and glyoxylate into malate is assumed to be available or not, like the enzyme citrate lyase. Because no feedback works on either reactions (4-1D) and (4-2B), the flux distribution of acetyl-CoA can be chosen rather arbitrary. Taking into account the purpose of the glyoxylate bypass as a method for the cell to compensate for losses caused by drains, it might be a good choice to give priority to the conversion of acetyl-CoA and glyoxylate into malate. In this way malate is produced, not only from succinate but also from acetyl-CoA and glyoxylate, which results in more oxaloacetate. If the conversion of acetyl-CoA and oxaloacetate into citrate would have priority, the concentration of oxaloacetate would drop rather fast when sufficient acetyl-CoA is available (simulation data not shown). It would stay low, because as soon as it is available, it reacts with acetyl-CoA into citrate. This causes acetyl-CoA to accumulate. In this way there is no balance between the concentration of acetyl-CoA and oxaloacetate. Therefore, the flux distribution in this part of the glyoxylate bypass is chosen to favour the formation of malate out of acetyl-CoA and glyoxylate instead of the conversion of acetyl-CoA and oxaloacetate into citrate.

4.2.2 DRAINS

The drains which have to be added to the simulation model are:

- a. lipids and amino acids drain from acetyl-CoA (4-3A);
- b. glutamate drain based on the reaction: α -ketoglutarate \rightarrow glutamate (4-3B);
- c. pyruvate drain, based on the reaction: malate \rightarrow pyruvate (4-3C);
- d. p-enol-pyruvate drain, based on the reaction: oxaloacetate \rightarrow p-enol-pyruvate (4-3D);
- e. nucleotides and amino acids drain from oxaloacetate (4-3E).

The concentration of glutamate, pyruvate and p-enol-pyruvate are incorporated in concentration blocks. Reaction (4-3B) is implemented in the reaction block which contains the conversion of α -ketoglutarate into succinate. Reaction (4-3C) is added to the reaction block which represents the formation of malate into oxaloacetate. Reactions (4-3D), (4-3E) and (4-3A) are implemented in the reaction block which contains the second part of the glyoxylate bypass (reactions (4-2B) and (4-1D)). The magnitude of all drains is a fixed percentage of the maximum available flux. These fixed percentages are based on the fluxes as calculated by Cortassa *et al.* [Cortassa *et al.* 1995], see table 4.3. A block diagram of the simulation model and the listing of the reaction block which contains the reactions (4-1D), (4-2B), (4-3A), (4-3D) and (4-3E) are given in appendix C.

Table 4.3. *Magnitudes of the drains according to Cortassa et al. as a percentage of the ethanol flux input.*

drain	attached to	f_i^{drain} (% of f_i^{eth})
amino acids, lipids	acetyl-CoA	8.8
glutamate	α -ketoglutarate	4.4
pyruvate	malate	7.7
p-enol-pyruvate	oxaloacetate	26.9
nucleotides, amino acids	oxaloacetate	4.4

4.3 SIMULATIONS

To test the simulation model a number of simulations have been done, of which 8 will be discussed. From the simulations it is expected that:

- a. the drains decrease the concentrations of the metabolites of the TCA cycle (simulation 1 and 2);
- b. the glyoxylate bypass can cover up the losses caused by the drains (simulation 2 and 3);
- c. the simulation model reaches a steady state after a while (simulation 3);
- d. the steady state depends only on the ethanol input (simulation 3, 4, 5 and 6);
- e. the flux distributions, from isocitrate and acetyl-CoA, do not cause a metabolite to accumulate unnecessary (simulation 6);
- f. the calculated concentrations and fluxes do not show unwanted values as a result of a deficiency in the computer program (simulation 6, 7 and 8).

Of each simulation the initial concentrations of the metabolites, the ethanol input, the status of the glyoxylate bypass and drains, the integration method and the simulation time are listed in table 4.4.

Table 4.4. Settings of the simulation parameters for simulation 1 to 8. $[X]_0$ = initial concentration of metabolite X ($\text{mol} \cdot \text{dm}^{-3}_{\text{cell}}$).

simulation	1	2	3	4	5	6	7	8
[ADH] ₀	0.9	0.9	0.9	0.2	0.6	0.6	0.6	0.6
[ACE] ₀	0.9	0.9	0.9	0.2	0.6	0.6	0.6	0.6
[ACO] ₀	0.9	0.9	0.9	0.2	0.6	0.6	0.6	0.6
[CIT] ₀	0.9	0.9	0.9	0.2	0.6	0.6	0.6	0.6
[ISO] ₀	0.9	0.9	0.9	0.2	0.6	0.6	0.6	0.6
[KET] ₀	0.9	0.9	0.9	0.2	0.6	0.6	0.6	0.6
[GLY] ₀	0.9	0.9	0.9	0.2	0.6	0.6	0.6	0.6
[SUC] ₀	0.9	0.9	0.9	0.2	0.6	0.6	0.6	0.6
[MAL] ₀	0.9	0.9	0.9	0.2	0.6	0.6	0.6	0.6
[OXA] ₀	0.9	0.9	0.9	0.2	0.6	0.6	0.6	0.6
ethanol input ($\text{mol} \cdot \text{s}^{-1}$)	0.3	0.3	0.3	0.3	0.3	0.25- 0.50- 0.75- 1.0	0.25- 0.50- 0.75- 1.0	0.25- 0.50- 0.75- 1.0
glyoxylate bypass	off	off	on	on	on	on	on	on
drains	off	on	on	on	on	on	on	on
integration method	linsim	linsim	linsim	linsim	linsim	linsim	gear	runge- kutta 5
simulation time (s)	30	100	50	30	30	200	200	200

The results of simulations 1-5, 7 and 8 are shown and discussed in appendix D, since these simulations show the expected results. The results of simulation 6 are shown in figure 4.2 because they reveal two deficiencies of the simulation model.

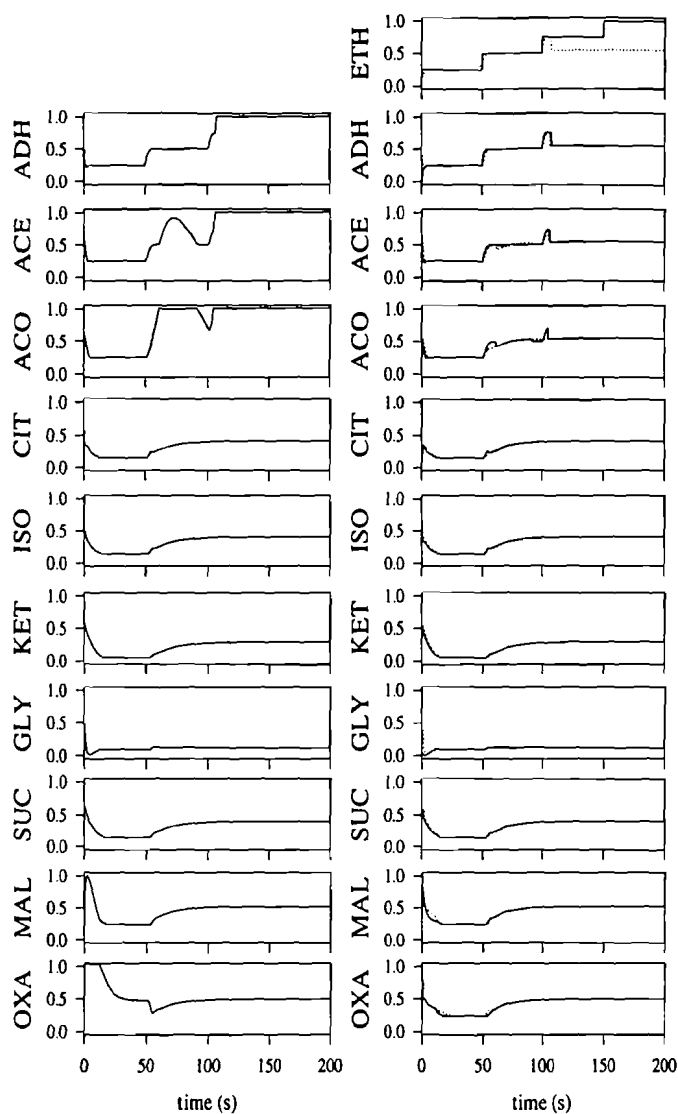


Figure 4.2. Results of simulation 6.

Graphs in left column, solid line: concentration of every metabolite ($\text{mol} \cdot \text{dm}_{\text{cell}}^{-3}$).
 Graphs in right column, solid line: f_i of every metabolite; dotted line: f_o of every metabolite ($\text{mol} \cdot \text{s}^{-1}$).

The results depicted in figure 4.2 show two deficiencies of the simulation model. The first one is that when the ethanol input gets above 0.5 (at $t = 100\text{s}$) the fluxes of the metabolites do not increase anymore. There is not enough oxaloacetate to react with acetyl-CoA into citrate, causing acetaldehyde, acetate and acetyl-CoA to accumulate. Apparently the glyoxylate bypass is pinched too much, resulting in a shortage of oxaloacetate. The second deficiency can be seen when the oxaloacetate concentration is examined. From $t=1\text{s}$ until $t=13\text{s}$ the oxaloacetate concentration is above the maximum level. This is a result of the if-then statement, which is used in every concentration block. Each timestep this if-then statement detects whether a concentration is equal or above a maximum level. When in one time step the concentration increases to the extent that it exceeds the maximum level, it is not set back to this maximum level. Instead, the concentration remains constant at too high a value until f_o becomes larger than f_i .

Summarizing the simulation results (see also appendix D), it can be concluded that:

- a. the glyoxylate bypass in the simulation model is able to cover up the losses caused by the drains in the TCA cycle (simulation 1, 2 and 3);
- b. the steady state values of a simulation depend only on the ethanol input and do not depend on the initial concentrations of the metabolites (simulations 3, 4 and 5);
- c. when the ethanol input reaches values above 0.5, the concentration of oxaloacetate becomes a limiting factor, preventing the fluxes of the metabolites to increase as much as the ethanol input does (simulation 6);
- d. concentrations can increase beyond the maximum level in consequence of the if-then statement used in the concentration block (simulation 6);
- e. although the increase of concentrations above the maximum level depends to a certain extent on the integration method used, each integration method shows this defect (simulation 6, 7 and 8).

Statement c, d and e will be dealt with in the following paragraph.

4.4 DEFICIENCIES OF THE SIMULATION MODEL

In the preceding paragraph, two problems of the simulation model were described which became clear during simulations. The first problem was an accumulation of acetyl-CoA because of a shortage of oxaloacetate. This happened when the ethanol input exceeded 0.5 and it was caused by the glyoxylate bypass, becoming pinched too much when the ethanol input exceeds 0.5. This problem will be dealt with in §4.4.2.

The second problem is a result of the use of an if-then statement in the determination of the maximum concentration of a metabolite. This allows the concentration to exceed the maximum level. This problem will be investigated in the following section and a possible solution will be given.

4.4.1 IF-THEN STATEMENT

To prevent the concentration from crossing the maximum level a state event could be used. This state event detects when the concentration equals one and adjusts the integration time step [Van den Bosch *et al.* 1994]. However, Simulink does not support state events, so another solution to the problem has to be found.

A possible solution could be the design of a special function. This function should take care that the concentration level gradually reaches the value of one, instead of exceeding it due to the discrete nature of the if-then statement.

The if-then statement in the concentration block of metabolite A is implemented as follows:

```

if { [A(t)] ≤ 0 and (fi(t) - fo(t)) < 0 } or { [A(t)] ≥ [A]max and (fi(t) - fo(t)) > 0 }      (4-5)
  d[A(t)]/dt = 0
else d[A(t)]/dt = fi(t) - fo(t)
end

```

The concentration of metabolite A, f_i^A and f_o^A are all limited to the area $[0,1]$. Other values are not valid. If f is defined as $f_i - f_o$, a so-called net flux, it contains the values $[-1,1]$. The concentration can be represented by a concentration vector $\underline{x}=[0,1]$ and the net flux by a flux vector $\underline{f}=[-1,1]$. Vector \underline{x} and \underline{f} span a surface S . With the vectors \underline{x} and \underline{f} , the if-then statement of equation (4-5) can be written in the following way:

$$d[A(t)]/dt = m_d(\underline{x},\underline{f}) \cdot (f_i(t) - f_o(t)) \quad (4-6)$$

In equation (4-6) $m_d(\underline{x},\underline{f})$ is a discrete function which provides a multiplier m_d for every coordinate of the surface S in the same way as the if-then statement would do. From equation (4-5) it can be derived that $m_d(\underline{x},\underline{f})$ should be zero for $\underline{x}=[0]$ and $\underline{f}=[-1,0]$ and for $\underline{x}=[1]$ and $\underline{f}=[0,1]$. For all other coordinates of surface S , $m_d(\underline{x},\underline{f})$ has a value of one. Figure 4.3 gives a graphical representation of $m_d(\underline{x},\underline{f})$.

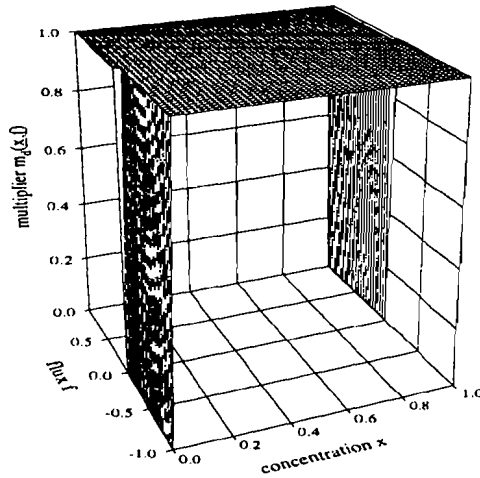


Figure 4.3. Values of multiplier $m_d(\underline{x},\underline{f})$ for every coordinate of surface S .

The discrete nature of the if-then statement and of $m_d(\underline{x},\underline{f})$ will result in the concentration crossing the maximum level. Therefore, function $m_d(\underline{x},\underline{f})$ is replaced by a continuous multiplier $m_c(\underline{x},\underline{f})$, which would lead the concentration gradually to the maximum level and thus preventing it from crossing this upper bound. A detailed derivation of multiplier $m_c(\underline{x},\underline{f})$ is given in appendix E, §E.1. A graphical representation of $m_c(\underline{x},\underline{f})$ is given in figure 4.4.

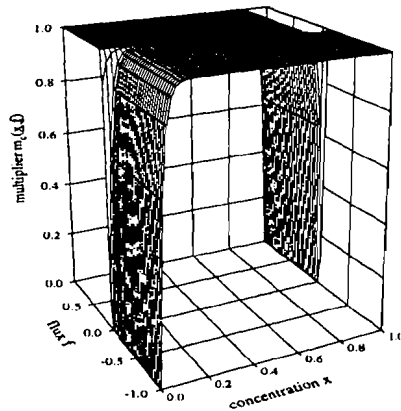


Figure 4.4. Values of multiplier $m_c(\underline{x},\underline{f})$ for every coordinate of surface S .

To decide whether multiplier $m_c(x,f)$ could replace the if-then statement, a comparison has been made on two issues. The first issue concerns the concentration level and the second one the required simulation time. A detailed description of this comparison is given in appendix E, §E.2. On both issues the if-then statement outperformed multiplier $m_c(x,f)$. Therefore, it can be concluded that the if-then can not be replaced by multiplier $m_c(x,f)$, with respect to the problem of the concentration exceeding the maximum value. There remains no other solution than to avoid the ethanol input to exceed 0.5 or to denormalise the concentration. Until the latter is done in §5.2, the ethanol input will be restricted to $[0,0.5]$.

4.4.2 FLUX DISTRIBUTION

The second problem which became clear during simulations was an accumulation of acetyl-CoA because of a shortage of oxaloacetate. This happened when the ethanol input exceeded the value 0.5. The concentration of oxaloacetate became a limiting factor, causing acetaldehyde, acetate and acetyl-CoA to accumulate. This situation was caused by the glyoxylate bypass, being pinched too much at that moment. When the ethanol input is increased, all concentrations increase too. Since malate and succinate have a negative feedback on the conversion of isocitrate into succinate and glyoxylate, the glyoxylate bypass is pinched more when the concentrations of malate and succinate increase. To increase the oxaloacetate concentration and eliminate the acetyl-CoA accumulation, the flux distribution of isocitrate should be changed in a way that the glyoxylate bypass becomes less pinched for the same concentration levels of malate and succinate.

Consider the flux distribution, which is implemented as follows:

$$a = \left(1 - \frac{[suc]}{[suc]_{max}} \right)^x \cdot \left(1 - \frac{[mal]}{[mal]_{max}} \right)^y \quad (4-7)$$

with $x, y = 1$;

$[suc]_{max}$ = maximum concentration of succinate;

$[mal]_{max}$ = maximum concentration of malate.

Exponent x and y are set to one for the simulations shown in §4.3. By varying these exponents, however, multiplier a can be changed. The exponents x and y should be altered in such a way that the difference between the concentration of acetyl-CoA and the concentration of oxaloacetate goes to a minimum.

To find this minimum and the corresponding exponents x and y the least square method (LSM) is used. The variables used in the LSM are the exponents x and y , and the difference between the oxaloacetate and acetyl-CoA concentration is the parameter which is minimised. The minimisation routine has been applied to different initial values of x and y (referred to as x_i and y_i) and different inputs of ethanol. The ethanol inputs which are used are depicted in figure 4.5.

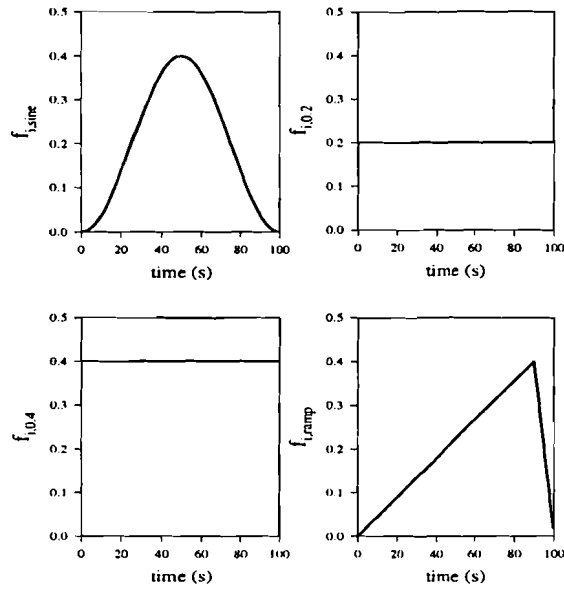


Figure 4.5. Ethanol inputs used in the LSM.

The following procedure has been applied:

- find an optimum setting for the LSM with fixed initial values x_i and y_i for one ethanol input;
- with this optimum setting and this ethanol input, but different values for x_i and y_i , check whether the same results are found for x and y ;
- with the optimum setting and different ethanol inputs, calculate the optimum values for x and y ;
- try to calculate a single optimum value for x and y for all ethanol inputs combined.

After the optimum setting was found with ethanol input $f_{i,sine}^{eth}$, different initial values for x and y were used. These values were chosen rather arbitrary, but it was checked with a simulation whether they were not way out of line. The results are listed in table 4.5. Some minimisations were interrupted, because the routine was stuck in a local minimum or the maximum number of iterations was exceeded.

Table 4.5. Minimisation results of ethanol input $f_{i,sine}^{eth}$.

* indicates that the minimisation has been interrupted.

minimisation	x_i	y_i	x	y	sum of squares
1	0.75	0.75	-5.5	4.19	0.206
2	2.25	2.25	1.15	0.46	0.263
3	2.25	-2.25	1.92	-2.00	13.12 *
4	-2.25	2.25	-5.5	4.19	0.206
5	-2.25	-2.25	-2.2505	-2.2497	2.19e17 *

Although the values for the exponents differ quite a lot, the values of the corresponding sum of squares (SSQ) of minimisation 1 and 2 differ only slightly. This indicates that there are more values for x and y which have as small a sum of squares as minimisation 2. To find this out the sum of squares for each coordinate of the surface spanned by $x=[-2.5,2.5]$ and $y=[-2.5,2.5]$ was calculated with steps of 0.02. In table 4.6 the values of x and y are listed for which the SSQ is equal to or smaller than the SSQ of minimisation 2.

Table 4.6. Sum of squares results with input $f_{i,sine}^{eth}$ of the surface spanned by $x=[-2.5,2.5]$ and $y=[-2.5,2.5]$ which are smaller than 0.263.

x	y	sum of squares	x	y	sum of squares
1.1	0.5	0.263	-1.9	2.1	0.248
0.7	0.7	0.262	-1.7	2.1	0.247
0.3	0.9	0.262	-2.3	2.3	0.249
-0.3	1.3	0.259	-2.1	2.3	0.241
-0.7	1.5	0.254	-2.5	2.5	0.236
-1.1	1.7	0.249	-2.3	2.5	0.260

The exponents x and y of table 4.5 with a sum of squares equal to or smaller than 0.263 and table 4.6 are shown in figure 4.6.

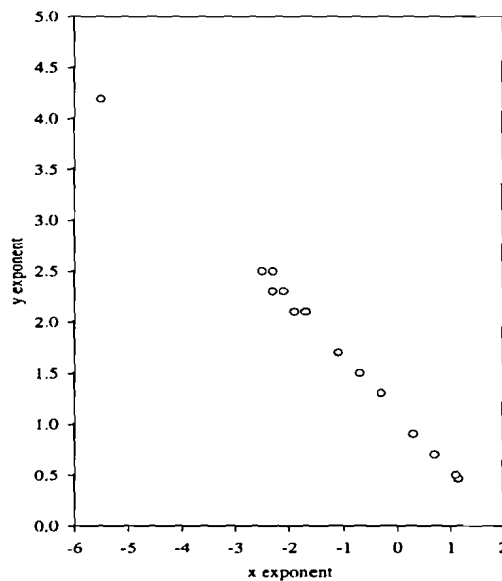


Figure 4.6. Exponents x and y with sum of squares equal to or smaller than 0.263 for the input $f_{i,sine}^{eth}$.

Figure 4.6 shows that all values of x and y , which have a SSQ equal to or smaller than 0.263, are lying on a single line. This implies that x and y can not be varied independently and, in consequence, all points on this line give a similar fit. In the same way as for the sinusoidal

input, x and y values were determined for the other three remaining inputs, showing a dependency of x and y too. These lines are depicted in figure 4.7 for all four inputs.

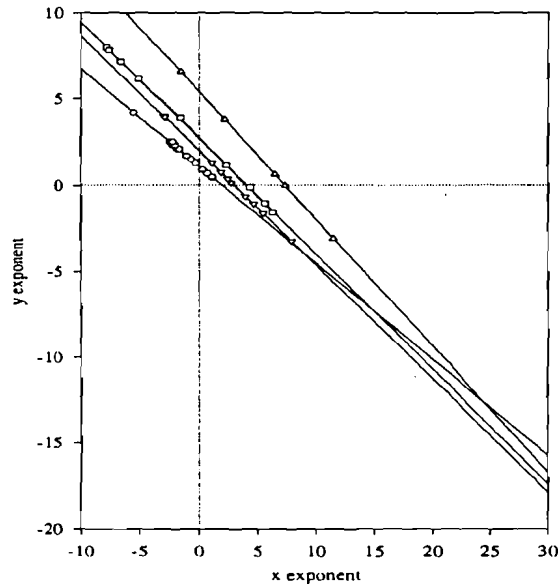


Figure 4.7. Relation between exponents x and y for all ethanol inputs.

$$\circ = f_{i,sine}^{eth}; \triangle = f_{i,0.2}^{eth}; \nabla = f_{i,0.4}^{eth}; \square = f_{i,ramp}^{eth}.$$

As can be seen from figure 4.7, there is no common coordinate in the xy-plane in which all lines cross.

There are several crosspoints of two lines, i.e. (8.83,-3.85), (14.85,-7.25) and (24.40,-12.60). These points contain, however, negative values for x and y. From equation (4-5) it can be seen that this is not allowed, since negative values for x and y would make multiplier a bigger than one. Therefore, it can be concluded that there is no single value for x and y which describes all ethanol inputs correctly.

4.5 CONCLUSIONS

By incorporating drains and the glyoxylate bypass an extended simulation model was build and 8 simulations done with this model were discussed. The simulations showed that the glyoxylate bypass implemented in the simulation model can compensate for the losses caused by the drains. Furthermore, the steady state values of a simulation depend on the ethanol input only. From the simulations it became also clear that both the if-then statement, which is used to calculate the maximum concentration, and the flux distribution, which determines the flux from isocitrate towards α -ketoglutarate and glyoxylate, did not function correctly.

It has been investigated whether the if-then statement could be replaced with a continuous function to prevent the concentration from exceeding the maximum level. This gave other additional problems and therefore no other solution remains than to avoid the ethanol input to exceed 0.5 or to denormalise the concentration.

By means of least square optimisation it was tried to find a flux distribution which performed well for various ethanol inputs. Although for a single ethanol input such an optimum could be found, there was not a flux distribution which could be used for all ethanol inputs combined. Therefore, the value of x and y which has to be used in practice depends on the relevance of the ethanol inputs used here with respect to the experimental data.

5

FITTING THE SIMULATION MODEL WITH EXPERIMENTAL DATA

5.1 INTRODUCTION

In this chapter the simulation model will be fitted to experimental data. For this, the simulation model has to be denormalised and the experimental data has to be adjusted (§5.2 and §5.3 respectively). In § 5.4 three simulations will be discussed, which show to what extent the simulation model can be tuned to the experimental data.

5.2 DENORMALISING THE SIMULATION MODEL

In order to do simulations with experimental data either the simulation model has to be denormalised or the experimental data has to be normalised. The problems described in §4.4, however, make it necessary to denormalise the simulation model anyway, so therefore this option is chosen here. Denormalising the simulation model comes down to denormalising the concentration, the flux and the flux distribution function, described in respectively §3.5.1, §3.5.2 and §4.4.2. They will be dealt with in this section.

Before denormalising the simulation model the units in which the concentrations and fluxes will be expressed, have to be chosen. The concentration will be expressed in $\text{mmol} \cdot \text{dm}_{\text{cell}}^{-3}$. The subscript 'cell' is necessary to make a distinction between the cell volume and the volume of the fermenter. The latter will be referred to with the subscript 'ferm'. The unit for fluxes will be changed into $\text{mmol} \cdot \text{s}^{-1} \cdot \text{dm}_{\text{cell}}^{-3}$ (see note in §3.5.1).

The concentration is at present implemented as a limited integrator with an upper and a lower bound. The lower bound of the concentration, which is equal to zero, remains zero since a concentration cannot be negative. The upper bound is released, i.e., it is given such a high value that the concentration will not reach it. No effort has yet been made to find out what the maximum concentration of each metabolite in the cell is, since this is not considered important

at this moment.

The flux was implemented as follows (equation (3-6)):

$$f_{o,\max}^A(t) = \frac{[A(t)]}{[A]_{\max}} \quad (3-6)$$

with $[A]$ = concentration of metabolite A ($\text{mol} \cdot \text{dm}_{\text{cell}}^{-3}$);

$[A]_{\max}$ = maximum concentration of metabolite A ($\text{mol} \cdot \text{dm}_{\text{cell}}^{-3}$).

In equation (3-6) $f_{o,\max}^A$ is dimensionless. The denormalised equation for the flux can be derived from the differential equation (5-1B) which describes the conversion of metabolite A into metabolite B (5-1A):



$$\frac{d[B(t)]}{dt} = k \cdot [A] \quad (5-1B)$$

with $[A]$, $[B]$ in $\text{mol} \cdot \text{dm}_{\text{cell}}^{-3}$;

k = rate constant (s^{-1}).

The term $d[B(t)]/dt$ in equation (5-1B) is the amount of metabolite B that is made each unit of time and this is equal to the amount of metabolite A that disappears each unit of time. Therefore, equation (5-1B) can be written as:

$$f_o^A = k \cdot [A(t)] \quad (5-2)$$

with f_o^A in $\text{mmol} \cdot \text{s}^{-1} \cdot \text{dm}_{\text{cell}}^{-3}$;

k in s^{-1} ;

$[A]$ in $\text{mmol} \cdot \text{dm}_{\text{cell}}^{-3}$.

Equation (5-2) is the denormalised equation for the flux¹. In the simulation model described in chapter 3 and 4 the rate constants k were implemented in the reaction blocks, from which they have to be removed. The magnitude of the rate constants will be discussed in §5.4.

The flux distribution function is at present implemented as follows (equation (4-5)):

$$a = \left(1 - \frac{[suc]}{[suc]_{\max}} \right)^x \cdot \left(1 - \frac{[mal]}{[mal]_{\max}} \right)^y \quad (4-5)$$

with x, y = constants;

$[mal]$ = malate concentration in $\text{mmol} \cdot \text{dm}_{\text{cell}}^{-3}$;

$[suc]$ = succinate concentration in $\text{mmol} \cdot \text{dm}_{\text{cell}}^{-3}$;

$[mal]_{\max}$ = maximum concentration of malate.

$[suc]_{\max}$ = maximum concentration of succinate.

¹Since the concentrations will not reach the maximum level, $f_{o,\max}^A$ is equal to f_o^A .

In equation (4-5) 'a' is the fraction of f_o^{50} that converts into glyoxylate and succinate. Denormalising this equation is difficult since the maximum concentrations are not known yet. It would be simpler to look for another function which would do essentially the same. In equation (4-5) 'a' is implemented as a fraction and therefore has values between zero and one. Beside this, 'a' has to be zero (or at least very small) when the concentration of malate and succinate are high and it has to be one (or very close to one) when the concentration of malate and succinate are very low. A function which suits this description is given in equation (5-3):

$$a = e^{-\frac{[suc]}{x}} \cdot e^{-\frac{[mal]}{y}} \quad (5-3)$$

with [suc] = succinate concentration ($\text{mmol} \cdot \text{dm}_{\text{cell}}^{-3}$);
 [mal] = malate concentration ($\text{mmol} \cdot \text{dm}_{\text{cell}}^{-3}$);
 x,y = coefficients ($\text{dm}_{\text{cell}}^3 \cdot \text{mmol}^{-1}$).

The coefficients x and y can be adjusted to regulate the flux through the glyoxylate bypass. They have values higher than zero. When the model is fitted to the experimental data, x and y can be used as tuning parameters. The listing of the altered concentration block, flux block and reaction block and the simulink diagram of the denormalised simulation model are given in appendix G.

5.3 PREPARING THE DATA

The experimental setup, which produces the raw data, is depicted in figure 5.1.

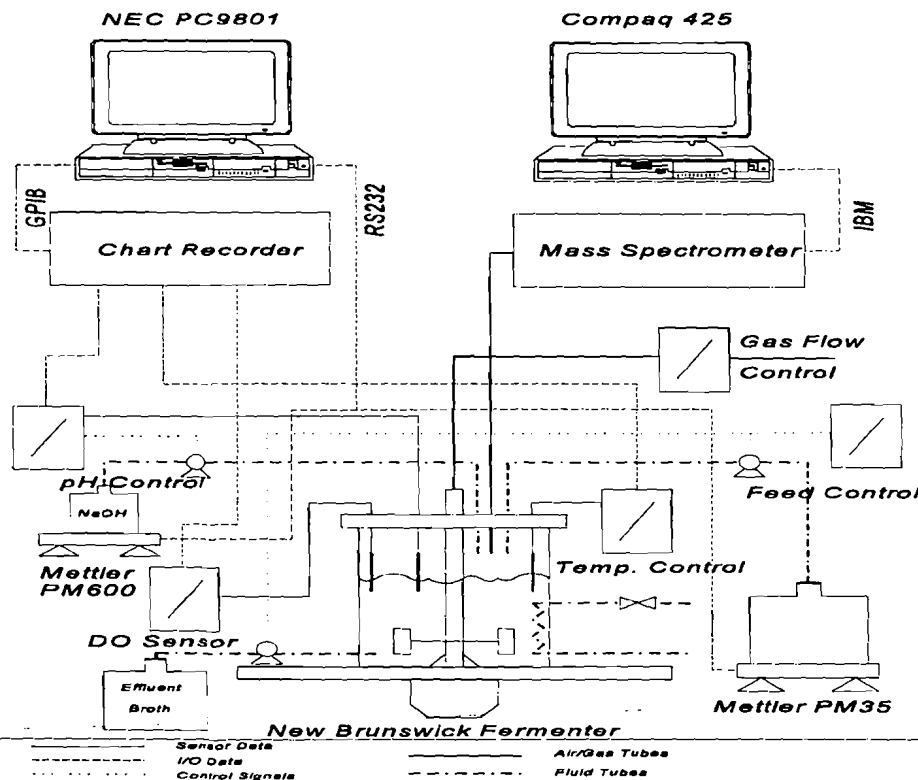


Figure 5.1. Experimental setup.

The continuous yeast culture is kept at a constant temperature of 30°C and at a constant pH of 4. The input of gas and medium are also constant in time. There is a continuous output of broth (content of the fermenter) and gas. The composition of this gas is determined in the mass spectrometer. To measure the concentration of a metabolite a sample of the fermenter content is taken every 4 minutes. More details can be found in the references [Keulers *et al.* 1994, Keulers *et al.* 1995]. The raw data which is available from experiments is listed in table 5.1. Raw data is referred to with the subscript 'raw'.

Table 5.1. Listing of the available raw data. For the oscillating parameters the mean value is given.

parameter	abbreviation	value	unit	oscillating
extracellular acetate	ACE_{ex}	$1.16 \cdot 10^{-4}$	$\text{mol} \cdot \text{dm}^{-3}_{\text{ferm}}$	yes
total acetate	ACE_{tot}	$3.01 \cdot 10^{-4}$	$\text{mol} \cdot \text{dm}^{-3}_{\text{ferm}}$	yes
carbon dioxide evolution rate	$f_{o, \text{raw}}^{CO_2}$	$1.56 \cdot 10^1$	$\text{mmol} \cdot \text{h}^{-1} \cdot \text{dm}^{-3}_{\text{ferm}}$	yes
ethanol input	$f_{i, \text{raw}}^{eth}$	2.76	$\text{mmol} \cdot \text{h}^{-1} \cdot \text{g}_{\text{cell}}^{-1}$	yes
cell volume	V_{cell}	$1.6 \cdot 10^{-3}$	$\text{dm}^3_{\text{cell}} \cdot \text{g}_{\text{wetcell}}^{-1}$	no
dry cell weight	DCW	6.70	$\text{g}_{\text{cell}} \cdot \text{dm}^{-3}_{\text{ferm}}$	no
wet cell/dry cell	$r_{W/D}$	3.77	$\text{g}_{\text{wetcell}} \cdot \text{g}_{\text{cell}}^{-1}$	no
volume of fermentor	V_{ferm}	1.15	$\text{dm}^3_{\text{ferm}}$	no

Before the raw data of table 5.1 can be applied to the simulation model their units have to be adjusted. The intracellular acetate concentration (referred to as ACE_{in}) is calculated as ACE_{tot} minus ACE_{ex} . The unit of this $ACE_{in, \text{raw}}$ is therefore $\text{mol} \cdot \text{dm}^{-3}_{\text{ferm}}$. To change this into $\text{mmol} \cdot \text{dm}^{-3}_{\text{cell}}$, $ACE_{in, \text{raw}}$ has to be multiplied by $10^3 \cdot V_{\text{cell}}^{-1} \cdot \text{DCW}^{-1} \cdot r_{W/D}$. All multiplication factors for the raw data are listed in table 5.2.

Table 5.2. Multiplication factors for the raw data parameters.

parameter	multiplication factor	new unit
ethanol input	$f_i^{eth} = f_{i, \text{raw}}^{eth} \cdot \frac{1}{3600 \cdot V_{\text{cell}} \cdot r_{W/D}}$	$\text{mmol} \cdot \text{s}^{-1} \cdot \text{dm}^{-3}_{\text{cell}}$
intracellular acetate	$ACE_{in} = ACE_{in, \text{raw}} \cdot \frac{10^3}{V_{\text{cell}} \cdot \text{DCW} \cdot r_{W/D}}$	$\text{mmol} \cdot \text{dm}^{-3}_{\text{cell}}$
carbon dioxide evolution rate	$f_o^{CO_2} = f_{o, \text{raw}}^{CO_2} \cdot \frac{1}{3600 \cdot V_{\text{cell}} \cdot \text{DCW} \cdot r_{W/D}}$	$\text{mmol} \cdot \text{s}^{-1} \cdot \text{dm}^{-3}_{\text{cell}}$

In table 5.3 additional information about the oscillation parameters is given.

Table 5.3. Prepared data.

parameter	period of oscillation (min)	mean value	unit	amplitude of oscillation (% of mean value)	phase shift with respect to extracellular ethanol input (rad)
ethanol input	40	$1.27 \cdot 10^{-1}$	$\text{mmol} \cdot \text{s}^{-1} \cdot \text{dm}_{\text{cell}}^{-3}$	44.2	0
intracellular acetate	40	4.57	$\text{mmol} \cdot \text{dm}_{\text{cell}}^{-3}$	31.1	$3\pi/4$
carbon dioxide evolution rate	40	$1.07 \cdot 10^{-1}$	$\text{mmol} \cdot \text{s}^{-1} \cdot \text{dm}_{\text{cell}}^{-3}$	17.7	$3\pi/4$

A remark has to be made about the phase shifts. The CO_2 evolution rate is measured outside the cell, however, the phase shift between intracellular and extracellular CO_2 evolution rate can be determined as follows. From literature it is known that the phase shift between intracellular CO_2 evolution rate and intracellular O_2 uptake rate and the phase shift between intracellular and extracellular O_2 uptake rate are negligible. The phase shift between the extracellular CO_2 evolution rate and extracellular O_2 uptake rate can therefore be seen as the phase shift between the intracellular and extracellular CO_2 evolution rate. This phase shift between the intracellular and extracellular CO_2 evolution rate has already been taken into account in table 5.3. Note that ethanol is measured outside the cell and is therefore an extracellular parameter. So when ethanol enters the cell the phase shift or the amplitude or both might change.

5.4 SIMULATIONS

A number of simulations have been done to test whether the simulation model is able to reproduce experimental results. Three of these simulations will be discussed in this section. The parameters of the simulation model which can be adjusted are the rate constants of all metabolites, the parameters x and y of the flux distribution from isocitrate (equation (5-3)), the flux distribution from acetyl-CoA and the magnitude of the drains. The drains are kept constant at the same magnitude as listed in table 4.3 and the flux distribution of acetyl-CoA will not be changed either, i.e. the conversion of acetyl-CoA and glyoxylate into malate has priority. For each simulation the initial concentration of the metabolites is $4.6 \text{ mmol} \cdot \text{dm}_{\text{cell}}^{-3}$, the integration method used is linsim and the simulated time is 100 minutes. The experimental data for the ethanol flux has been smoothed with a sinus function and this function is used as input for the simulation model. The ethanol input of the simulation model is an oscillating parameter and therefore the oscillation is imposed on the simulation model. However, the supply of ethanol medium to the culture is constant and therefore the oscillation is not imposed on the yeast culture.

Table 5.4. *Settings of the simulation parameters for simulation 1, 2 and 3.*

simulation	1	2	3
k_{ADH}	0.5	0.0278	0.0278
k_{ACT}	0.5	0.0278	0.0278
k_{ACO}	0.5	0.0278	0.5
k_{CIT}	0.5	0.0278	0.5
k_{ISO}	0.5	0.0278	0.5
k_{KET}	0.5	0.0278	0.5
k_{GLY}	0.5	0.0278	0.5
k_{SUC}	0.5	0.0278	0.5
k_{MAL}	0.5	0.0278	0.5
k_{OXA}	0.5	0.0278	0.5
x	1.3	20	1.3
y	1.3	20	1.3

The magnitude of the rate constants used in the first simulation are chosen as high as possible, in accordance with the assumption that the time constant of the chemical reactions involved is much smaller than the physical time constant. For values higher than 0.5 the required simulation time increased rapidly and therefore this value was chosen. The parameters x and y were adjusted manually in a way that gave the best results for the CO₂ evolution rate. The results of simulation 1 are shown in figure 5.2.

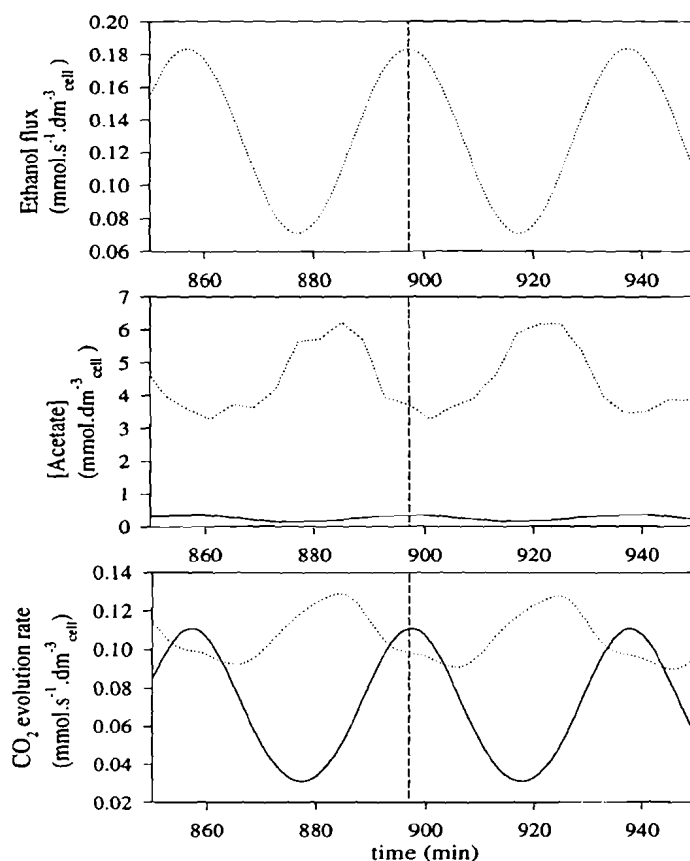


Figure 5.2. Results of simulation 1.

Top graph, dotted line: smoothed ethanol flux.

Middle graph, dotted line: experimental acetate concentration; solid line: simulated acetate concentration; broken vertical line: see text.

Bottom graph, dotted line: experimental CO₂ evolution rate; solid line: simulated CO₂ evolution rate; broken vertical line: see text.

Figure 5.2 shows several things:

1. There is a phase shift between the simulation data and experimental data for the acetate concentration as well as for the CO₂ evolution rate, but there is no phase shift between the ethanol flux on one hand and the simulated CO₂ evolution rate and acetate concentration on the other hand (see vertical broken lines in graphs). This is a result of the high value of the rate constants.
2. The mean value of the simulated CO₂ evolution rate is lower than the mean value of the experimental CO₂ evolution rate. The simulated CO₂ evolution rate is a summation of three fluxes, namely the flux from isocitrate to α -ketoglutarate, the flux from α -ketoglutarate to succinate and the flux from oxaloacetate to p-enol-pyruvate. Therefore, it depends on the magnitude of the p-enol-pyruvate drain, on the magnitude of the glutamate drain, on the flux distribution from isocitrate and acetyl-CoA and on the magnitude of the ethanol flux. It does not depend on the rate constants of the metabolites.
3. The relative amplitude of the simulated CO₂ evolution rate is bigger than the relative amplitude of the experimental CO₂ evolution rate. This fact could be caused by CO₂, which has to diffuse from the inside of the mitochondrion to the outside of the cell.

4. The mean value of the simulated acetate concentration is much lower than the mean value of the experimental acetate concentration. Since a ethanol flux is the input of the simulation model and the flux is calculated as $f_o(t) = k \cdot [A(t)]$ (equation (5-2)), the concentration of a metabolite A is determined through its rate constant and the ethanol input flux. The combination of the small ethanol flux with a mean value of $0.13 \text{ mmol} \cdot \text{s}^{-1} \cdot \text{dm}^{-3}_{\text{cell}}$ and a high value of 0.5 for the rate constants, results in a low concentration level.

First remark 4 will be addressed. For this, the rate constants of all metabolites have to be decreased. The new magnitude is calculated as the rate constant of simulation 1 times the mean value of the simulated acetate concentration divided by the mean value of the experimental acetate concentration.

The results of this second simulation are shown in figure 5.3.

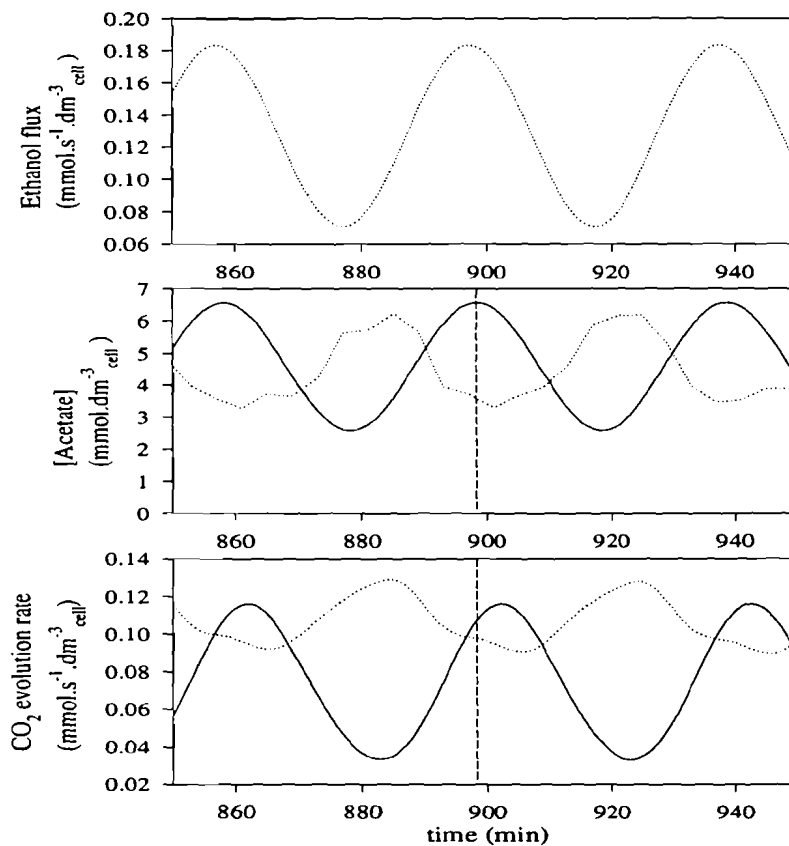


Figure 5.3. Results of simulation 2.

Top graph, dotted line: smoothed ethanol flux.

Middle graph, dotted line: experimental acetate concentration; solid line: simulated acetate concentration; broken vertical line: see text.

Bottom graph, dotted line: experimental CO_2 evolution rate; solid line: simulated CO_2 evolution rate; broken vertical line: see text.

Figure 5.3 shows that:

1. The mean value of the simulated acetate concentration is equal to the mean value of the experimental acetate concentration.
2. The amplitude of the simulated acetate concentration is almost the same as the amplitude of the experimental acetate concentration. The rather 'square' shape of the experimental acetate

concentration is caused by a sampling rate of 4 minutes.

- There is a rather big phase shift between the simulated acetate concentration and the simulated CO_2 evolution rate. By decreasing the rate constants, the time constant of the chemical reactions involved is no longer much lower than the physical time constant. This results in a phase shift between the simulated acetate concentration and the simulated CO_2 evolution rate.

To solve remark 3 the rate constants for the TCA cycle and glyoxylate bypass metabolites have to be increased again to the same level as in simulation 1. As was seen in figure 5.2 there was no phase shift between the simulated acetate concentration and the simulated CO_2 evolution rate in this situation. The rate constant of acetate has to be kept at the lower value used in simulation 2 to maintain the correct acetate concentration. Since the rate constant of a metabolite only effects it's own concentration, the rate constant of acetaldehyde can be either low or high. The rate constant of acetaldehyde is arbitrary given the same value as the rate constant of acetate. The results of simulation 3, in which two different values for the rate constants are used, are shown in figure 5.4.

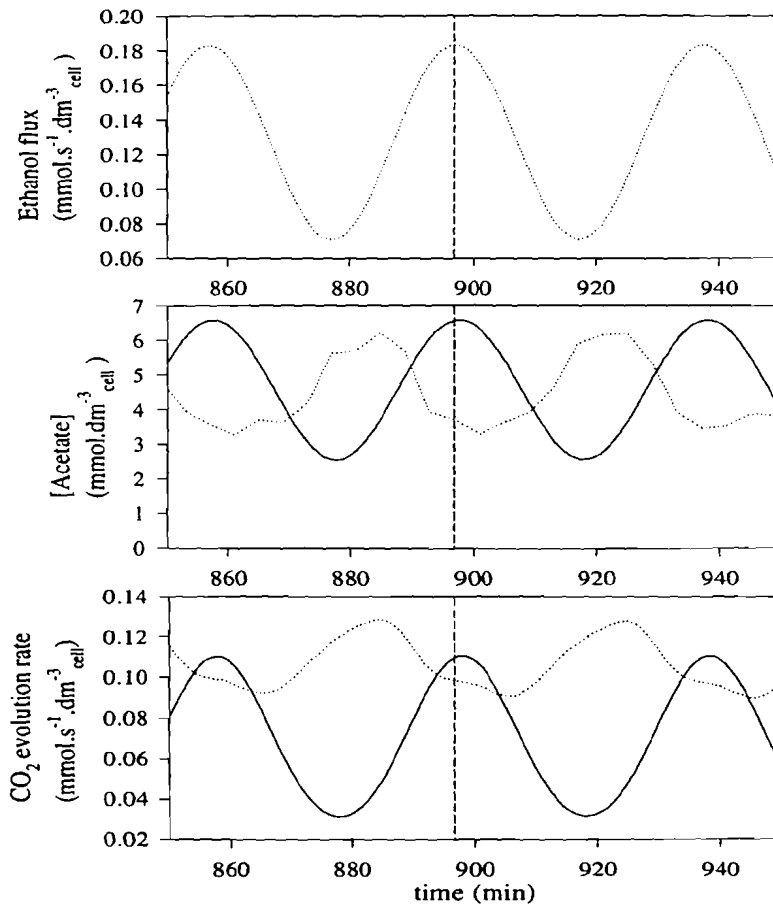


Figure 5.4. Results of simulation 3.

Top graph, dotted line: smoothed ethanol flux; broken vertical line: see text.

Middle graph, dotted line: experimental acetate concentration; solid line: simulated acetate concentration; broken vertical line: see text.

Bottom graph, dotted line: experimental CO_2 evolution rate; solid line: simulated CO_2 evolution rate; broken vertical line: see text.

Compared to figure 5.3, figure 5.4 shows that the phase shift between the simulated acetate concentration and the simulated CO₂ evolution rate has disappeared as expected and that the mean value of acetate is correct. Still two problems remain. First, there is a phase shift between the experimental and the simulated data of the acetate concentration and CO₂ evolution rate. Secondly, the simulation of the CO₂ evolution rate has to be improved.

The first problem could be solved by assuming that extracellular and intracellular ethanol have a phase shift which is equal to the phase shift between the simulated and experimental acetate concentration. This would eliminate the apparent phase shift for both acetate and CO₂ evolution rate, since the simulated acetate concentration and CO₂ evolution rate do not have a phase shift towards the intracellular ethanol flux.

The second problem is somewhat more complicated. As mentioned in remark 2 from figure 5.2 the simulated CO₂ evolution rate is influenced by the magnitude of the p-enol-pyruvate and glutamate drains, by the flux distribution from isocitrate and acetyl-CoA and it also depends on the ethanol flux. With these parameters the mean value of the simulated CO₂ evolution rate can be tuned. But, since so many parameters have an influence it is very likely that more than one combination of these parameters gives the correct results for the simulated CO₂ evolution rate. To find the correct combination, additional experiments have to be done to find e.g., the magnitude of the p-enol-pyruvate and glutamate drains or to be able to determine the amount of flux from isocitrate to α -ketoglutarate. The amplitude of the simulated CO₂ evolution rate, which might then still be too large, can be adjusted with a diffusion model. This is valid since the CO₂ evolution rate is determined extracellularly.

5.5 CONCLUSIONS

The simulation model has been denormalised by denormalising the concentration block, the flux block and the flux distribution of isocitrate. With this denormalised simulation model and experimental data for the ethanol flux, the acetate concentration and the CO₂ evolution rate three simulations have been discussed.

These simulations have shown several things. First, the concentration of the metabolites can be adjusted through changes in the rate constants. The simulated acetate concentration was adjusted to the experimental acetate concentration through decreasing the rate constant of acetate. Secondly, the experimental acetate concentration and the experimental CO₂ evolution rate show no phase shift, but for low rate constants a phase shift appeared between the simulated acetate concentration and the simulated CO₂ evolution rate. Whether the simulation model can be seen as a chemical model or a physical model depends on the magnitude of the flux with respect to the fluctuation of the experimental value of the metabolite concentrations. Third, a phase shift exists between the ethanol flux on one hand and the simulated acetate concentration and CO₂ evolution rate on the other hand. This problem can be solved in assuming that there exists a phase shift between the extracellular and intracellular ethanol. Finally, the simulated CO₂ evolution rate is influenced by several parameters and variables, like the ethanol input, the magnitude of the p-enol-pyruvate and glutamate drains and by the flux distribution from isocitrate. In order to simulate the CO₂ evolution rate correctly additional experimental data is necessary to determine the value of these parameters and variables.

6

CONCLUSIONS AND FUTURE WORK

A literature research of biochemical computer programs has been done to find out whether these programs could serve as a basis for a simulation model of the TCA cycle and glyoxylate bypass. However, neither one of the computer programs could handle steady states and dynamic behaviour as well as calculate fluxes and concentrations. For this reason a new simulation model was made.

Three simulation models are described and tested in this thesis. The first simulation model is based on a simplified version of the TCA cycle. Its main function is to test the three different building blocks of which it is made of. Simulations done with this simulation model show that all building blocks operate correctly. The second simulation model is based on an extended version of the TCA cycle and it also incorporates the glyoxylate bypass and several drains. Simulations done with this second simulation model show a deficiency in the if-then statement used in the concentration block and a deficiency in the flux distribution function of isocitrate. The deficiency caused by the if-then statement could not be solved, unless the simulation model would be denormalised. By means of least square optimisation a flux distribution was found which performed well for different ethanol inputs. However, a flux distribution suitable for an ethanol input that was a combination of different shaped signals could not be found. The third simulation model is a denormalised version of the second simulation model. A number of simulations have been done to test whether this denormalised simulation model can produce signals with the same amplitude and phase shift as obtained from experiments. The simulated acetate concentration could be adjusted to the experimental acetate concentration through tuning of the rate constant. The phase shift between ethanol on one hand and the simulated acetate concentration and CO₂ evolution rate on the other hand can be solved when it is assumed that this phase shift results from ethanol going into the cell. However, to simulate the CO₂ evolution rate, additional experimental data is necessary.

The simulation model is made as a tool in finding the cause of a metabolic oscillation. However, the simulation model, as described in chapter 5, is not able to produce such an oscillation. The turning rate of the TCA cycle and glyoxylate bypass, which has a magnitude of a few seconds,

is too fast for the period of oscillation, which is 40 minutes. To generate oscillations with the simulation model additional feedback mechanisms, most likely located outside the TCA cycle, need to be implemented.

Future work will be focussed on implementing additional feedback mechanisms and on obtaining additional experimental data. Such a feedback mechanism could be the influence of the CO₂ concentration inside the cell on the ethanol uptake rate of the cell. In the simulation model the CO₂ evolution rate is influenced by the ethanol input, the magnitude of the p-enol-pyruvate and glutamate drains and by the flux distribution from isocitrate and acetyl-CoA. Since the ethanol input is known, the additional experimental data which has to be measured could be:

- two of the following fluxes: the flux from isocitrate to α -ketoglutarate, the flux from α -ketoglutarate to succinate, the flux from oxaloacetate to p-enol-pyruvate;
- the flux from isocitrate to α -ketoglutarate, the flux from isocitrate to glyoxylate and the magnitude of either the p-enol-pyruvate drain or the glutamate drain;
- the flux from acetyl-CoA to malate, the flux from acetyl-CoA to citrate and the magnitude of either the p-enol-pyruvate drain or the glutamate drain.

In order to continue with the simulation model in a meaningful and relevant direction, it is suggested that one of the above mentioned combinations is experimentally determined.

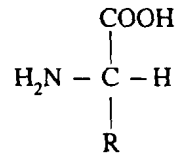
REFERENCES

- Barnett, J.A., R.W. Payne and D. Yarrow** (1990). Yeasts: characteristics and identification. Second edition. Cambridge University Press, Cambridge.
- Brown, G., R. Hafner and M. Brand** (1990). A 'top-down' approach to the determination of control coefficients in metabolic control theory. *Eur. J. Biochem.* **188**: 321-325.
- Burns, J.A. et al.** (1985). Control analysis of metabolic systems. *Trends Biochem. Sci.* **10**: 16.
- Cornish-Bowden, A. and J.-H.S. Hofmeyr** (1991). MetaModel: a program for modelling and control analysis of metabolic pathways on the IBM PC and compatibles. *Comput. Appl. Biosci.* **7**: 89-93.
- Cornish-Bowden, A.** (1995). Metabolic control analysis in theory and practice. *Adv. Mol. and Cell Biol.* **11**: 21-64.
- Cortassa, S., J.C. Aon and M.A. Aon** (1995). Fluxes of carbon, phosphorylation, and redox intermediates during growth of *Saccharomyces cerevisiae* on different carbon sources. *Biotechn. Bioeng.* **47**: 193-208.
- Fell, D.A. and H.M. Sauro** (1985). Metabolic control and its analysis. Additional relationships between elasticities and control coefficients. *Eur. J. Biochem.* **148**: 555-561.
- Fell, D.A.** (1992). Metabolic Control Analysis: a survey of its theoretical and experimental development. *Biochem. J.* **286**: 313-330.
- Garfinkel, D., L. Garfinkel, M. Pring, S.B. Green and B. Chance** (1970). Computer applications to biochemical kinetics. *Annu. Rev. Biochem.* **39**: 473-498.
- Heinrich, R. and T.A. Rapoport** (1974a). A linear steady-state treatment of enzymatic chains. General properties, control and effector strength. *Eur. J. Biochem.* **42**: 89-95.
- Heinrich, R. and T.A. Rapoport** (1974b). A linear steady-state treatment of enzymatic chains. Critique of the crossover theorem and a general procedure to identify sites with an effector. *Eur. J. Biochem.* **42**: 97-105.
- Higgins, J.J.** (1965). Dynamics and control in cellular reactions. *Control of Energy Metabolism* (Chance, Estabrook and Williamson eds.) pp. 13-46. Academic Press, New York.
- Kascser, H. and J.A. Burns** (1973). The control of flux. *Symp. Soc. Exp. Biol.* **32**: 65-104.
- Kell, D.B. and H.V. Westerhoff** (1986). Metabolic control theory: its role in microbiology and biotechnology. *FEMS Microbio. Rev.* **39**: 305-320.
- Keulers, M.L.B.** (1993). Identification and control of a fed-batch process; application to culture of *Saccharomyces cerevisiae*. *Ph.D. Thesis*. Technische Universiteit Eindhoven, Eindhoven, the Netherlands.
- Keulers, M., T. Asaka and H. Kuriyama** (1994). A versatile data acquisition system for physiological modelling of laboratory fermentation processes. *Biotechn. Techn.* **8**: 879-884.
- Keulers, M. and H. Kuriyama** (1995). Effect of gas flow rate and oxygen concentration on the damping (filtering) action of fermenter head space. *Biotechn. Letters* **17**: 675-680.
- Kornberg, H.L. and N.B. Madsen** (1957). Synthesis of C₄-dicarboxylic acids from acetate by a "glyoxylate bypass" of the tricarboxylic acid cycle. *Biochim. Biophys. Acta* **24**: 651-653.
- Krebs, H.A.** (1940). The citric acid cycle. *Biochem. J.* **34**: 460-463.
- Letellier, T., C. Reder and J.-P. Mazat** (1991). CONTROL: software for the analysis of the control of metabolic networks. *Comput. Appl. Biosci.* **7**: 383-390 (not available to the author).
- Lodder, J. and N.J.W. Kreger-van Rij** (1967). The yeast, a taxonomic study. Second printing. North-Holland Publishing Company, Amsterdam.
- Maclean, N.** (1987). Macmillan dictionary of genetics and cell biology. The Macmillan Press LTD, London.
- Mendes, P.** (1993) GEPASI: a software package for modelling the dynamics, steady states and control of biochemical and other systems. *Comput. Appl. Biosci.* **9**: 563-571.
- Regan, L. and M. Gregory** (1995). Flux analysis of microbial metabolic pathways using a visual programming environment. *J. Biotech.* **42**: 151-161.
- Reder, C.** (1988). Metabolic Control Theory: a structural approach. *J. Theor. Biol.* **135**: 175-201.

- Sauro, H.M., J.R. Small and D.A. Fell** (1987). Metabolic control and its analysis. Extensions to the theory and matrix method. *Eur. J. Biochem.* **165**: 215-221.
- Sauro, H.M. and D.A. Fell** (1991). SCAMP: a metabolic simulator and control analysis program. *Math. Comput. Modelling* **15**: 15-28.
- Savageau, M.A.** (1969a). Biochemical Systems Analysis. I. Some mathematical properties of the rate law for the component enzymatic reactions. *J. Theoret. Biol.* **25**: 365-369.
- Savageau, M.A.** (1969b). Biochemical systems Analysis. II. The steady-state solutions for a n-pool system using a power-law approximation. *J. Theoret. Biol.* **25**: 370-379.
- Savageau, M.A.** (1969c). Biochemical systems analysis. III. Dynamic solutions using a power-law approximation. *J. Theoret. Biol.* **26**: 215-226.
- Savageau, M.A.** (1976). Biochemical Systems Analysis. Addison-Wesley, London.
- Savageau, M.A.** (1990) Biochemical Systems Theory: alternative views of metabolic control. *Control of Metabolic Processes* (Cornish-Bowden and Cárdenas eds.), pp. 69-88. Plenum Press, New York.
- Schulz, A.R.** (1991). Algorithms for the derivation of flux and concentration control coefficients. *Biochem. J.* **278**: 299-304.
- Stryer, L.** (1988). Biochemistry. Third edition. W.H. Freeman and Company, New York.
- Thomas, S. and D.A. Fell** (1993). A computer program for the algebraic determination of control coefficients in Metabolic Control Analysis. *Biochem. J.* **292**: 351-360.
- Van den Bosch, P.P.J. and A.C. van der Klauw** (1994) Stochastische systeemtheorie, modeling, identification and simulation of dynamical systems. Collegediktaat nr. 5686. Eindhoven University of Technology, Eindhoven.
- Walker, P.M.B.** (1989). Chambers biology dictionary. W&R Chambers LTD, Edinburgh.
- Westerhoff, H.V. and Yi-Der Chen** (1984). How do enzyme activities control metabolite concentrations? An additional theorem in the theory of metabolic control. *Eur. J. Biochem.* **142**: 425-430.
- Westerhoff, H.V. et al.** (1991). Quantitative approaches to the analysis of the control and regulation of microbial metabolism. *Antonie van Leeuwenhoek* **60**: 193-207.

NOMENCLATURA

Amino acid The basic structural unit of proteins, varying in size, shape, charge, hydrogenbonding capacity and chemical reactivity. Their common structure is:



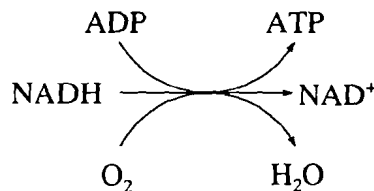
	with individual side chains attached at the R position.
Anabolism	A metabolic process of the formation of complex molecules from simpler ones.
ADP	Adenosine diphosphate, the hydrolysed form of ATP.
ATP	Adenosine triphosphate, carrier of free energy in biological systems.
Batch culture	A culture initiated by the inoculation of cells into a finite volume of fresh medium and terminated at a single harvest after the cells have grown.
Budding	A method of asexual reproduction by growth and specialisation, followed by the separation by constriction of a part of the parent.
Carbohydrates	A group of compounds represented by the general formula $\text{C}_x(\text{H}_2\text{O})_y$.
Catabolism	A metabolic process of breaking down complex molecules into simpler ones.
Chemostat	A culture vessel in which steady state growth is maintained by adding medium to the vessel with the same flow rate as cell culture is being removed from the vessel.
Citric acid cycle	The final common cyclical pathway for the oxidation of fuel molecules. It also provides intermediates for the biosynthesis.
Conserved cycle	Cycle in which the total concentration of the metabolites involved remains constant.
Continuous culture	A culture maintained at a steady state over a period, usually in a chemostat.
FADH₂	Flavin adenine dinucleotide, used primarily for the generation of ATP.
Fermentation	Production of chemical energy in the form of ATP through the degradation of carbohydrates and other organic molecules in a reaction that does not require molecular oxygen.
Gluconeogenesis	Metabolic pathway that converts pyruvate into glucose.
Glycogen	Readily mobilized storage form of glucose.
Glycolysis	Metabolic pathway that converts glucose into pyruvate.
<i>in vitro</i>	Term used to describe the experimental reproduction of biological processes in the more easily defined environment of the culture vessel, plate or testtube.
<i>in vivo</i>	Term used to describe biological processes occurring within the living organism or cell.
Lipids	Water-insoluble biomolecules with a variety of biological functions like membrane compound, highly concentrated energy storages and signal molecules.
K_m	The metabolite concentration at which the enzymatic conversion rate is half of the maximum.
Metabolism	The sum of chemical reactions within a cell or organism, including the energy-releasing breakdown (catabolism) and the synthesis (anabolism) of complex molecules.
Metabolite	Product of metabolism.
Mitochondrion	A cytoplasmic organelle whose main function is the generation of ATP by aerobic respiration.
NAD	Nicotinamide adenine dinucleotide, the oxidised form of NADH.
NADH	Nicotinamide adenine dinucleotide, used primarily for the generation of ATP.

Nucleotide	The individual components of a nucleic acid.
Protein	A molecule that consists of one, or a small number of polypeptide chains each of which is a linear polymer of several to several hundred amino acids; being able to recognize and interact with highly diverse molecules they serve in all cells as sensors that control the flow of energy and matter.
Rate constant (k)	Determines the rate at which a reaction takes place; $[k]=(\text{dm}^{-3})^n\text{mol}^{-n}\text{s}^{-1}$ for a reaction of order $(n+1)$.
Rate law	Gives the relation between concentration of metabolites and rate constants of a reaction; eg., the rate law of reaction $A \xrightleftharpoons[k_2]{k_1} B$ is written as

$$\frac{d[A]}{dt} = -k_1[A] + k_2[B];$$

$$\frac{d[B]}{dt} = k_1[A] - k_2[B].$$

Respiratory chain	An ATP-generating process in which NADH is converted into NAD with the aid of O_2 :
-------------------	--



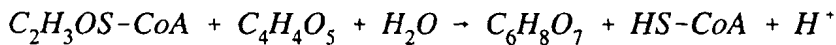
Steady state	Equilibrium between the flow of fresh medium into the bioreactor and the yeast cells suspension that is removed from the bioreactor which results in a constant biomass production rate and a constant consumption rate of components of the fresh medium.
Stoichiometry	Gives the relation between proportions of compounds in a reaction or of elements in a compound.
v_{\max}	The maximum conversion rate of an enzyme.
Vacuole	A membrane-bounded chamber in a cell containing fluid or gas.
Yeast	Unicellular fungus reproducing asexually by budding or division.

A

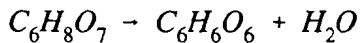
CHEMICAL REACTIONS

CHEMICAL REACTIONS OF THE TCA CYCLE:

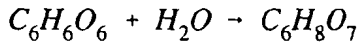
acetyl-CoA + oxaloacetate → citrate



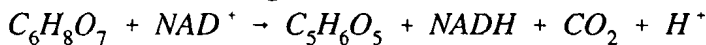
citrate → cis-aconitate



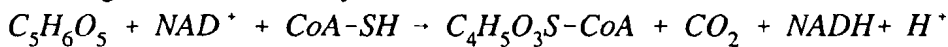
cis-aconitate → isocitrate



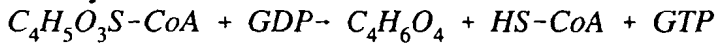
isocitrate → α-ketoglutarate



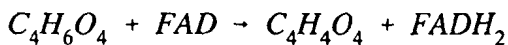
α-ketoglutarate → succinyl-CoA



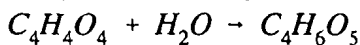
succinyl-CoA → succinate



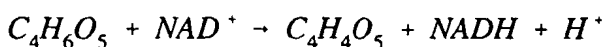
succinate → fumarate



fumarate → malate

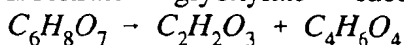


malate → oxaloacetate

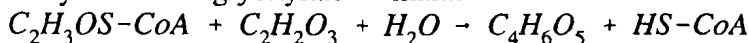


CHEMICAL REACTIONS OF THE GLYOXYLATE BYPASS:

isocitrate → glyoxylate + succinate



acetyl-CoA + glyoxylate → malate

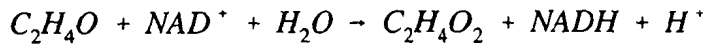


CHEMICAL REACTIONS OF THE CONVERSION OF ETHANOL INTO ACETYL-COA:

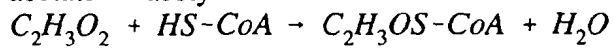
ethanol → acetaldehyde



acetaldehyde → acetate



acetate → acetyl-CoA



B

LISTING OF CONCENTRATION BLOCK, FLUX BLOCK AND REACTION BLOCK

CONCENTRATION BLOCK

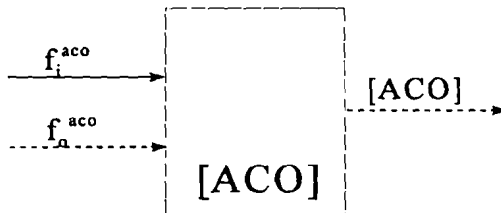


Figure B.1. Block diagram of the acetyl-CoA concentration block.

f_i^{aco} = flux in of acetyl-CoA;
 f_o^{aco} = flux out of acetyl-CoA;
 $[ACO]$ = concentration of acetyl-CoA.

LISTING OF ACETYL-CoA CONCENTRATION BLOCK

```
function[sys,x0] = Aco(t,x,u,flag,acomax,x0Aco)
% ACO calculates the concentration of acetyl-CoA

% u(1) = flux in;
% u(2) = flux out;
% x0Aco = initial concentration of acetyl-CoA;
% acomax = maximum concentration of acetyl-CoA;
% x = [acetyl-CoA];
% y = x;

if abs(flag) == 1 % xdot
    if ((x<=0)&((u(1)-u(2))<0))|((x>=acomax)&((u(1)-u(2))>0))
        sys = 0;
    else
        sys = u(1) - u(2);
    end;
end;
```

```

elseif flag == 3      % output y
    sys = x;

elseif flag == 0     % return sizes of parameters and initial conditions
    sys = [ 1, 0, 1, 2, 0, 0];

    % sys(1) is number of continuous states
    % sys(2) is number of discrete states
    % sys(3) is number of outputs
    % sys(4) is number of inputs
    % sys(5) is number of roots that the system has
    % sys(6) is set to 0 because the system has no direct feed-through
    % of its inputs (see file Matlab/toolbox/simulink/blocks/sfunc.m)

    x0 = [x0Aco];

else                  % only continuous states
    sys = [ ];
end;

```

FLUX BLOCK

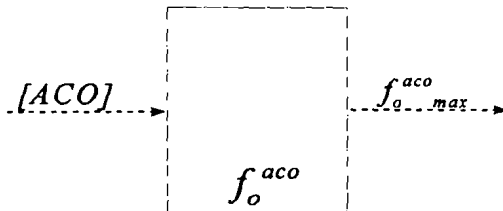


Figure B.2. *Blockdiagram of the acetyl-CoA flux block.*
 $[ACO]$ = concentration of acetyl-CoA;
 $f_o^{aco,max}$ = maximum possible flux out of acetyl-CoA.

LISTING OF ACETYL-CoA FLUX BLOCK

```

function[sys,x0] = acoflux(t,x,u,flag,acomax)
% ACOFLUX determines the flux out of the acetyl vessel

% acomax = maximum concentration of acetyl-CoA;
% u = [acetyl];
% y = flux-out;

if abs(flag) == 1      % xdot
    sys = [ ];

```

```

elseif flag == 3           % output y
    sys = (u)/(acomax);

elseif flag == 0         % return sizes of parameters and initial conditions
    sys = [ 0, 0, 1, 1, 0, 1];
    x0 = [];
else
    % only continuous states
    sys = [ ];
end;

```

REACTION BLOCK

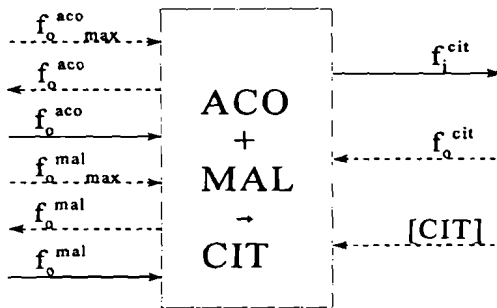


Figure B.3. Blockdiagram of a reaction block.

$f_{o,max}^{aco}$ = maximum possible flux out of acetyl-CoA;
 f_o^{aco} = flux out of acetyl-CoA;
 $f_{o,max}^{mal}$ = maximum possible flux out of malate;
 f_o^{mal} = flux out of malate;
 f_i^{cit} = flux in of citrate;
 f_o^{cit} = flux out of citrate;
 $[CIT]$ = concentration of citrate.

LISTING OF 'MALATE + ACETYL-COA → CITRATE' REACTION BLOCK

```

function [sys, x0] = mac(t,x,u,flag,Kmac)
% MAC Chemical reaction as an M-file
% MAC performs a chemical reaction on malate and acetyl to form citrate,

% u(1) = maximum flux out of acetyl vessel;
% u(2) = maximum flux out of malate vessel;
% u(3) = [citrate];
% u(4) = flux-out of citrate vessel;
% y = flux into the citrate vessel and out of the acetyl and malate vessel;
% Kmac = rate constant of the reaction;

if abs(flag) == 1 % if flag = 1, return state derivatives xdot
    sys = [ ];

```

```
elseif flag == 3 % if flag = 3, return output y
    if (u(3)<1)
        sys = Kmac*( min(u(1), u(2)));
    elseif (u(3)>=1)
        s = (min(u(1), u(2)));
        sys = Kmac*(min(u(4),s));
    end;

elseif flag == 0 % if flag = 0, return sizes of parameters and initial conditions
    sys = [ 0, 0, 1, 4, 0, 1 ];
    x0 = [];

else % only continuous state
    sys = [ ];
end;
```

C

LISTING OF A REACTION BLOCK AND SIMULINK DIAGRAM OF THE NORMALISED SIMULATION MODEL

LISTING OF 'ACETYL-CoA + GLYOXYLATE → MALATE / ACETYL-CoA + OXALOACETATE → CITRATE' REACTION BLOCK

```
function [sys, x0] =
oacgam31(t,x,u,flag,k2,k9,cith,acgma,Malsyn,oxah,oxal,oxpe,Phocar,k11,droxa,drace)
% OACGAM31 Chemical reaction as an M-file
% OACGAM31 performs two chemical reactions:
% acetyl CoA + oxaloacetate -> citrate,
% acetyl CoA + glyoxylate -> malate
% incorporates the drains:
% oxaloacetate -> p-enol-pyruvate
% oxaloacetate -> amino acids and nucleotides
%acetyl-CoA -> amino acids and lipids

% u(1) = maximum flux out of acetyl vessel           = Fmace1;
% u(6) = maximum flux out of glyoxylate vessel       = Fmgly;
% u(3) = maximum flux out of oxaloacetate vessel     = Fmoxal;
% u(5) = [citrate]                                   = cit;
% u(4) = flux-out of citrate vessel                   = Focit;
% u(2) = [oxaloacetate]                              = oxa;

% y(2) = flux into the citrate vessel;
% y(3) = flux into malate vessel and out of glyoxylate vessel;
% y(1) = flux out of acetyl vessel;
% y(5) = flux into p-enol-pyruvate vessel;
% y(4) = flux out of oxaloacetate vessel;

% k2 = rate constant of oxa + ace -> cit;
% k9 = rate constant of gly + ace -> mal;
% droxa = oxaloacetate drain;
% drace = acetyl drain;
% acgma = part of ace flux going into glyoxylate bypass;
```



```

% oxpe = part of oxa flux going to pep;
% Malsyn = malate synthase, ace + gly -> mal;
% Phocar = phosphopyruvate carboxylase, oxa -> pep;

% drains are a fixed percentage of flux;

if abs(flag) == 1 % if flag = 1, return state derivatives xdot
    sys = [ ];

elseif flag == 3 % if flag = 3, return output y

    Fmace1 = u(1);
    Fmgly = u(6);
    Fmoxa1 = u(3);
    cit = u(5);
    Focit = u(4);
    oxa = u(2);

    oxadrain = Fmoxa1*droxa; % droxa = percentage oxadrain
    Fmoxa = Fmoxa1 - oxadrain;

    acedrain = Fmace1*drace; % drace = percentage acedrain
    Fmace = Fmace1 - acedrain;

% the reaction ace + gly -> mal has priority

if (Malsyn>0) % Gly-bypass on
    s1 = acglma*Fmace;
    Fgam = k9*min(s1,Fmgly); % flux from gly and ace to mal
    s2 = Fmace - Fgam; % remaining part of Foutace

if (Phocar>0) % pep drain open
    s3 = oxpe*Fmoxa;
    Fop = k11*s3; % flux from oxa to pep
    s4 = Fmoxa - Fop; % remaining part of Foutoxa

if (cit<cith)
    Foac = k2*min(s2,s4); % flux from oxa and ace to cit
else
    s5 = min(s2,s4);
    Foac = k2*min(s5,Focit);
end;
else
    Fop = 0; % pep drain off
if cit<cith;
    Foac = k2*min(s2,Fmoxa);
else

```

```

    s6 = min(s2,Fmoxa);
    Foac = k2*min(s6,Focit);
end;
end;

else % Gly-bypass off
    Fgam = 0;
    if (Phocar>0) % pep drain open
        s7 = oxpe*Fmoxa;
        Fop = k11*s7;
        s8 = Fmoxa - Fop;
        if (cit<cith)
            Foac = k2*min(Fmace,s8);
        else
            s9 = min(Fmace,s8);
            Foac = k2*min(s9,Focit);
        end;
    else
        Fop = 0; % pep drain off
        if cit<cith;
            Foac = k2*min(Fmace,Fmoxa);
        else
            s10 = min(Fmace,Fmoxa);
            Foac = k2*min(s10,Focit);
        end;
    end;
end;
end;

sys(2) = Foac;
sys(3) = Fgam;
sys(1) = Foac + Fgam + acedrain;
sys(5) = Fop;
sys(4) = Foac + Fop + oxadrain;

elseif flag == 0 % if flag = 0, return sizes of parameters and initial conditions
    sys = [ 0, 0, 5, 6, 0, 1 ];
    % sys(1) is number of continuous states
    % sys(2) is number of discrete states
    % sys(3) is number of outputs
    % sys(4) is number of inputs
    % sys(5) is number of roots that the system has
    % sys(6) is set to 1 because the system has direct feed-through
    % of its inputs (see file Matlab/toolbox/simulink/blocks/sfunc.m)
    x0 = [];
else % only continuous state
    sys = [ ];
end;

```

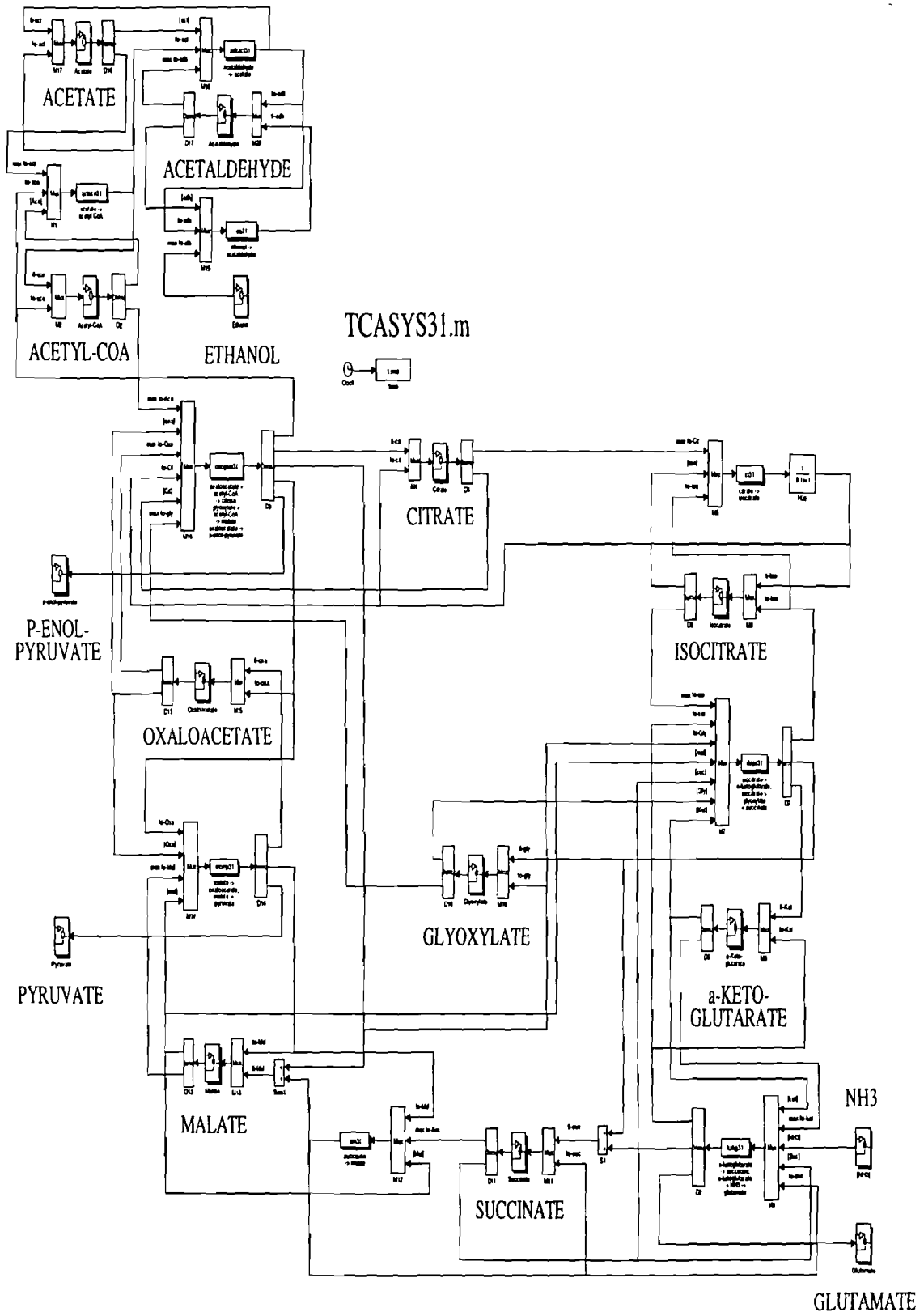


Figure C.1. Simulink diagram of the normalised simulation model, described in chapter 4.

D

SIMULATION RESULTS

A total of 8 simulations have been done to test the simulation model described in §4.2. Table D.1, which is exactly the same as table 4.4, shows all the settings of the simulation parameters.

Table D.1. *Settings of the simulation parameters for simulation 1 to 8.*
 $[X]_0 = \text{initial concentration of metabolite } X \text{ (mol} \cdot \text{dm}^{-3}_{\text{cell}})$.

simulation	1	2	3	4	5	6	7	8
$[\text{ADH}]_0$	0.9	0.9	0.9	0.2	0.6	0.6	0.6	0.6
$[\text{ACE}]_0$	0.9	0.9	0.9	0.2	0.6	0.6	0.6	0.6
$[\text{ACO}]_0$	0.9	0.9	0.9	0.2	0.6	0.6	0.6	0.6
$[\text{CIT}]_0$	0.9	0.9	0.9	0.2	0.6	0.6	0.6	0.6
$[\text{ISO}]_0$	0.9	0.9	0.9	0.2	0.6	0.6	0.6	0.6
$[\text{KET}]_0$	0.9	0.9	0.9	0.2	0.6	0.6	0.6	0.6
$[\text{GLY}]_0$	0.9	0.9	0.9	0.2	0.6	0.6	0.6	0.6
$[\text{SUC}]_0$	0.9	0.9	0.9	0.2	0.6	0.6	0.6	0.6
$[\text{MAL}]_0$	0.9	0.9	0.9	0.2	0.6	0.6	0.6	0.6
$[\text{OXA}]_0$	0.9	0.9	0.9	0.2	0.6	0.6	0.6	0.6
ethanol input ($\text{mol} \cdot \text{s}^{-1}$)	0.3	0.3	0.3	0.3	0.3	0.25→ 0.50→ 0.75→ 1.0	0.25→ 0.50→ 0.75→ 1.0	0.25→ 0.50→ 0.75→ 1.0
glyoxylate bypass	off	off	on	on	on	on	on	on
drains	off	on	on	on	on	on	on	on
integration method	linsim	linsim	linsim	linsim	linsim	linsim	gear	runge- kutta 5
simulation time (s)	30	100	50	30	30	200	200	200

The results of simulation 1-5, 7 and 8 will be discussed in this appendix. For all figures depicted in this appendix the graphics in the left column present the concentrations of the metabolites. The graphics in the right column show the corresponding f_i and f_o of these metabolites. For an explanation of the abbreviations see the glossary.

In simulation 1 the glyoxylate bypass and all drains are shut off. The results are shown in figure D.1. Ethanol provides just enough C-atoms to cover the losses caused by CO_2 in the cycle. As a result of this the summation of the concentrations of the metabolites in the TCA cycle remains constant throughout the simulation (see §3.6 simulation 2 and the footnote).

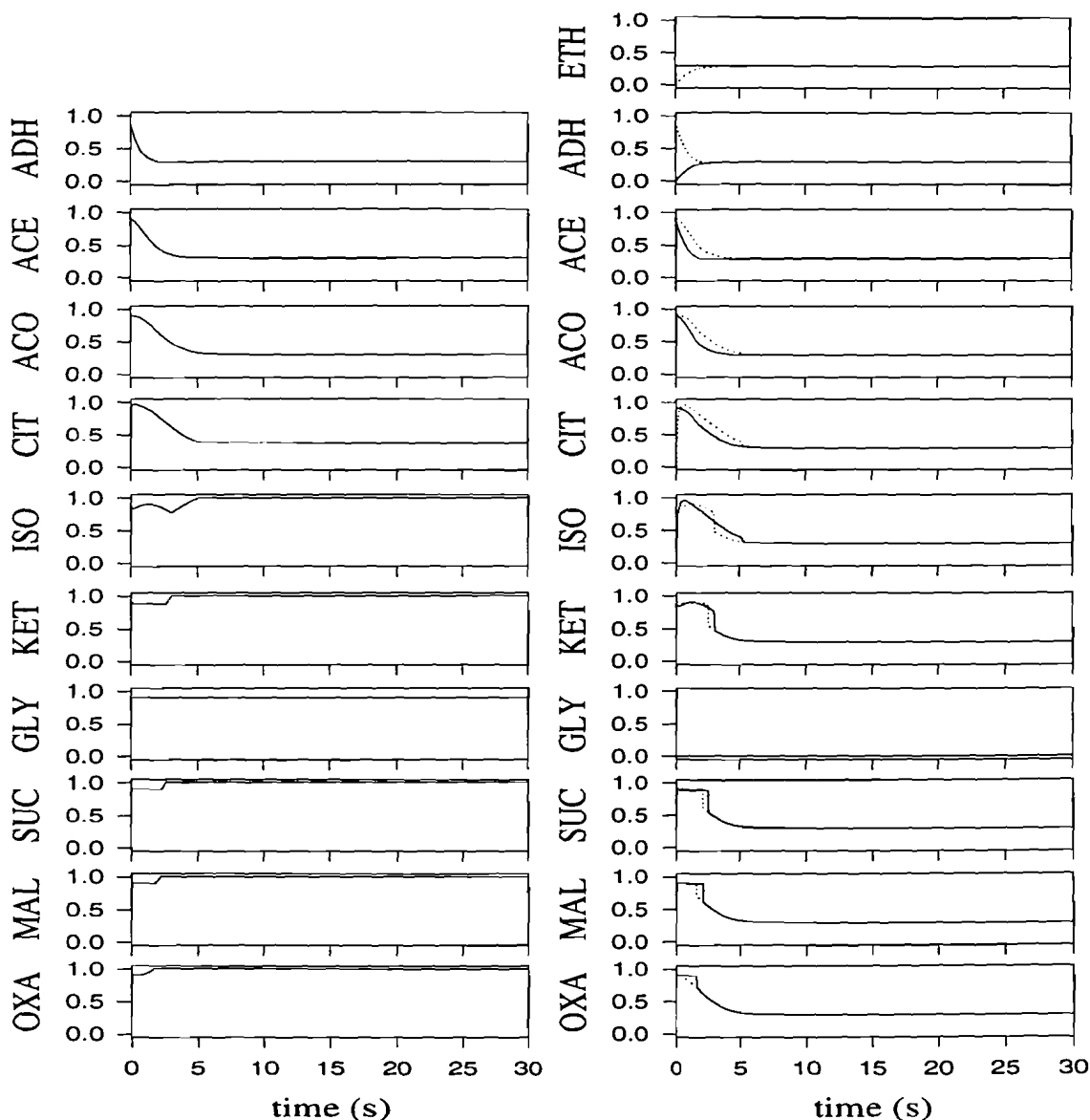


Figure D.1. Results of simulation 1.

Graphs in left column, solid line: concentration of every metabolite ($\text{mol} \cdot \text{dm}_{\text{cell}}^{-3}$).
 Graphs in right column, solid line: f_i of every metabolite; dotted line: f_o of every metabolite ($\text{mol} \cdot \text{s}^{-1} \cdot \text{dm}_{\text{cell}}^{-3}$).

In simulation 2, of which the results are shown in figure D.2, the drains are open, while the glyoxylate bypass is still turned off. Ethanol is no longer able to cover all the losses of the TCA cycle. This causes acetaldehyde, acetate and acetyl-CoA to accumulate, while all other metabolites drop slowly in time. When simulation 1 and 2 are compared, it can be seen that the drains empty the TCA cycle, causing the TCA cycle to stop after some time.

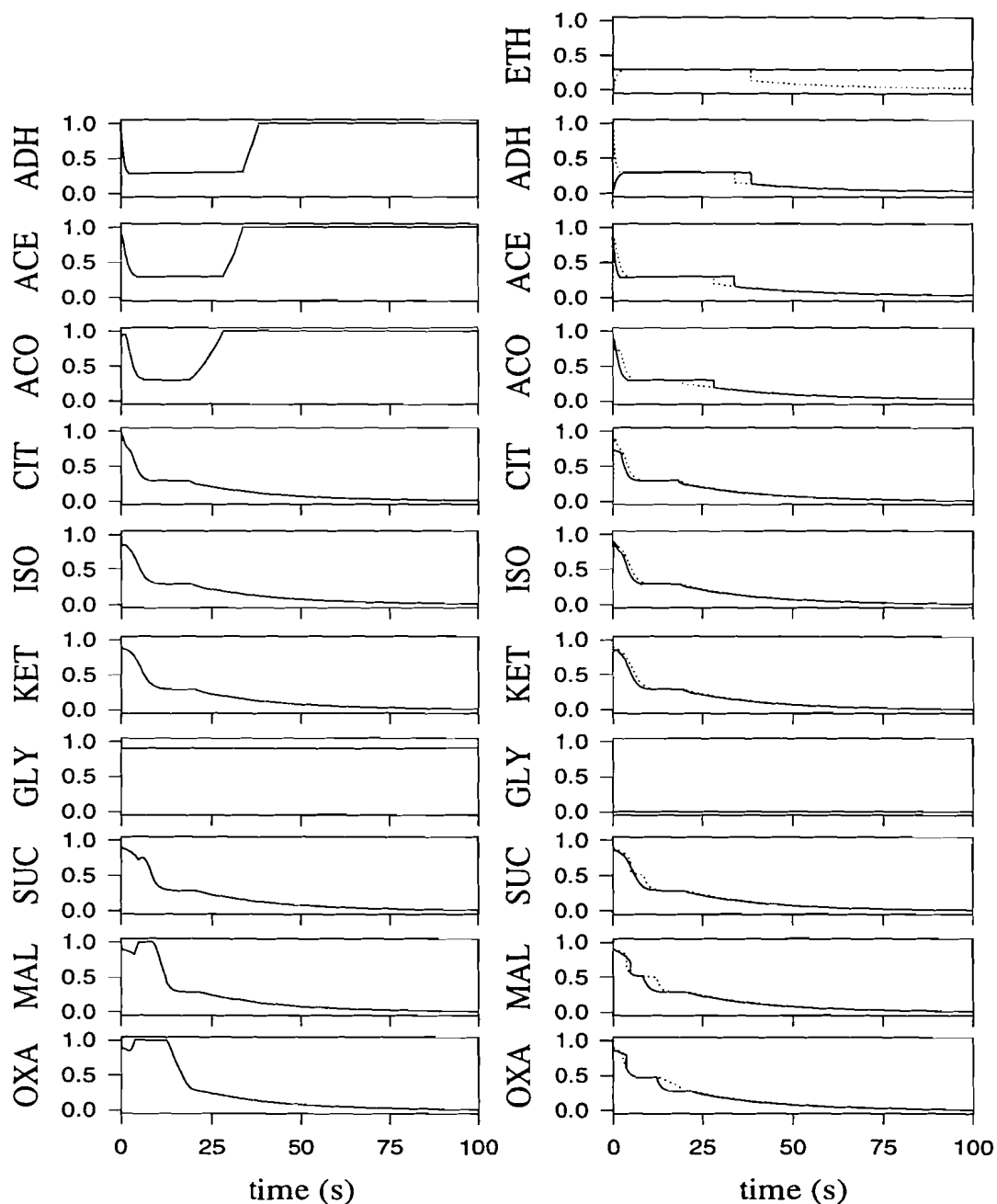


Figure D.2. Results of simulation 2.

Graphs in left column, solid line: concentration of every metabolite ($\text{mol} \cdot \text{dm}_{\text{cell}}^{-3}$).
 Graphs in right column, solid line: f_i of every metabolite; dotted line: f_o of every metabolite ($\text{mol} \cdot \text{s}^{-1} \cdot \text{dm}_{\text{cell}}^{-3}$).

To cover the losses caused by CO_2 and the drains, the glyoxylate bypass should be opened. This is done in simulation 3. Although the concentrations of most metabolites drop in the beginning, a steady state is reached after approximately 40s. When simulation 3 is compared with simulation 2, one can see that the glyoxylate bypass is able to compensate for the losses of the drains of the TCA cycle. The results are shown in figure D.3.

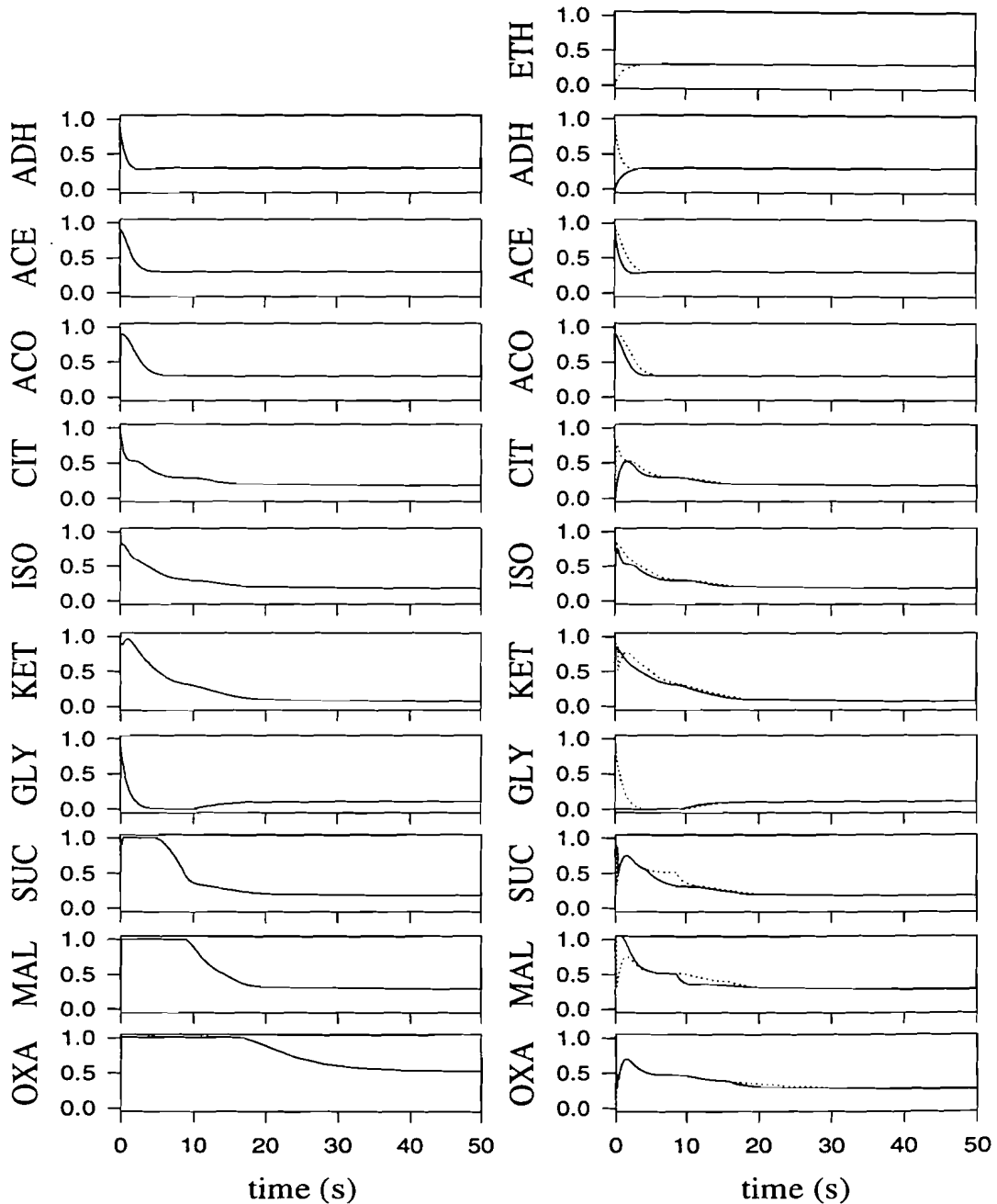


Figure D.3. Results of simulation 3.

Graphs in left column, solid line: concentration of each metabolite ($\text{mol} \cdot \text{dm}^{-3}_{\text{cell}}$).
 Graphs in right column, solid line: f_i of every metabolite; dotted line: f_o of every metabolite ($\text{mol} \cdot \text{s}^{-1} \cdot \text{dm}^{-3}_{\text{cell}}$).

Two simulations, 4 and 5, have been done with different initial concentrations of the metabolites, compared to simulation 3. When simulation 3, 4 and 5 are compared, they show that the steady state values of the model do not depend on the initial concentrations of the metabolites. The results are shown in figure D.4 and D.5.

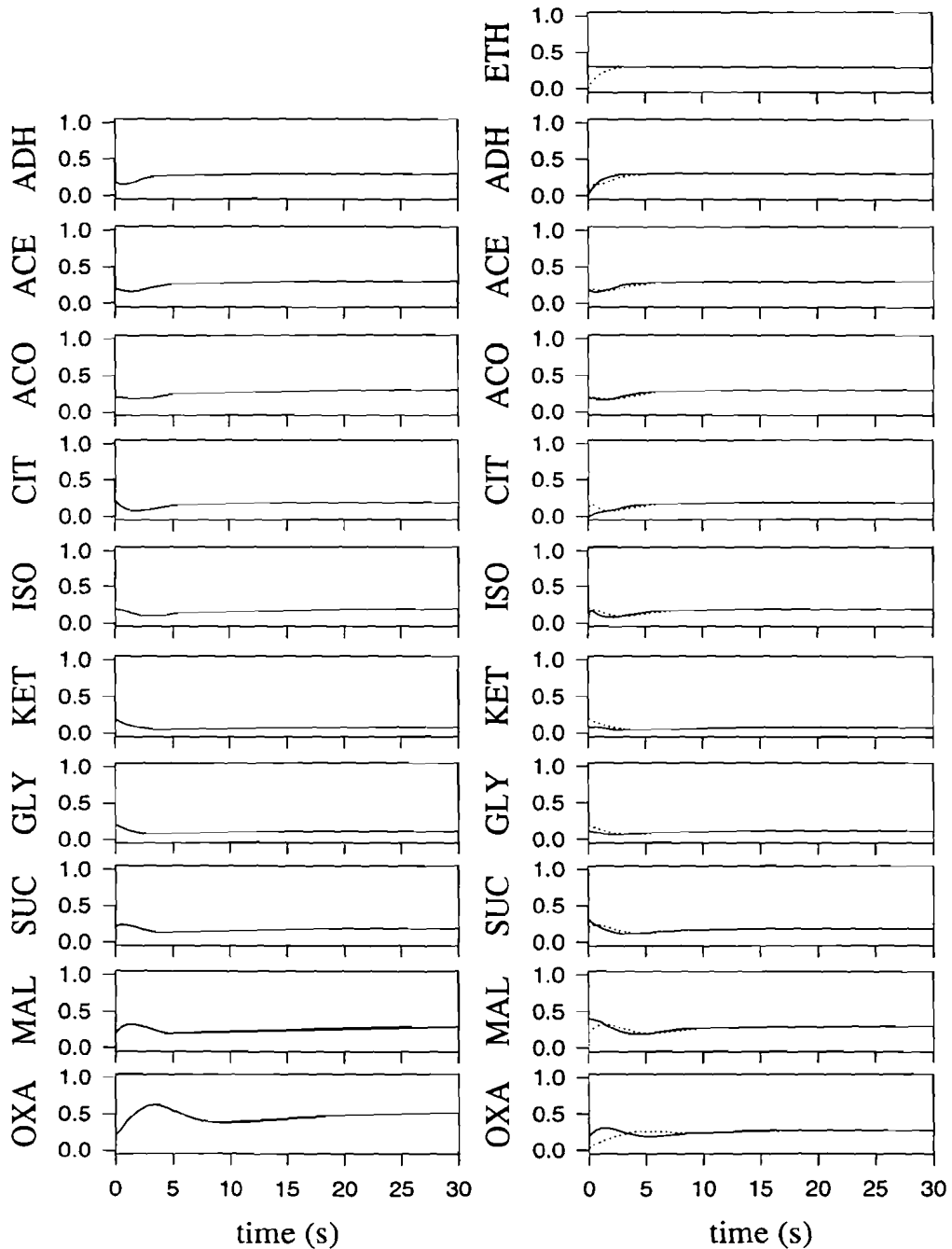


Figure D.4. Results of simulation 4.

Graphs in left column, solid line: concentration of each metabolite ($\text{mol} \cdot \text{dm}_{\text{cell}}^{-3}$).
 Graphs in right column, solid line: f_i of every metabolite; dotted line: f_o of every metabolite ($\text{mol} \cdot \text{s}^{-1} \cdot \text{dm}_{\text{cell}}^{-3}$).

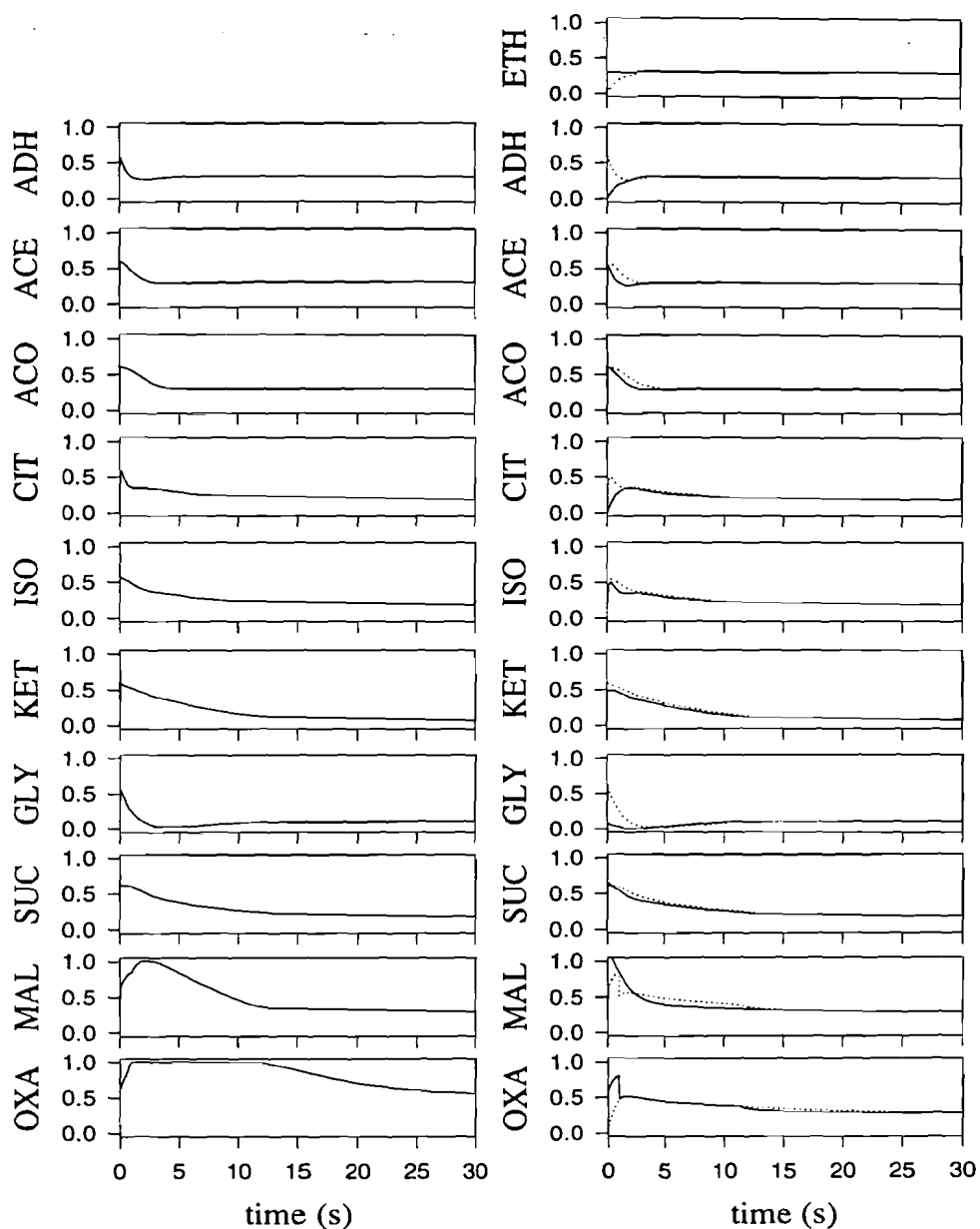


Figure D.5. Results of simulation 5.

Graphs in left column, solid line: concentration of each metabolite ($\text{mol} \cdot \text{dm}_{\text{cell}}^{-3}$).
 Graphs in right column, solid line: f_i of every metabolite; dotted line: f_o of every metabolite ($\text{mol} \cdot \text{s}^{-1} \cdot \text{dm}_{\text{cell}}^{-3}$).

To show that the steady state values do depend on the ethanol input, simulation 6 is done. This simulation is similar to simulation 5, only the ethanol input is changed. The ethanol input of simulation 5 remains at a constant value throughout the simulation, whereas in simulation 6 it is increased every 50s with 0.25, starting from 0.25. The results, depicted in figure 4.2 and discussed in §4.3, show that when the ethanol input gets above 0.5 the fluxes of the metabolites do not increase anymore. There is not enough oxaloacetate to react with acetyl-CoA into citrate, causing acetaldehyde, acetate and acetyl-CoA to accumulate. Apparently the glyoxylate bypass is pinched too much, resulting in a shortage of oxaloacetate.

Examining the oxaloacetate concentration in simulation 6 another deficiency can be seen. From $t=1s$ until $t=13s$ the oxaloacetate concentration is above the maximum level. This is a result of the if-then statement, which is used in every concentration block. Each timestep this if-then statement detects whether a concentration is equal or above a maximum level. When in one time step the concentration increases to the extent that it exceeds the maximum level, it is not set back to this maximum level. Instead the concentration remains constant at too high a value until f_o becomes larger than f_i .

To check whether the choice of integration method would have an influence on this phenomenon, simulation 7 and 8 were done. They both differ from simulation 6 only in applied integration method. Simulation 6 is done with the linsim integration method, simulation 7 is done with the Gear integration method and simulation 8 with the Runge-Kutta 5 integration method. From these 3 integration methods linsim performed best and Runge-Kutta 5 worst. Nevertheless, all three integration methods showed the unwanted effect. The results are depicted in figure D.6.

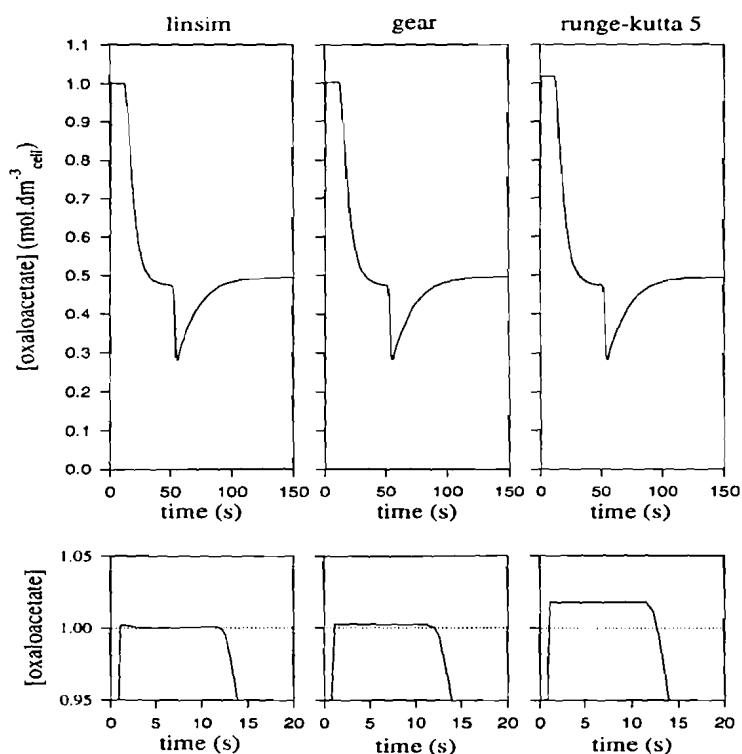


Figure D.6. Oxaloacetate concentration calculated with the linsim, Gear and Runge-Kutta 5 integration methods.

Upper graphs, solid line: oxaloacetate concentration.

The lower graphs are an enlargement from the first 20 seconds of the upper graphs, solid line: oxaloacetate concentration ($\text{mol} \cdot \text{dm}^{-3}_{\text{cell}}$).

From the simulations discussed in this appendix it can be concluded that:

- a. The glyoxylate bypass is able to compensate for the losses caused by the drains (simulation 1, 2 and 3);

- b. The steady state values of the simulation model depend only on the ethanol input (simulation 3, 4 and 5);
- c. Above an ethanol input of 0.5 the concentration of oxaloacetate becomes a limiting factor and as a result of this the fluxes do not show the same increment as the ethanol flux (simulation 6);
- d. Concentrations can increase above the maximum level (simulation 6);
- e. Preventing the concentrations from crossing the maximum value cannot be done by choosing another integration method, because each integration method shows this deficiency to a extend (simulation 6, 7 and 8).

E

IF-THEN STATEMENT

One of the problems which resulted from the simulations done in §4.3 is the concentration exceeding the maximum level. This is a result of the use of an if-then statement in the determination of the maximum concentration of a metabolite. A possible solution to this problem will be investigated in this appendix.

E.1 CONTINUOUS FUNCTION

A solution for the problem could be the design of a special function. This function should take care that the concentration level gradually reaches a value of one, instead of exceeding it due to the discrete nature of the if-then statement.

The if-then statement in the concentration block of a metabolite A is implemented as follows:

$$\begin{aligned} &\text{if } \{ [A(t)] \leq 0 \text{ and } (f_i(t) - f_o(t)) < 0 \} \text{ or } \{ [A(t)] \geq [A]_{\max} \text{ and } (f_i(t) - f_o(t)) > 0 \} \\ &\quad d[A(t)]/dt = 0 \\ &\text{else } d[A(t)]/dt = f_i(t) - f_o(t) \\ &\text{end.} \end{aligned} \quad (\text{E-1})$$

The concentration, f_i^A and f_o^A of metabolite A are all limited to the area $[0,1]$. Other values are not valid. If f is defined as f_i^A minus f_o^A , a so-called net flux, it contains the values $[-1,1]$. The concentration can be represented by a concentration vector $\underline{x}=[0,1]$ and the net flux by a flux vector $\underline{f}=[-1,1]$. Vector \underline{x} and \underline{f} span a surface S. With the vectors \underline{x} and \underline{f} , the if-then statement of equation (E-1) can be written in the following way:

$$d[A(t)]/dt = m_d(\underline{x}, \underline{f}) \cdot (f_i(t) - f_o(t)) \quad (\text{E-2})$$

In equation (E-2) $m_d(\underline{x}, \underline{f})$ is a discrete function which provides a multiplier m_d for every coordinate of the surface S in the same way as the if-then statement would do. From equation (E-1) it can be derived that $m_d(\underline{x}, \underline{f})$ should be zero for $\underline{x}=[0]$ and $\underline{f}=[-1,0]$ and for $\underline{x}=[1]$ and $\underline{f}=[0,1]$. For all other coordinates of surface S, $m_d(\underline{x}, \underline{f})$ has a value of one. Figure E.1 gives a graphical representation of $m_d(\underline{x}, \underline{f})$.

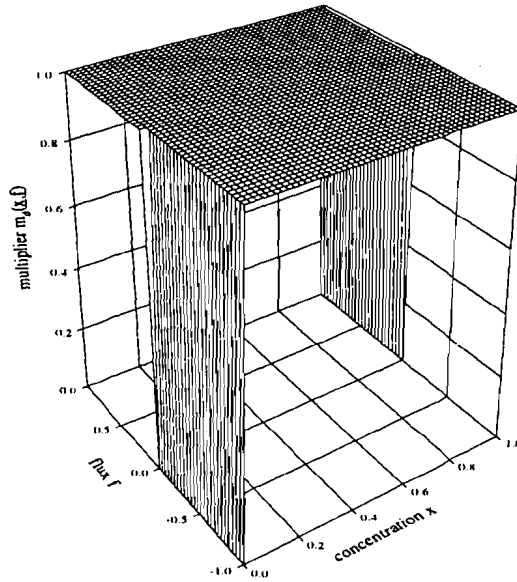


Figure E.1. Values of multiplier $m_d(\underline{x},f)$ for every coordinate of surface S .

The discrete nature of the if-then statement and of $m_d(\underline{x},f)$ will result in the concentration crossing the maximum level. Therefore, the discrete function $m_d(\underline{x},f)$ is replaced by a continuous multiplier $m_c(\underline{x},f)$, which would lead the concentration gradually to the maximum level and thus preventing it from crossing this upper bound.

The continuous multiplier $m_c(\underline{x},f)$ is designed in two steps. In the first step the line spanned by $f=[-1,1]$ and $\underline{x}=[-1]$ is considered. Figure E.2 shows $m_{d1}(\underline{x},f)$ for which a continuous function has to be designed.

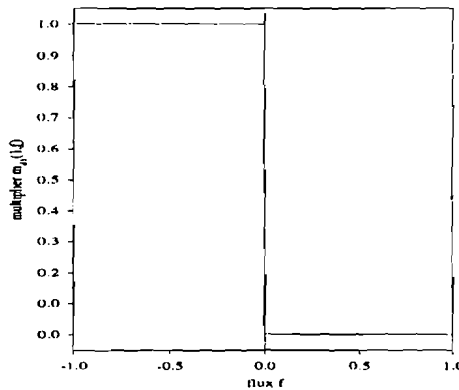


Figure E.2. Graphical representation of multiplier $m_{d1}(1,f)$ for $f=[-1,1]$.

The function shown in figure E.2 can be approximated by a tangent hyperbolic. Important is the fact that $m_{c1}(\underline{x},f)$ has to be zero for $f=[0 \dots 1]$ and $\underline{x}=[1]$, because only a negative flux can alter the concentration. The function

$$m_{c1} = 0.5 + 0.5 \tanh(-50f - 3) \tag{E-3}$$

appears to be a suitable approximation, as shown in figure E.3.

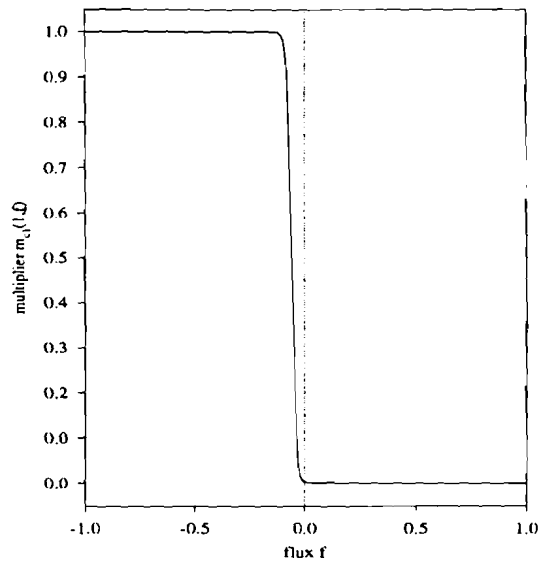


Figure E.3. Graphical representation of multiplier $m_{c1}(1, f)$ for $f \in [-1, 1]$.

Figure E.4 shows the ideal multiplier $m_{d2}(0, f)$ and a suitable continuous multiplier $m_{c2}(0, f)$ as an approximation for the line $f \in [-1 \dots 1]$. Multiplier $m_{d2}(0, f)$ and $m_{c2}(0, f)$ are shown in figure E.4.

$$m_{c2} = 0.5 + 0.5 \tanh(50f - 3) \quad (\text{E-4})$$

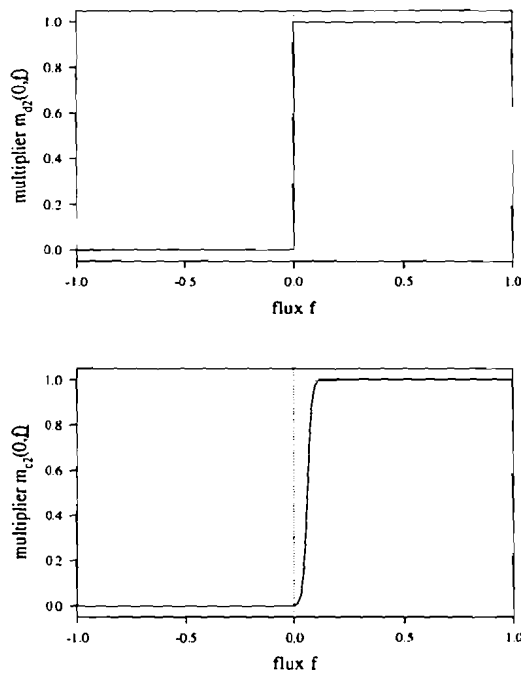


Figure E.4. Upper graph: multiplier $m_{d2}(0, f)$ for $f \in [-1 \dots 1]$.
 Lower graph: multiplier $m_{c2}(x, f)$ for $f \in [-1 \dots 1]$.

Equations (E-3) and (E-4) can be written in a more general form as

$$m_{c1} = a_1 + b_1 \tanh(-50f - 3) \quad (\text{E-5A})$$

$$m_{c2} = a_2 + b_2 \tanh(50f - 3) \quad (\text{E-5B})$$

The second step in developing a continuous representation for an if-then statement consists of designing continuous functions for the variables a_1 , a_2 , b_1 and b_2 . These variables have to be adjusted for different values of concentration x . Figure E.5 shows different functions of multiplier $m_{c1}(x,f)$ and $m_{c2}(x,f)$ for different values of concentration x . For simplicity the changes of $m_{c1}(x,f)$ and $m_{c2}(x,f)$ are linear. These different functions are listed in table E.1.

Table E.1. Different functions of multiplier m_{c1} and m_{c2} for different values of concentration x .

x	f	$m_{c1}(x,f)$	x	f	$m_{c2}(x,f)$
1	[-1... 1]	$0.5+0.5 \cdot \tanh(-50f-3)$	0	[-1... 1]	$0.5+0.5 \cdot \tanh(50f-3)$
$1-\delta$	[-1... 1]	$0.55+0.45 \cdot \tanh(-50f-3)$	δ	[-1... 1]	$0.55+0.45 \cdot \tanh(50f-3)$
$1-2\delta$	[-1... 1]	$0.60+0.40 \cdot \tanh(-50f-3)$	2δ	[-1... 1]	$0.60+0.40 \cdot \tanh(50f-3)$
$1-10\delta$	[-1... 1]	$1+0 \cdot \tanh(-50f-3)$	10δ	[-1... 1]	$1+0 \cdot \tanh(50f-3)$

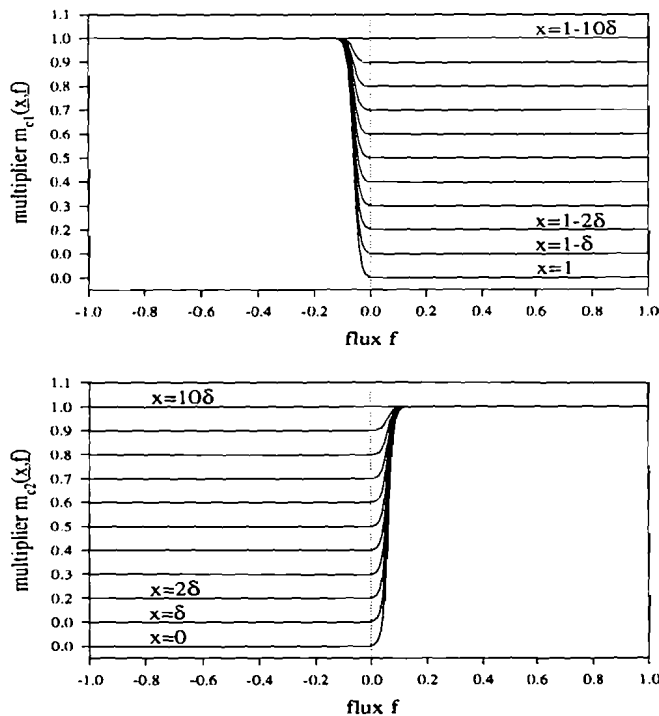


Figure E.5. Functions $m_{c1}(x,f)$ and $m_{c2}(x,f)$ for different values of concentration x . δ is a very small number.

Table E.1 shows that variable a_1 goes from 0.5 to 1 and variable b_1 goes from 0.5 to 0 when the concentration increases from 0 to 10δ . Variable a_2 increases from 0.5 to 1 and variable b_2 decreases from 0.5 to 0 if the concentration decreases from 1 to $1-10\delta$. The values of a_1 , b_1 , a_2 and b_2 can be seen as minimum and maximum bounds of these variables. The variables can be represented by continuous functions that start from the minimum bound and reach the maximum bound fast. These continuous functions can be approximated by an exponential function. Figure E-6 shows for each variable a suitable function. These functions are:

$$a_1 = 1 - \frac{1}{3.81 \cdot 10^{21}} \exp(50x - 1) \quad (\text{E-6A})$$

$$b_1 = \frac{1}{3.81 \cdot 10^{21}} \exp(50x - 1) \quad (\text{E-6B})$$

$$a_2 = 1 - \frac{1}{2.82 \cdot 10^{22}} \exp(50(-x + 1) + 1) \quad (\text{E-6C})$$

$$b_2 = \frac{1}{2.82 \cdot 10^{22}} \exp(50(-x + 1) + 1) \quad (\text{E-6D})$$

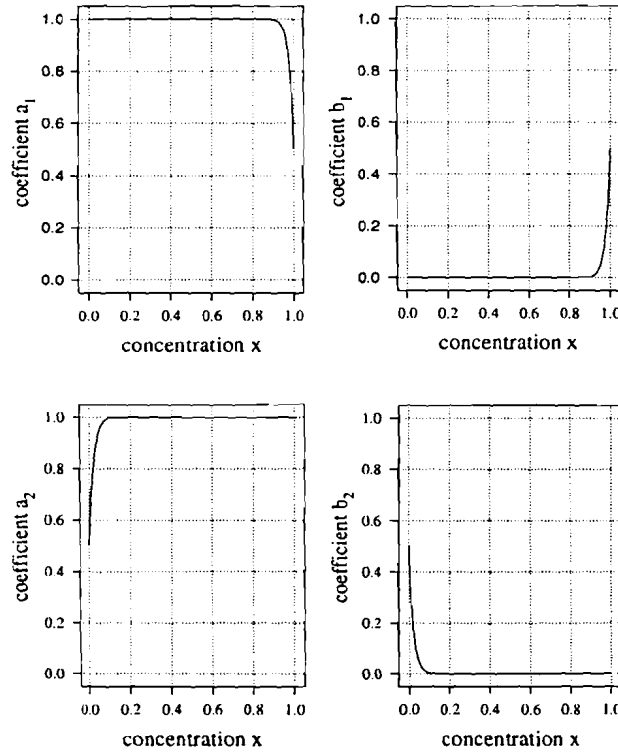


Figure E.6. Graphical representation of equations (E-6A-D).

When equations (E-6A-D), (E-5A) and (E-5B) are combined the continuous function $m_c(x,f)$ which can replace the if-then statement is formed. This continuous function is given in equation (E-7) and shown in figure E.7.

$$m_c(x,f) = m_{c1}(x,f) + m_{c2}(x,f);$$

$$= \left(\begin{array}{l} 1 - \frac{1}{3.81 \cdot 10^{21}} \exp(50x-1) + \frac{1}{3.81 \cdot 10^{21}} \exp(50x-1) \cdot \tanh(-50f-3) \\ 1 - \frac{1}{2.82 \cdot 10^{22}} \exp(50(-x+1)+1) + \frac{1}{2.82 \cdot 10^{22}} \exp(50(-x+1)+1) \cdot \tanh(50f-3) \end{array} \right) \quad (\text{E-7})$$

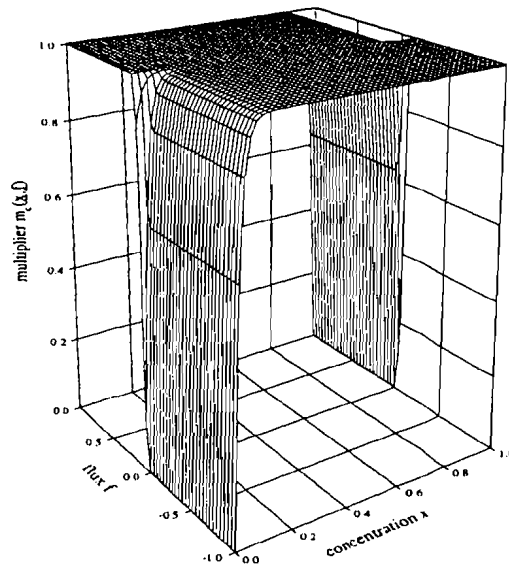


Figure E.7. Graphical presentation of $m_c(x,f)$ (equation (E-7)).

E.2 COMPARISON BETWEEN IF-THEN STATEMENT AND CONTINUOUS FUNCTION

The behaviour of the simulation model with the continuous function or the if-then statement has been compared on two issues. The first issue concerns the concentration level and the second one the required simulation time.

The if-then statement as it is used in calculating the concentration of a metabolite is exchanged by the continuous function of equation (E-7). The implementation of the continuous function in the simulation program becomes:

$$\frac{dx}{dt} = m_c(x,f) \cdot (f_i - f_o)$$

$$= \left(\begin{array}{l} 1 - \frac{1}{3.81 \cdot 10^{21}} \exp(50x-1) + \frac{1}{3.81 \cdot 10^{21}} \exp(50x-1) \cdot \tanh(-50f-3) \\ 1 - \frac{1}{2.82 \cdot 10^{22}} \exp(50(-x+1)+1) + \frac{1}{2.82 \cdot 10^{22}} \exp(50(-x+1)+1) \cdot \tanh(50f-3) \end{array} \right) \cdot (f_i - f_o) \quad (\text{E-8})$$

The implementation of the if-then statement is shown in §E.1. Each implementation is put in a S-functions in Simulink. Two small simulation models were made to calculate the concentration of a metabolite. One contained the if-then statement and the other one the continuous function. Each simulation model has two inputs: flux in and flux out. With these simulation models it was checked whether the calculated concentrations were equal and whether there was a difference in required simulation time.

E.2.1 CONCENTRATION

First of all it is examined whether there is a difference in calculating the concentration. This is done by putting the same net flux on both simulation models. The calculated concentration levels are subtracted from each other, in order to demonstrate the difference. This is shown in figure E.8A-F for three different net fluxes. Figure E.8A, E.8C and E.8E show the net flux and concentration level calculated with the if-then statement. Figure E.8B, E.8D and E.8F give concentration levels calculated with the if-then statement and continuous function and furthermore, they show the difference between these calculated concentration levels.

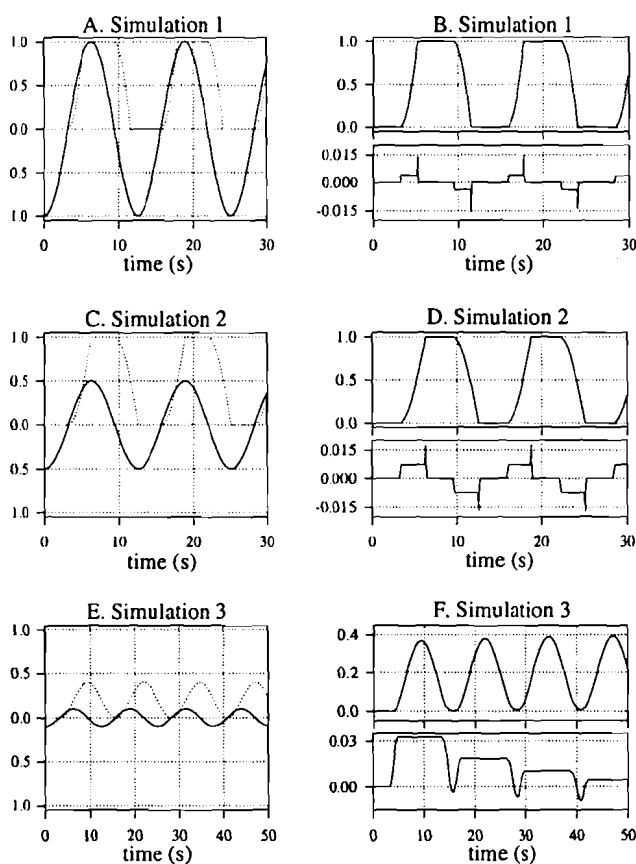


Figure E.8. Net fluxes, concentration and difference in concentration levels for 3 simulations. Graph A, C, E: solid line: concentration ($\text{mol} \cdot \text{dm}_{\text{cell}}^{-3}$); dotted line: net flux ($\text{mol} \cdot \text{s}^{-1}$). Upper graph of B, D, F: concentration calculated with continuous function. Lower graph of B, D, F: concentration of if-then statement minus concentration of continuous function.

Figure E.8 shows that there is no difference in calculated concentration when the concentration is at the maximum or minimum level. If the net flux is changing and the concentration is somewhere between the upper and lower bound there is a difference in calculated concentration. Both the lower graphs of figure E.8B and E.8D show a spike and a platform, whereas the lower graph of figure E.8F only shows a platform. Figure E.9 shows a contourplot of simulation 1 and 2.

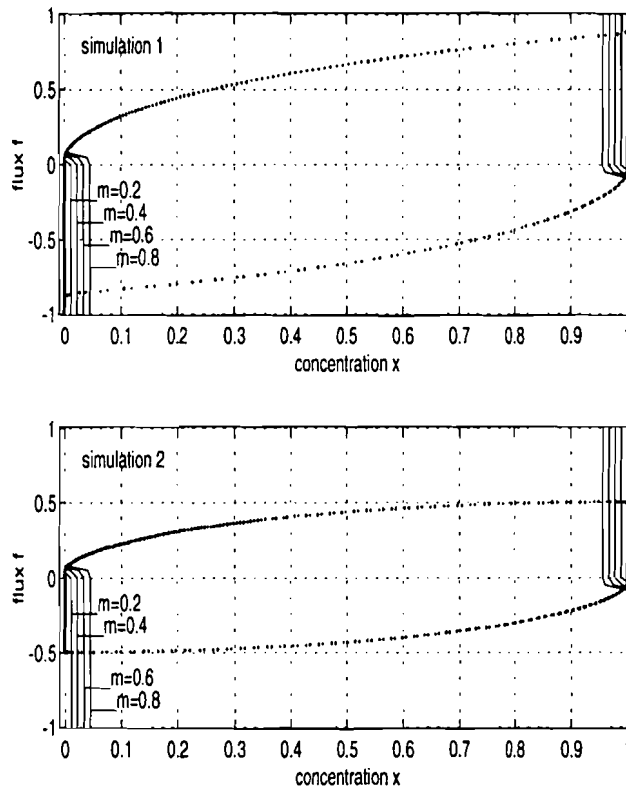


Figure E.9 Contourplots of simulation 1 and 2.

Both graphs: solid line: contourlines of multiplier m , each line shows an increment of 0.2; dotted line: trajectory of concentration x and flux f .

With the upper graph in figure E.9 the difference in calculated concentration for simulation 1 can be explained. Each period of the flux, starting at $f=-1$ (see figure E.8A) the trajectory follows the path from (x,f) is $(0,0)$, $(1,0.8)$, $(1,1)$, $(1,0)$, $(0,-0.8)$ to $(0,-1)$. The platform, shown in the lower graphs of figure E.8B, E.8D and E.8F occurs after $(x,f) = (0,0)$. In this case the if-then statement reaches value one in just one step, whereas multiplier $m_c(x,f)$ needs more time to reach value one. The same happens when concentration x approaches value one. Multiplier $m_c(x,f)$ then decreases compared to the if-then statement. The difference in this case is even larger, causing the spike. The magnitude of the spike is larger than the magnitude of the platform because of the difference in density of the contourlines for $(x,f)=(0,0 \dots 0.1)$ and $(1,0.9 \dots 1)$. In other words, the tangent hyperbolic part of equation (E-7) reaches one faster than the exponential part.

The fact that the difference in calculated concentration for simulation 2 is larger than for simulation 1 can be explained with figure E.10. The simulations are done with fixed time steps of 0.05 s. Figure E.10 makes clear that simulation 2 needs 10 steps to go from $(x,f) = (0,0.04)$ and cross the contourline $m_c=0.8$. Simulation 1 does this in 6 steps. This results in a faster increasing multiplier $m_c(x,f)$ for simulation 1, making the difference in calculated concentration smaller than in the case of simulation 2.

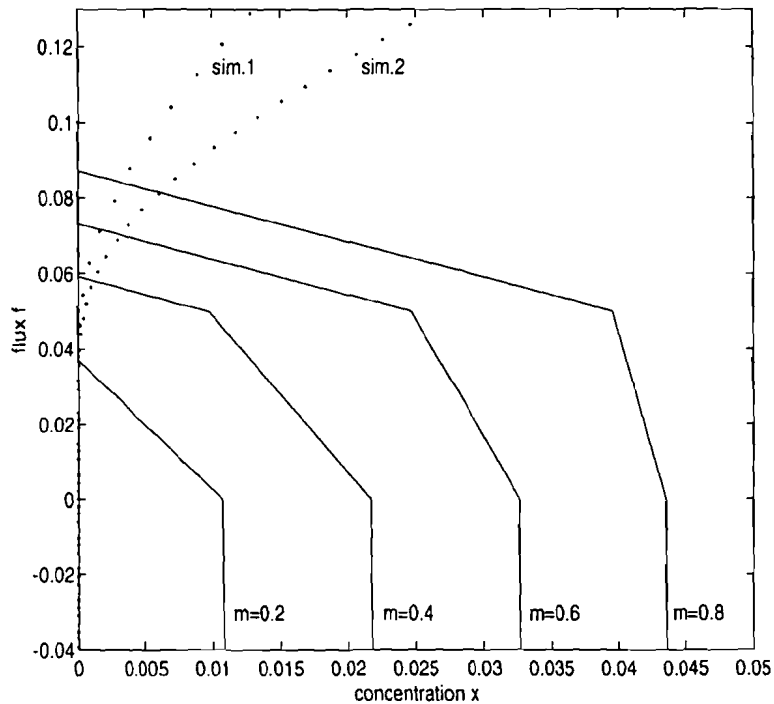


Figure E.10. *Contourplot of multiplier $m_c(x,f)$ and the trajectories of simulation 1 and 2. Solid lines: contourlines, each line shows an increment of 0.2; dotted lines: trajectory of concentration x and flux f of simulation 1 and 2.*

The difference in calculated concentration of figure E.8F is explained with figure E.11.

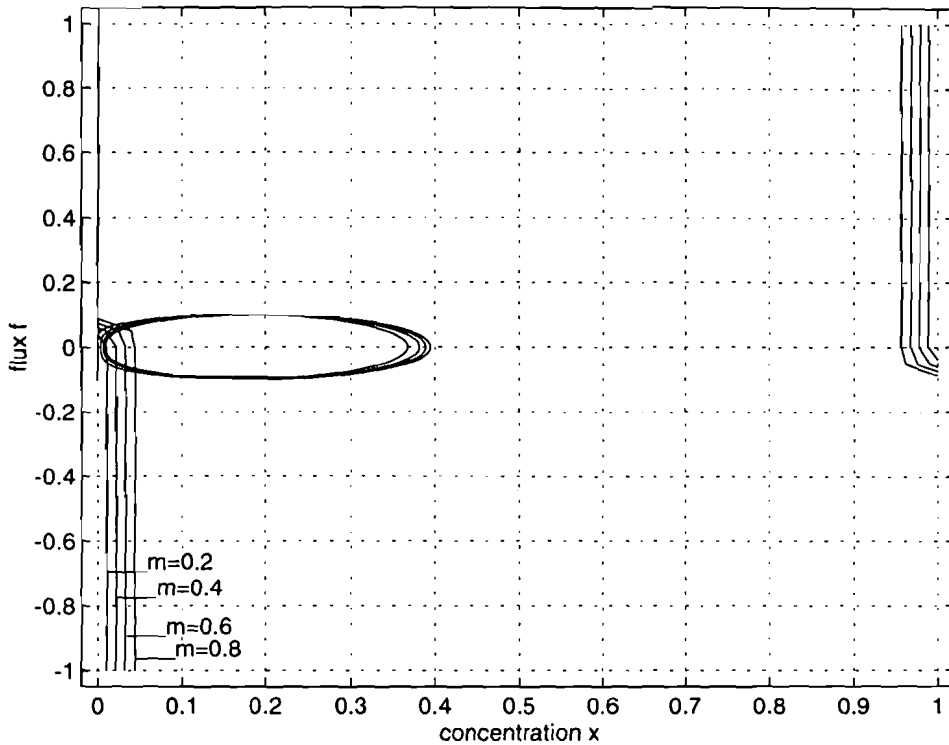


Figure E.11. Contourplot of simulation 3.

Solid line: contourlines of multiplier $m_c(x, f)$, each line shows an increment of 0.2.

Broken line: trajectory of concentration x and flux f .

In figure E.11 the trajectory turns clockwise in time. When concentration x increases from 0 to 0.5 multiplier $m_c(x, f)$ reaches value one faster than in the situation where x decreases from 0.5 to 0. As a result of this an ever increasing concentration is calculated with the continuous function, making the difference in calculated concentration larger each period of flux f .

E.2.2 REQUIRED SIMULATION TIME

The two simulation models were also used to check whether there was a difference in required simulation time between the continuous function and the if-then statement. The parameters which could influence the simulation time are minimum and maximum stepsize and tolerance. For different maximum and minimum stepsize and different tolerance, the required simulation time when the net flux is oscillating is given in table E.1.

Table E.1. *Required simulation time with an oscillating net flux.*

simulation n	minimum stepsize	maximum stepsize	tolerance	if-then statement	continuous function
1	0.01	0.01	1e-8	27 s	41 s
2	0.01	1	1e-8	2 s	8s
3	0.001	0.1	1e-8	4s	9 s
4	0.001	1	1e-8	2 s	8 s
5	0.001	1	1e-6	2 s	7 s
6	0.001	1	1e-4	2 s	4 s
7	0.001	1	1e-10	4 s	17 s
8	0.001	1	1e-15	17 s	110 s

Table E.2 shows that in all simulations the continuous function is slower than the if-then statement. Simulation 1 shows that for a fixed stepsize the continuous function is almost once as slow as the if-then statement. This is due to the number of calculations which have to be made in the continuous function. Simulation 1 and 2 show that increasing the maximum stepsize the if-then statement becomes almost 14 times faster, whereas the simulation time for the continuous function is reduced by a factor 5. A tenfold smaller minimum stepsize (simulation 2 and 4) has no effect on the required simulation time.

When the tolerance is reduced (simulation 4, 5 and 6) the continuous function becomes faster, whereas the tolerance is increased (simulation 4, 7 and 8) the continuous function slows down more than the if-then statement.

E.3 CONCLUSIONS

The difference in calculated concentration for the if-then statement and the continuous function is only zero when the concentration is constant in time. When there is no steady state, i.e. the net flux has a slope larger than zero, a difference in calculated concentration occurs. This is due to the fact that the continuous function needs a number of steps to reach value zero or one. The worst case appears when the net flux is oscillating and the concentration does not reach the maximum level. In this case the difference between the if-then statement and the continuous function reveals a strange course: the deviation starts off with a positive value and ends with a significantly negative value.

It has been checked whether the required time for a simulation depends on minimum or maximum stepsize or tolerance. The results show that they all influence the simulation time. In all cases a simulation with the continuous function needed more time. It differed from twice as much when the minimum and maximum stepsize are equal to eleven times as much when the minimum and maximum stepsize were different and the tolerance was very small.

The above results show that the if-then statement can not be replaced by the continuous function, given in equation (E-7). Not only is the required time for a simulation with the continuous function larger, also the deviations, which occur at an oscillating net flux and a concentration level which does not reach a maximum, are unacceptable.

F

LISTING OF MINXY, TCAMIN AND WINDOW

For the minimisation procedure described in chapter 4, one matlab routine, named MINXY, and two matlab functions, named MINTCA and WINDOW, were written. The function MINTCA runs a simulation and determines concentrations and fluxes of all metabolites for a given value of exponent x and y . The function WINDOW takes that part of the acetyl-CoA and oxaloacetate concentration vector for which the sum of squares (SSQ) has to be determined and calculates it. This sum of squares is passed on to the routine MINXY, where new values for x and y are calculated. These new values of x and y are passed on to MINTCA to run another simulation. The WINDOW function is written to be able to leave out transient states in the minimisation procedure. During transient states, the concentration of acetyl-CoA and oxaloacetate can differ to such an extent that it would have too big an influence on the minimisation results.

LISTING OF MINXY

```
% name: minxy.m
% minimalise x and y of ikigs33.m in tcasys33.m
% first run initca33 and fiteth3 in matlab workspace
% write in workspace global x y fid;
%         fid=fopen('010496-1.txt','wt');
%         x= ...;
%         y= ...;

xz0=[x y] % initial values for x and y;

options(3)=[0.01]; % termination tolerance on F
options(16)=[0.001]; % minimum change in variables for fin.diff.grad.
options(17)=[0.1]; % maximum change in variables for fin.diff.grad.
options(18)=[0.1]; % steplength

fprintf(fid,'size(e)  x      y      sum of squares \n');

xy=leastsq('mintca',xy0,options);

p1=[x];
p2=[y];
fprintf(fid,'ready \n');
```



```
fprintf(fid,'c1 = %f.\n',p1);
fprintf(fid,'c2 = %f.\n',p2);
fclose('all');
```

```
disp('ready');
xy=[x y]
```

LISTING OF MINTCA

```
function y=mintca(xy)
% MINTCA minimalises xy=[x,y] of ikigsmin.m
% goes with tcasymin.m
% is used in minxy.m
```

```
global c1 c2 fid;
x=xy(:,1);
y=xy(:,2);
```

```
options(2)=[1]; % minimum stepsize
options(3)=[1]; % maximum stepsize
options(6)=[2]; % plot parameter off
```

```
linsim('tcasys31',2400,[],options);
load oxaloace;
load acetyl;
```

```
% acetyl window
ACE=window(50,2390,acetyl');
```

```
% oxaloacetate window
OXA=window(50,2390,oxaloace');
```

```
e=OXA(:,2)-ACE(:,2);
y=e;
sosq=e'*e;
```

```
p=[size(e) x y sosq];
q=[x y sosq]
```

```
fprintf(fid,'%4.0f %2.0f %10.4f %10.4f %10.6f\n',p);
```

LISTING OF WINDOW

```
function y=window(b,e,x);
% WINDOW puts a window over x':
% b<= window < e.
% b and e refer to values of the first column of x'.
```

```
g=find(x(:,1)>e);  
n=size(g);
```

```
X=flipud(x);  
X(1:n(:,1),:)=[];  
x=flipud(X);
```

```
g=find(x(:,1)<b);  
n=size(g);
```

```
x(1:n(:,1),:)=[];  
y=x;
```

G

LISTING OF ALTERED CONCENTRATION BLOCK, FLUX BLOCK AND REACTION BLOCK AND SIMULINK DIAGRAM OF DENORMALISED SIMULATION MODEL

LISTING OF ALTERED ACETYL-CoA CONCENTRATION BLOCK

```
function[sys,x0] = aco(t,x,u,flag,acoh,x0Aco,Acecar,kaco)
% ACO.m calculates the concentration of acetyl-CoA,

% u(1) = flux in;
% u(2) = flux out;
% x0Aco = initial concentration of acetyl;
% x = [acetyl-CoA];
% Kaco = rate constant of acetyl-CoA;
% Acecar = acetyl-CoA carboxylase enzyme for
% amino acids and lipids drain form acetyl-CoA;
% acoh = maximum concentration of acetyl-CoA;

% y(1) = x;
% y(2) = acetyl drain to amino acids and lipids

if abs(flag) == 1 % xdot
    if ((x<=0)&((u(1)-u(2)-kaco*x*Acecar)<0))|((x>=acoh)&((u(1)-u(2)-kaco*x*Acecar)>0))
        sys(1) = 0;
    else
        sys(1) = u(1) - u(2) - kaco*x*Acecar;
    end;

elseif flag == 3 % output
    sys(1) = x;
    sys(2) = kaco*x*Acecar; % acetyl drain

elseif flag == 0 % return sizes of parameters and initial conditions
    sys = [ 1, 0, 2, 2, 0, 0];
```

```

% sys(1) is number of continuous states
% sys(2) is number of discrete states
% sys(3) is number of outputs
% sys(4) is number of inputs
% sys(5) is number of roots that the system has
% sys(6) is set to 0 because the system has no direct feed-through
%   of its inputs (see file Matlab/toolbox/simulink/blocks/sfunc.m)

x0 = [x0Aco];

else           % only continuous states
    sys = [ ];
end;

```

LISTING OF ALTERED ACETYL-CoA FLUX BLOCK

```

function[sys,x0] = acoflux(t,x,u,flag,kaco)
% ACOFLUX determines the flux out of the acetyl vessel,

% u = [acetyl-CoA];
% y = flux-out;

if abs(flag) == 1           % xdot
    sys = [];

elseif flag == 3           % output
    sys = kaco*u;

elseif flag == 0           % return sizes of parameters and initial conditions
    sys = [ 0, 0, 1, 1, 0, 1];
    x0 = [];

else           % only continuous states
    sys = [ ];
end;

```

LISTING OF ALTERED 'ACETYL-COA + GLYOXYLATE -> MALATE / ACETYL-COA + OXALOACETATE -> CITRATE' REACTION BLOCK

```

function [sys, x0] = oacgam(t,x,u,flag,cith,Malsyn)
% OACGAM performs two chemical reactions:
% acetyl CoA + oxaloacetate -> citrate,
% acetyl CoA + glyoxylate -> malate and

% u(1) = maximum flux out of acetyl vessel      = Fmace;
% u(2) = maximum flux out of oxaloacetate vessel = Fmoxa;
% u(3) = flux-out of citrate vessel             = Focit;

```

```

% u(4) = [citrate] = cit;
% u(5) = maximum flux out of glyoxylate vessel = Fmgly;
% y(1) = flux out of acetyl vessel;
% y(2) = flux into the citrate vessel and flux out of oxaloacetate vessel;
% y(3) = flux into malate vessel and out of glyoxylate vessel;
% cith = maximum concentration of citrate;
% Malsyn = malate synthase, enzyme of reaction ACE + GLY -> MAL;

if abs(flag) == 1 % if flag = 1, return state derivatives xdot
    sys = [ ];
elseif flag == 3 % if flag = 3, return output y
    Fmace = u(1);
    Fmoxa = u(2);
    Focit = u(3);
    cit = u(4);
    Fmgly = u(5);

% the reaction ace + gly -> mal has priority
if (Malsyn>0) % Gly-bypass on
    Fgam = min(Fmace,Fmgly); % flux from gly and ace to mal
    s1 = Fmace - Fgam; % remaining part of Foutace
    if (cit<cith)
        Foac = min(s1,Fmoxa); % flux from oxa and ace to cit
    else
        s2 = min(s1,Fmoxa);
        Foac = min(s2,Focit);
    end;
else % Gly-bypass off
    Fgam = 0;
    if (cit<cith)
        Foac = min(Fmace,Fmoxa);
    else
        s3 = min(Fmace,Fmoxa);
        Foac = min(s3,Focit);
    end;
end;

sys(1) = Foac + Fgam;
sys(2) = Foac;
sys(3) = Fgam;
elseif flag == 0 % if flag = 0, return sizes of parameters and initial conditions
    sys = [ 0, 0, 3, 5, 0, 1 ];
    x0 = [];
else % only continuous state
    sys = [ ];
end;

```

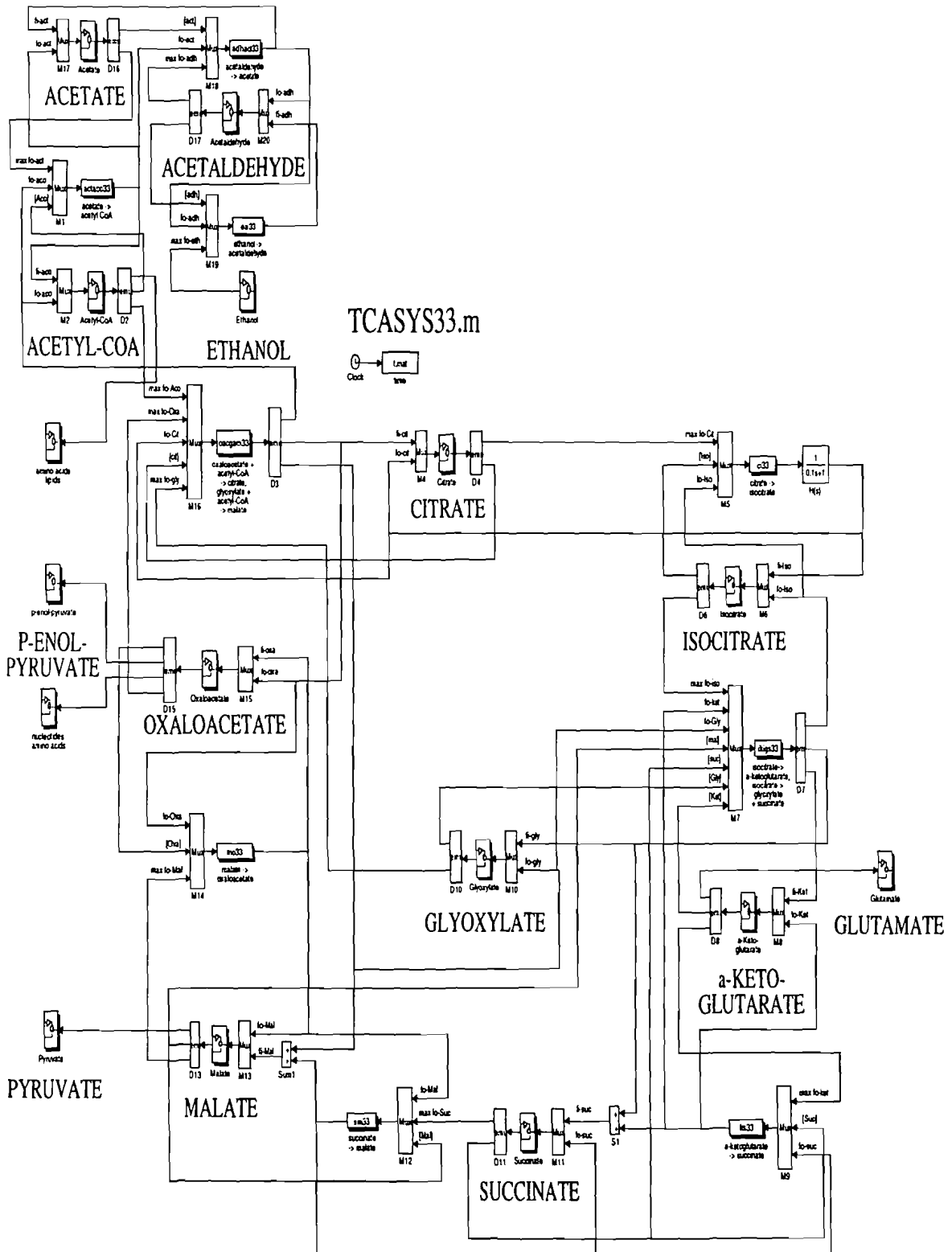


Figure G.1. Simulink diagram of the denormalised simulation model, described in chapter 5.

要 旨

生物の主要代謝経路の一つであるトリカルボン酸 (TCA) サイクルとグリオキシル酸側路よりなる複合反応サイクル系を対象とし、その中間代謝産物の生成・消費速度及び濃度の時間変化を算出することを可能とするシミュレーションモデルを開発した。本モデルを酵母 *Saccharomyces cerevisiae* がエタノールを炭素源とする連続培養において示す自律的代謝振動現象のデータ解析に適用し、本現象の機構の検討を行った。

本シミュレーションモデルは、3つの異なった構成ブロック、即ち、各々の中間代謝産物の濃度を示す濃度ブロック、各代謝産物の速度を表す速度ブロック及び各反応ステップの収支を表現する反応ブロックより構成される。濃度ブロックにおいては、各中間代謝産物の濃度変化を流入 (Flux_{in}) と流出フロー (Flux_{out}) の差に基づいて算出する。速度ブロックは基質となる代謝物質の濃度及び反応速度定数を基に Flux_{out} を算出する。反応ブロックでは各反応ステップの物質収支を算出する。グリオキシル酸側路へ分流するフラックスは、物質収支及び2つの生成物による負のフィードバック制御を考慮したフラックス分配関数を組み込んだ反応ブロックにより算出する。

これらの構成ブロックによりTCAとグリオキシル酸側路より構成される代謝回転のシミュレーションが可能となった。シミュレーションに用いた実験データは細胞へのエタノール流入速度、細胞内酢酸濃度及び炭酸ガスの生成速度である。細胞内酢酸濃度の周期的変動の幅は酢酸反応ブロックの速度定数を適切に設定することにより可能となった。同様に炭酸ガス速度変化のシミュレーションを試みたが、その生成経路が数カ所であり多数の定数が含まれているため事実上困難であった。また、エタノール消費速度変化と酢酸濃度、炭酸ガス生成速度変化との間に認められる位相のズレを本シミュレーションモデルで説明することは難しく、炭酸ガスの解離・拡散及びエタノール消費速度のフィードバック制御機構を含めたモデルの開発ならびに実験的検証が必要であることが示された。

SAMENVATTING

Een simulatiemodel van de citroenzuurcyclus en de glyoxylaats bypass is ontwikkeld. Met dit model kunnen de concentratie van een metabool en de hoeveelheid van deze metabool die per tijdseenheid wordt omgezet, berekend worden. Dit simulatiemodel kan gebruikt worden als hulpmiddel bij het onderzoek naar de oorzaak van een autonome, metabole oscillatie die voorkomt in een continue cultuur van de gist *Saccharomyces cerevisiae* gevoed met ethanol.

Het simulatiemodel bestaat uit 3 verschillende bouwstenen; een concentratieblok voor elke metabool, een fluxblok voor elke metabool en een reactieblok voor elke reactie. In het concentratieblok wordt de verandering in de concentratie berekend als het verschil van de hoeveelheid van de metabool die per tijdseenheid gegenereerd wordt (aangeduid met $flux_{in}$) en de hoeveelheid van deze metabool die per tijdseenheid verdwijnt (aangeduid met $flux_{uit}$). Het flux blok bepaalt de $flux_{uit}$ van een metabool als het produkt van de reactieconstante en de concentratie van de betreffende metabool. Een reactieblok bevat de stoichiometrie van een reactie. De grootte van de flux die de glyoxylaats bypass in gaat, wordt bepaald aan de hand van een zogenaamde fluxdistributiefunctie in het betreffende reactieblok. Deze fluxdistributie-functie bevat de negatieve terugkoppeling van twee metabolen.

Met de beschreven bouwstenen is het mogelijk om een simulatiemodel van een cyclische metabole route te maken. Het is getest of het simulatiemodel gefit kan worden op experimentele data. De experimentele data die beschikbaar was bestond uit een oscillerende ethanol flux die de cel in gaat, een oscillerende acetaat concentratie en een oscillerende CO_2 produktie. Er zijn verschillende simulaties gedaan om te bepalen of het simulatiemodel dezelfde amplitude en faseverschuiving kon produceren als aanwezig in de experimentele data. De amplitude van de gesimuleerde acetaat concentratie is gelijk te krijgen aan de amplitude van de experimentele acetaat concentratie door de reactieconstante te variëren. De faseverschuiving tussen de experimentele ethanol flux en de experimentele acetaat concentratie kon niet worden gesimuleerd. Deze faseverschuiving zou dan ook veroorzaakt kunnen worden door het feit dat ethanol de cel in moet. Het simuleren van de amplitude van de CO_2 produktie is gecompliceerder, omdat de CO_2 produktie niet alleen afhangt van diverse fluxen, maar ook van de fluxdistributiefuncties van de glyoxylaats bypass en de ethanol input. Om de simulatie van de CO_2 produktie goed te krijgen is additionele experimentele data nodig.

ACKNOWLEDGEMENTS

The research described in this thesis was carried out at the Biochemical Engineering Laboratory of the National Institute of Bioscience and Human-Technology in Tsukuba, Japan. I would like to thank dr. Hiroshi Kuriyama and dr. Marc Keulers for creating this opportunity for me and for their support and help during my ten months stay. The japanese summary was kindly provided by dr. Kuriyama. The support of prof.dr.ir. P. van den Bosch and dr.ir. Ad van de Boom from the Netherlands is kindly appreciated. Especially professor Van den Bosch has been very stimulating and encouraging during his visit to Tsukuba in January 1996.

Miriam van Santen.
Eindhoven, 23th April 1996.